INVESTIGATING THE PERFORMANCE OF EARTHEN LEVEE STRUCTURES WITH INDUCED INTERNAL DETERIORATION

Gholamreza Saghaee

Doctor of Philosophy

Department of Civil Engineering and Applied Mechanics

McGill University

Montreal, Quebec, Canada

July 2017

A thesis submitted to McGill University in partial fulfilment of the requirements for the degree for Doctor of Philosophy

ABSTRACT

Earthen levees are constructed worldwide as flood control infrastructure and are important components of public safety in the areas they protect. Among the factors which negatively impact the stability and serviceability of earthen levees, internal deteriorations are known to be the most critical type of structural problem. A common type of internal deterioration, animal burrows dug into earthen levee embankments are reported to be the cause of failure in many cases of earthen levees breaches. Globally, the annual cost of damage resulting from failure of earthen structures and associated infrastructure due to invasive wildlife activities is estimated to be many billions of dollars. Understanding the mechanisms of wildlife-caused earthen levee failure is a key component of preventing future breaches. Much of the literature in the area of nuisance wildlife investigates the ecological and environmental impacts of animal activities and habitat, however, studies related to failure mechanisms of earthen structures due to invasive wildlife activities are limited and require a geotechnical engineering perspective. This research aims to identify the mechanics that govern the progress of failure within wildlife-induced levees deteriorations. Investigation of the impact of animal burrows on the hydraulic performance and stability of levee structures is performed using centrifuge modeling. Scaled-down earthen levee models with both landside and waterside burrows as well as a benchmark intact levee model are built and tested at 35g during the centrifuge experiments. The centrifuge experiments are monitored and recorded for deformation, seepage, and pore pressure measurements. Particle Image Velocimetry (PIV)

analyses are performed on series of images captured during the centrifuge flights to calculate global deformation of the levee models. Finite element models are developed based on the experiments and used to conduct parametric studies on the impacts of burrow configurations on the stability of the deteriorated levees. The studies investigate key parameters which governs levee safety: burrow length, burrow depth and levee side slope ratio. Details and results of the experimental and numerical work are presented in this thesis along with conclusions and recommendations for future research.

RÉSUMÉ

Les digues de terre sont construites dans le monde entier en tant qu'infrastructure de lutte contre les inondations et sont des composantes importantes de la sécurité publique dans les zones qu'elles protègent. Parmi les facteurs qui ont une incidence négative sur la stabilité et la facilité d'utilisation des digues de terre, les détériorations internes sont connues pour être le type le plus critique de problème structurel. Un type courant de détérioration interne, les terriers d'animaux creusés dans des digues en terre de levée sont rapportés comme étant la cause d'échec dans de nombreux cas de brèches. Globalement, le coût annuel des dommages résultant de l'échec des structures en terre et d'infrastructures connexes en raison d'activités envahissantes de la faune est estimé à plusieurs milliards de dollars. La compréhension des mécanismes de défaillance de levée de terre causée par la faune est un élément clé de la prévention des brèches futures. Une grande partie de la littérature dans le domaine de la faune nuisible enquête sur les impacts écologiques et environnementaux des activités animales, cependant, les études liées aux mécanismes de défaillance des structures de terre en raison des activités de la faune envahissante sont limitées et nécessitent une perspective d'ingénierie géotechnique. Cette recherche vise à identifier les mécanismes qui régissent la dégradation des digues causée par la faune. L'étude de l'impact des terriers sur la performance hydraulique et la stabilité des structures de digues est effectuée en utilisant la modélisation par centrifugation. Des modèles de digues de terre à échelle réduite avec des terriers terrestres et des terriers situés au bord de l'eau, ainsi qu'un modèle de digues intactes de référence sont

construits et testés à 35g lors des expériences de centrifugation. Les expériences de centrifugation servent à surveiller et enregistrer les mesures de déformation, d'infiltration et de pression des pores. Les analyses de vélocimétrie d'image de particules (PIV) sont effectuées sur les milliers d'images capturées lors des vols de centrifugation pour calculer la déformation globale des modèles de levée. Les modèles d'éléments finis sont développés sur la base du travail de centrifugation expérimentale et utilisés pour effectuer des études paramétriques sur les impacts de la configuration des terriers sur la stabilité des digues détériorées. Les études évaluent les principaux paramètres qui déterminent la sécurité des digues: la longueur du terrier, la profondeur du terrier et le rapport de la pente latérale. Les détails et les résultats du travail expérimental et numérique sont présentés dans cette thèse ainsi que des conclusions et des recommandations pour des recherches futures.

ACKNOWLEDGMENTS

I would like to extend my sincere gratitude to my advisor Professor Mohamed A. Meguid for his mentorship over the course of my doctoral studies. It has been an honor to work with him as a member of the Geo-Group at McGill University. His excellent scientific supervision during my research is deeply appreciated.

Many thanks to C-Core and Memorial University of Newfoundland scientists, engineers and technicians-notably Dr. Ryan Philips and Gerry Piercy- whose collaborations made the experimental component of this research possible and successful. It is a pleasure to thank Dr. Ahmed Mousa for his contributions to this research. I would like to thank Dr. Hori Toshikazu and École de Technologie Supérieure (ÉTS) of Montreal, for their assistance in this project. A special mention of thanks to Holly Cronin for her invaluable help with this thesis.

My deepest appreciation to my family for their continuous support during my academic journey. I am forever indebted to my mother Khadijeh Alizadeh for her endless love and to my father Ramezan Saghaee, a great man and entrepreneur whose integrity is always his priority, for all his inspirations in my life. Last but certainly not least, I am thankful to my wonderful sisters, Robabeh, Sarah and Freshteh, for always being there for me. I believe standing at this point would not have been possible without my family, and I dedicate this milestone to them.

The research presented in this thesis is supported by the Natural Sciences and Engineering Research Council of Canada (NSERC) under grant number 311971-11.

CONTRIBUTIONS OF AUTHORS

Authorship

This manuscript-based thesis is comprised of the materials from published and under-review articles. The list of journal articles and conference papers is included below. These papers were written in collaboration with other authors. However, the author of this thesis is the first author and the sole student, among the co-authors. He was responsible for conducting the research, experiments, modeling, data analysis, as well as for preparing the manuscripts and presenting the research in conferences.

List of publications

Saghaee, G., Meguid, M. A., and Bayoumi, A., (2017), "Synthesis of Wildlife-Triggered Failures in Earth Levees", *Canadian Geotechnical Journal, NRC Research Press, DOI: 10.1139/cgj-2016-0484.*

[Chapter 4 of this thesis]

Saghaee, G., Meguid, M. A., and Bayoumi, A., (2016), "Experimental Evaluation of the Performance of Earth Levees Deteriorated by Wildlife Activities", *Acta Geotecnica, Springer, DOI: 10.1007/s11440-015-0373-0*.

[Chapter 3 of this thesis]

Saghaee, G. and Meguid, M. A., (2013), “Investigating the Failure Mechanism of Earthen Embankments due to Animal Burrows”, *Canadian Dam Association Conference,* Montreal, Canada, October 5-10, 2013.

Saghaee, G., Meguid, M. A., and Bayoumi, A., (2012), “On the Effects of Animal Burrows on the Performance of Homogeneous Earthen Structures”, *Canadian Geotechnical Society Conference,* Winnipeg, Canada, September 30 - October 3, 2012.

Saghaee, G., Meguid, M. A., and Bayoumi, A., (2012), “An Experimental Procedure to Simulate the Effects of Animal Burrows on Existing Levee Structures”, *Eurofuge: Physical modelling in Geotechnical Engineering,* Delft, Netherland, April 23-24, 2012.

TABLE OF CONTENTS

LIST OF FIGURES

LIST OF TABLES

[Blank]

1 INTRODUCTION

1.1 General

Earthen levees are constructed worldwide to protect dry lands and populations from floods and high water levels. In the United States alone, there are more than 150,000 kilometres of earthen levees [1]. The integrity and serviceability of these structures are important to public safety, as levee failure can result in disasters [2]. Among the issues which can seriously compromise the safety of earthen levees is damage resulting from wildlife activities. Animal burrows have long been observed to negatively impact the hydraulic performance and structural integrity of levees and earth dams. Failure of earthen structures and other infrastructure due to animal burrows often causes billions of dollars worth of damage [3]. The majority of research on the topic of animal activities and habitat related to earthen structures focuses on the ecological and environmental impacts. However, studies which assess failure mechanisms of earthen structures due to wildlife-based damages appear to be absent from the literature. The studies presented in this thesis are intended to initiate geotechnical engineering-based investigations of the issue.

Earthen levees are typically constructed using fine-grained soil materials. Such soil types provide desirable habitat for burrowing species of animals. Due to the mechanical properties of these soils, burrows are stable and easy to dig, which makes levees attractive targets for burrowing animals. The presence of animal burrows in levee embankments indicates that a portion of the soil materials composing the body of the earthen structure has been lost. Since the stability of levee side slopes is provided by the mobilised shear strength of the soil, losing any soil particles from within a levee negatively impacts the stability of its slopes. In addition, the presence of burrows within a levee's embankment, alters the expected water flownet configurations. Slope stability depends directly on the shear strength of soil, which is related linearly to the level of effective stress.

Change in water seepage paths in the soil body can threaten the stability of slope and lead to levee breach. Levee breaches are generally caused by excessive force from the water they were built to retain, weakness in levee materials or foundations, and seismic activities. Extensive research, including back-analysis of previously failed levees (e.g. [2]), has been undertaken to investigate the mechanisms that lead to levee breach and failure, such as erosion (e.g. [4]) or overtopping (e.g.[5]). However, the failure mechanisms of earthen levee collapse due to animal burrow damage are still not well understood.

1.2 Motivation

Understating the failure mechanisms of earthen levee breaches caused by wildlife activities is a first step and a key aspect of preventing failure. Post-failure analyses of breeched earthen levees are complex and sometimes impossible because the evidence is usually washed away during and following failure. Conventionally, dealing with the influence of burrowing species on levees is considered a maintenance matter. Due to the lack of a valid procedure to evaluate the effects of animal burrows within levees, the conducted evaluations are inaccurate and the resulting maintenance actions are not fully effective. Some maintenance codes and guidelines do exist for earthen levees [6], but sufficient and accurate information on the behaviour of deteriorated levees is lacking. This research aims to understand the failure mechanisms of internally-deteriorated earthen levees using both physical and numerical models. The results of these studies are intended to contribute to more proper evaluations of the safety and performance of existing earthen levee structures. These finding may also prove advantageous in designing new earthen levees with potential to be damaged by wildlife activities.

1.3 Objective and scope

The main objectives of this research are:

- To develop an experimental method to simulate the presence of animal burrows in an existing levee using a physical model;
- To implement the experimental method developed to simulate the failure mechanism of an earthen levee;
- To build numerical models of deteriorated earthen levees based on the outcomes of centrifuge experiments;
- To evaluate parameters that impact the stability and hydraulic performance of earthen levees.

1.4 Overview

This thesis consists of six chapters, which summarize the work undertaken during the author's doctoral research. The order of the chapters reflects the general flow of the work performed. This first chapter introduces the research and the outline of the thesis. Chapter two presents a summary of the literature review and background information focusing on animal burrows in earthen structures, internal erosion, centrifuge modeling, and numerical analysis of earthen levees. Chapter three explains the method used to conduct the physical modeling. The performed centrifuge experiments together with the details of the tests and results are also presented in chapter three. Chapter four investigates failure mechanisms for three different burrow scenarios and demonstrates the numerical model built based on the results of the centrifuge experiments. Chapter five presents the results of a parametric study conducted on levee models to investigate the effect of animal burrow characteristics on levee stability and performance. Finally, chapter six summarizes the conclusions made in each of the prior chapters then research outcomes and offers suggestions for futures studies.

1.5 Original contributions

The body of research presented in this thesis makes the following contributions to the fields of earthen levee engineering:

- Appling physical modeling to study the effect of animal burrows on earthen levees
- Introducing a burrow simulation mechanism to enable centrifuge modelling of internally deteriorated earthen levees
- Proposing failure mechanisms of earthen levee breaches caused by animal burrows
- Developing finite element models of deteriorated earthen levees
- Conducting a parametric study of the effects of animal burrow configurations on the stability and hydraulic performance of earthen levees

2 LITERATURE REVIEW

2.1 Wildlife activities and earthen levees

The presence and the consequences of animal burrows on earthen levees are to some extent understood by the agencies involved in maintaining levees. However, insufficient attention is paid to the severity of the impacts of these burrows on the integrity of earthen structures. The problems associated with burrowing animals are generally considered to be maintenance issues and are typically addressed by implementing some form of wildlife management plan. Yet, in the United States (US) alone, wildlife activities impacting earthen levees have been reported in the 48 states, of which only nine have official guidance on responding to damages caused by these animals [6]. Animal burrows can alter the hydraulic performance of levee structures and cause surface and internal erosion. Internal erosion is among the most common causes of levee structure failures [7]. The severity of the damage to a levee by burrowing animals depends on the size, length, and connectivity of the burrow network. The configuration of a given animal burrow depends on specific type of animal involved and the soil properties of the embankment. Table 2.1 presents the severity of the problems caused by animal intrusions on earthen dam and levee structures.

Table 2.1. Representative selection of intrusive animal species in the US [3]

Species	Magnitude of reported damages %	Number of states
Muskrats	71	34
Beavers	67	32
North American Badgers	17	8
Ground Squirrels	15	6

The presence of animal burrows inside levees endangers the integrity of the earthen structures. A network of these burrows can be expanded extensively within a levee embankment. Such a network can have openings on both the waterside and the landside of a levee at the same time [8]. Figure 2.1 illustrates schematically how animal burrows may present in an earthen levee. The development of animal burrows can lead to local collapse of either the crest or the slope of an embankment due to the instability caused by the animal burrow chambers [6].

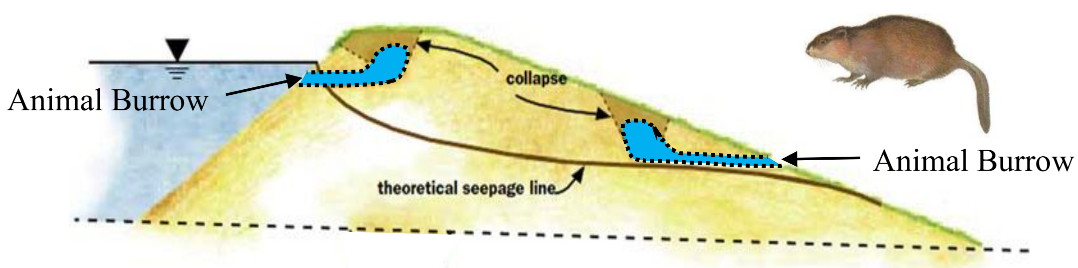

Figure 2.1. Schematic example of animal burrows in an earthen levee [6]

Burrow length, depth, and size are dependent on both the characteristics of the animal species that dug the burrow and the characteristics of the soil used to construct the levee [9]. In particular, burrow length and complexity change in relation to the percentages of silt and clay in the soil [10]. The direction of an animal burrow is typically independent of the hillslope, despite the tendency of burrowing animals to minimize the energy they expend on digging; pocket gophers in particular tend to burrow horizontally [11]. The geometrical properties of an animal burrow have significant impacts on the type and magnitude of damage they cause to an earthen levee. Key burrow characteristics for a selection of common species are summarized in Table 2.2.

Table 2.2. Burrows characteristics for selected species [3, 4]

Species	Typical burrows characteristics	Attack side
Muskrats	Burrows as deep as 10 ft below water level	Waterside
Beavers	Tunnels, dens,1-9 ft deep, 2 ft high chambers	Waterside
Pocket Gophers	Burrows 40 ft long and 10 ft deep	Landside
North American Badgers	Large burrows 5–30 ft long and 2–3 ft chambers. Single elliptical entrance with 1 ft diameter	Waterside
Ground Squirrels	Large colonies. Burrows 2–10 in diameter, and 10 ft long	Both sides

Many cases of levee breaches have been reported around the world for which the presence of animal burrows is considered the primary cause of failure. Notable among these failures are: the 1980 Lower Jones Tract levee failure in California due to seepage and rodent activity [12]; followed by the 2004 Upper Jones Tract levee failure [13]; the 2008 Winfield Pin Oak levee failure in Missouri due to muskrat activity [14]; and more recently a 2014 levee failure in San Matteo, Italy [15].

Detecting animal burrows is a critical component of accurately evaluating a deteriorated levee. In order to remediate the damages caused by a burrow network, determining its configuration is vital. Various methods are used to detect animal burrows including the gravity survey method which measures density [16], the resistivity method which measuring electrical resistivity [17], the seismic reflection method which measures seismic velocity [18, 19], and the ground penetrating radar (GPR) method which measures dielectric constants [1, 20, 21]. Identifying the configurations of animal burrows in an existing levee and understanding the behaviour of these burrows is necessary to enables proper evaluation of the safety and serviceability of the levee. This research aims to contribute to the literature on wildlife activities and earthen levees by investigating the effects of animal burrows on levee models and elucidating mechanisms by which the intrusions can lead to the failure of earthen structures.

2.2 Causes of levee failure

Earthen levee failure results from a single problem or the combination of multiple problems. These problems usually develop over time but also can occur suddenly. Levees are normally made of soil without surface protection to resist surface erosion, which makes them sensitive to overtopping. Overtopping occurs when the water level on the waterside of a levee rises above the levee crest. The overtopping of levees has been studied experimentally by Schmocker and Hager [22, 23] who built and tested physical models with different configurations, and their results determined that sediment size has a significant effect on breach process.

A common safety threat, erosion, is another key cause of levee failure [24]. Erosion happens when soil particles are displaced due to an external force [25]. Surface erosion is a type of erosion that occurs on the surface of an earthen levee, for instance due to water flow of a canal along levee embankment or overtopping event. Surface erosion can be prevented by using erosion-resistant materials such as concrete blocks or geogrids on the crest and slopes [26, 27]. A particularly dangerous type of erosion, internal erosion, can be more of a hazard to levee safety than other types of erosion because it can remain undiscovered for a long time before its effects are visible. However, recent research by Planes et al. [28] has found that measuring ambient seismic noise could be a good tool for discovering internal erosion in earth dam and levees. Figure 2.2 presents an example of a typical problem resulting from internal erosion in an earthen embankment [29].

Figure 2.2. Internal erosion a) Tunbridge dam in Australia that experienced failure due to internal erosion (piping); b) seepage exit points on the land side slope; c) the evacuated town downstream [29]

Internal erosion occurs in different ways: concentrated leak, backward erosion, contact erosion, and suffusion. Each of these scenarios follows the general pattern of internal erosion leading to levee failure, which can be divided into four stages: initiation, continuation, progression, and failure.

Figure 2.3 illustrates the initiation stage of three scenarios of internal erosion relevant to this research. Animal burrows related breaches typically follow scenario where a concentrated leak due to the presence of cavities in the embankment initiates a levee failure. Scenario b and c represent potential internal erosion initiation patterns less commonly associated with animal burrow levee failure.

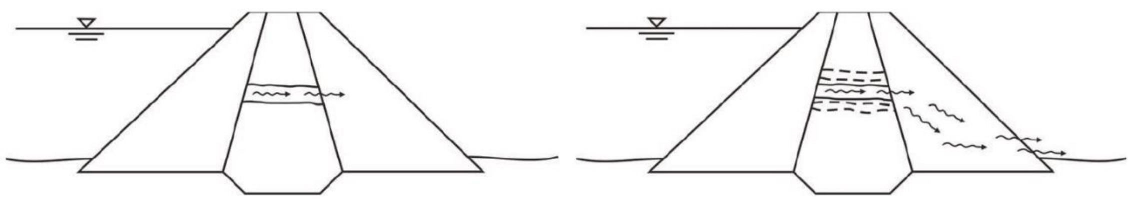

a) Internal erosion in the embankment initaited by concentrated leak

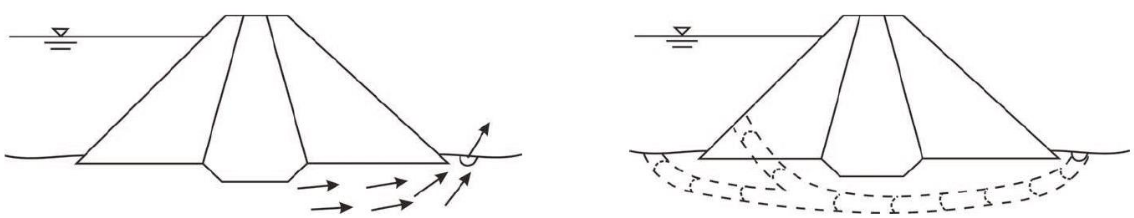

b) Internal erosion in the foundation initiated by backward erosion

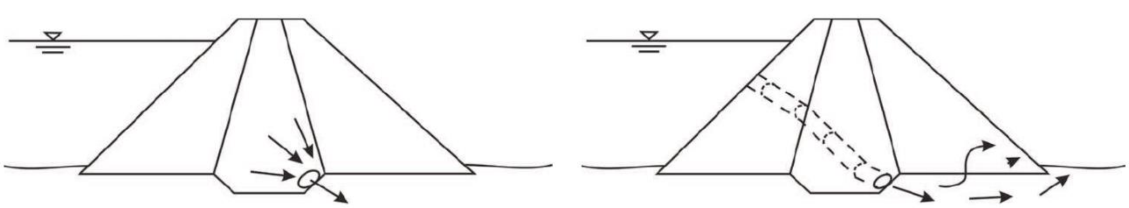

c) Internal erosion from the embankment to the foundation initiated by backward erosion

Figure 2.3. Selected internal erosion initiation scenarios in earthen levees [30]

2.3 Approaches to study levee performance and failure

Several methods can be used to analyze earthen levees, including physical modelling. The physical modeling of levees is conducted by building a large-scale model or using small-scale centrifuge models. Full-scale levee models have been built by Van Beek et al. [31] and Koelewijn et al. [32] to study the effects of internal erosion on earthen levees. All four stages of internal erosion were observed during these experiments. Due to the large size of the levee structures, building full-scale models is costly, time-consuming, and sometimes not even feasible [33].

Small-scale centrifuge models provide a comparably powerful yet relatively cost and time effective alternative. Raising gravity level in a centrifuge reproduce in a small-scale model the stress level experienced by a prototype levee structure [34]. The ability to increase gravity level is necessary for accurate small-scale physical modeling of earthen levee because soil shear strength is dependent on stress level [35]. A centrifuge machine is used to apply high g-level to the models. Depending on the type of the centrifuge used, a model is usually built and then loaded in to the centrifuge basket. Beam centrifuges are the most common type of geotechnical centrifuge and can spin heavier payloads at higher g-levels than other types. (Figure 2.4).

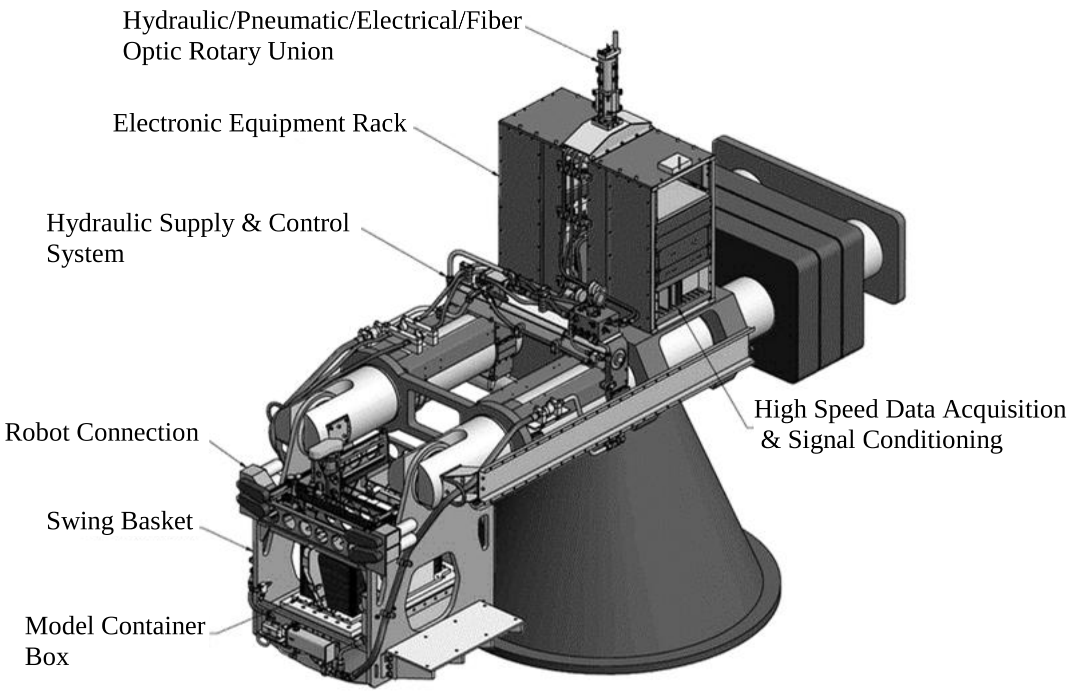

(a)

(b)

Figure 2.4. a) Schematic drawing of a beam centrifuge [36], b) C-Core's 5.5m-radius, 200G payload capacity beam centrifuge used in this study

The agreement between the results of field investigations and centrifuge models supports the effectiveness of the method in simulating levee structures and studying soil-structure interaction problems. Post-failure studies of the New Orleans levee system failure due to hurricane Katrina, the worst recorded natural disaster in US history, have been conducted using centrifuge models. For one such study, Ubilla et al. [37] built 50g models of three different cross sections of the New Orleans' levee (Figure 2.5). The same technique was used by Steedman and Sharp [2] to study the failure mechanism of earthen levees.

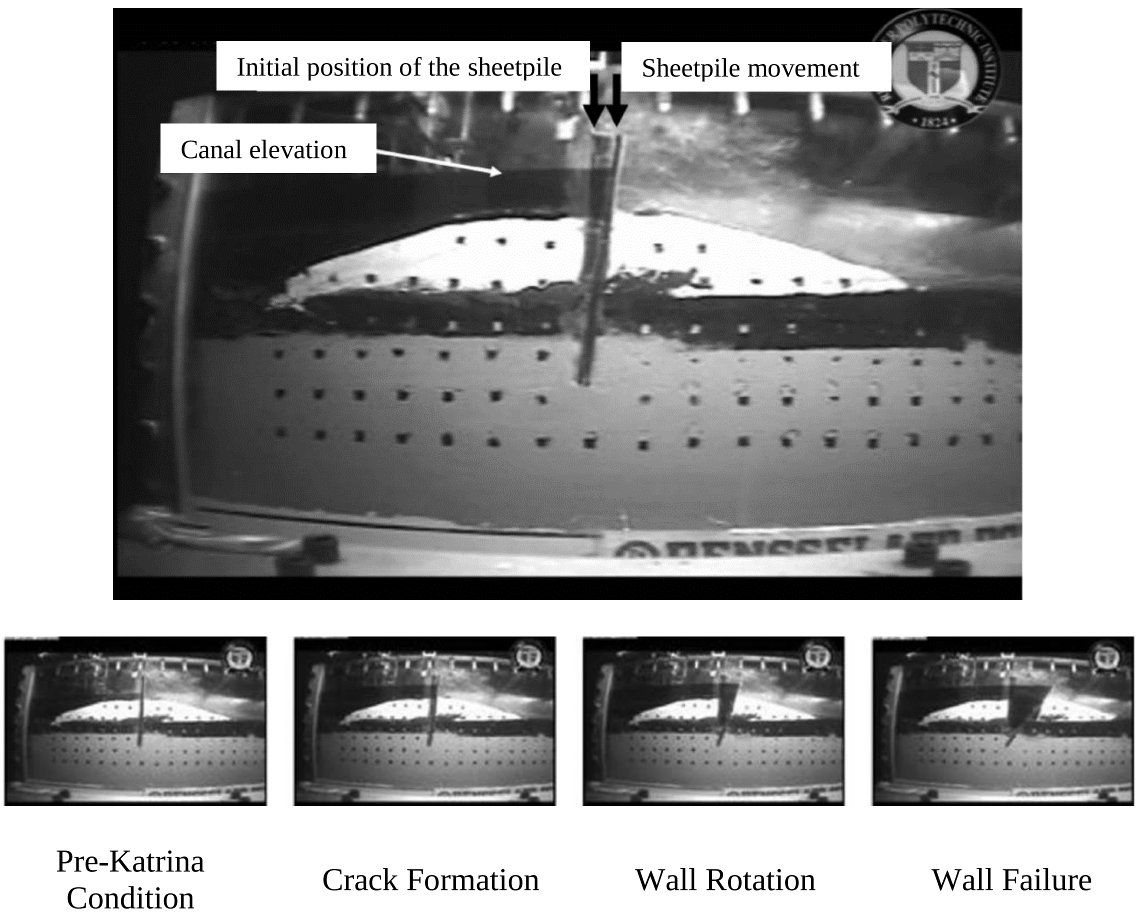

Figure 2.5. Failure stages for New Orleans levee (London Avenue) models [37]

Centrifuge modeling has also been used to study the seismic performance of levees. A clay levee built on a peat layer of the Sacramento delta was modeled at 57g by Cappa et al. [38]. The liquefaction of the levee foundation as a side product of earthquakes has been studied using centrifuge modeling. Maharjan and Takahashi [39] studied the ground motion effects on the deformation of 2H:1V slope levee foundation using a 1/40 scaled model. The results showed that foundations resting on non-homogenous layers suffer more damages as compared to the uniform sand layers. Backward erosion beneath the earthen levees has been investigated using centrifuge models by Koito et al. [40]. They built half levee models using kaolin clay and silica sand and tested under static conditions. The results illustrated backward erosion patterns for the studied cases. The behavior of non-homogeneous earthen levee models, with a mixed clay-bentonite core, has been investigated during raising water level in centrifuge experiments by Lee et al. [41]. The research results showed that a rapid increase in water level can cause hydraulic fracture in the levee core.

Beside physical modeling, numerical modeling and analytical approaches are also employed to study earthen levees. Numerical modeling has been used for a long time to simulate geotechnical engineering problems. Currently, finite element, finite difference and discrete element methods are used to analyze complicated problems related to earthen levees. For instance, Jafari el al. [42] has conducted 3D finite element analysis of seepage through a complex curved levee. Shi-igai et al. [43] used an analytical approach to study the amount of wave overtopping on levees for given conditions. Kaunda [44] has also employed artificial neural networks to estimate backward erosion in earthen levees.

3 EXPERIMENTAL EVALUATION OF THE PERFORMANCE OF EARTH LEVEES DETERIORATED BY WILDLIFE ACTIVITIES

3.1 Preface

In this study, an earth levee model is constructed to investigate the impact of animal burrows on the integrity and performance of earthen structures. A series of centrifuge experiments are conducted on homogenous scaled-down 1H:1V levee models built from the natural Kasama soil. Both intact and deteriorated models were subject to a 35g acceleration level. Invasive animal intrusions were introduced in the form of horizontal array of idealized cylindrical burrows at the mid height of the levee. The water level was gradually increased during the centrifuge flight and the response of the levee was monitored throughout the test. Pore pressures were recorded using pressure transducers placed at pre-selected locations within the model. Surface displacements were measured using laser LVDTs and supplemented with three digital cameras for tracking the overall deformation pattern of the levee model. A summary of the test procedure and selected results are presented herewith. The observed deformation mechanism due to the presence of animal burrows is also described. As compared with the intact levee, the presence of burrows is found to alter the pattern of the water flow through the deteriorated levee structure - leading to a notable increase in the exit hydraulic gradient, internal erosion and subsequently slope failure.

3.2 Introduction

Levee breaches are typically driven by excessive forces from the retained water (floods), weaknesses in the levee material or its foundation, and seismic events. Invasive animal activities have been known to negatively impact the hydraulic performance and often the structural integrity of levees and earth dams. The possible types of deterioration in levees due to wildlife activities can be categorized into structural damage, surface erosion, and hydraulic alterations [6]. The latter, one of the most common causes of failure in earthen structures, can develop in the form of distortion in flow net, internal erosion and piping [45]. Internal erosion and piping develops in four phases: initiation of erosion, continuation of erosion, forming internal channels, and finally breach [45]. This form of damage may not be visible until the safety of the earth structure is already jeopardized. Internal erosion typically develops when cracks or cavities exist within the earth structure.

The invasive wildlife activities in earthen structures are globally spotted. The estimated worldwide annual cost of damage or failure of earthen structures and the associated infrastructure due to these activities exceeds billions of dollars [3]. Selected case studies of earth structure failures related to wildlife are summarized in Table 3.1. Although several methods have been used to detect and locate animal cavities in earthen structures, e.g. gravity survey, resistivity methods, seismic reflection, and ground penetrating radar, the damage caused by these nuisance activities could remain concealed for a long time [46].

Extensive research has been done on intact earth structures to study the mechanisms of piping [33, 47-49], erosion [50-52], overtopping [23, 53], and their back analysis [54]. A significant amount of the literature in the area of wildlife investigates the ecological and environmental impact of animal activities and habitat [3]. However, the literature pertinent to the synthesis of failure mechanisms of earth structures due to invasive wildlife activities is very scarce.

Table 3.1. Reported levee and earth dam failures induced by wildlife invasive activities

Case	Location	Year	Failure Mode
Sid White	Near Omak, Washington	1971	Seepage through animal burrows caused dam to fail and dumped debris into town of Riverside
Lower Jones Tract	California Delta	1980	Seepage and rodent activities
Water's Edge	North of Cincinnati, Ohio	1992	Water flow through animal burrows
Iowa Beef Processor Waste Pond	Wallula near Richland, Washington	1993	Uncontrolled seepage through the animal burrows, exiting on the downstream face and causing erosion
Persimon Creek Watershed-Site 50	Mississippi	1998	The dam failed due to erosion of an emergence spillway Ongoing beaver activities clogged primary spillway
Sunrise Duck Club (Suisun Marsh)	Suisum Marsh, California	1999	High tide and possible beaver activities
Pischieri Pond	Cleveland, Ohio	1999	The dam was breached when an inspection found a void within its body
Upper Jones Tract	California Delta	2004	High tide, under-seepage and rodent activities
Foema Stream	Sinalunga, Italy	2006	Porcupine burrow, internal erosion and levee subsidence
Truckee Canal	Femley, Nevada	2008	Woody vegetation and animal burrows present
Pin Oak	Winfield, Missouri	2008	Muskrat burrows
Secchia River	San Matteo, Italy	2014	Presence of animal burrows is recognized to be the cause of failure

This study experimentally investigates the effects of invasive animal activities on the hydraulic performance and stability of levees. Description of the physical model, the methodology used to introduce animal burrows within the model, and details of the performed centrifuge testing are presented. The test results of an instrumented intact (reference) levee model, including surface displacements and pore pressures, are summarized and compared with those measured for deteriorated levee models. The changes to phreatic surface and the progressive failure developing along the side slopes of deteriorated levees are discussed.

3.3 Significance and scope of work

The invasive wildlife activities in earth structures have been traditionally dealt with as a maintenance issue rather than a challenging design problem and a long-term performance concern. It is, therefore, instrumental to capture the distinctive hydraulic characteristics as well as the stability of earth structures deteriorated by these intruding activities. The introduction of animal burrows unquestionably alters the original design of earth structures beyond expectations; hence the challenge in addressing this problem in geotechnical engineering.

Due to the complicated nature of the problems and lack of experimental data needed for validating numerical models, centrifuge testing has been initially chosen for the proposed experimental program on the deteriorated levees. The reported geometry and location of burrows within a levee have been found to vary depending on the water level, animal type and levee material [3]. Chlaib et al. [20] indicated that animal burrows are mostly found on the waterside of levees and close to horizontal. For the purpose of this experimental study, animal burrows are idealized as a series of cylindrical openings introduced at the mid-height of the levee along the waterside.

This study aims at identifying the mechanics that govern the progress of failure within the deteriorated levees. Investigation of their hydraulic performance and the impact on stability is closely investigated. Details of the levee model testing are provided in the subsequent section.

3.4 Experimental program

In preparation for an optimized model, a series of simplified two-dimensional limit equilibrium analyses has been performed using SLIDE software with different levee geometries, side slopes and water levels. The intact levee stability was investigated using Spencer's method for three side slopes: 2.5H: 1V, 1.5H: 1V, and 1H: 1V. Based on the preliminary numerical simulations, an optimized levee section with equal side slopes and a toe drain is proposed for the purpose of this investigation. The 1H: 1V side slope has been found to provide an acceptable balance between stability of the intact levee and a reasonable vulnerability to failure of the deteriorated levee during the proposed testing. An array of equally spaced horizontal burrows was then introduced on the waterside at the mid-height of the symmetrical levee. This numerically-driven idealizing scheme enabled proper guidance for the design of the physical model used in the study.

The experimental program involves building a scaled-down levee and introduction of idealized animal burrows within the model. Upon completion of the burrow construction, the model was subjected to a gradual increase in water level during centrifuge testing until failure is reached at a predefined gravity acceleration (g) level.

Previous studies showed that burrowing animals tend to smartly dig in relatively loose soils that exhibit some cohesion. These favorable geologic conditions ensure efficient excavation while maintaining stability of burrows [55]. The natural Kasama soil, successfully used in similar centrifuge experiments [56], was utilized in this study to mimic these favorable conditions. Kasama soil gradation has been determined based on ASTM D6913 [57] and ASTM D422 [58] (Figure 3.1). The soil is classified as silty sand (SM) based on the USCS classification system, with 52% sand, 38% silt and 10% clay content. A summary of the basic soil properties is given in Table 3.2. Figure 3.2 shows the standard proctor results used to determine the maximum dry density of the soil based on ASTM D698 [59].

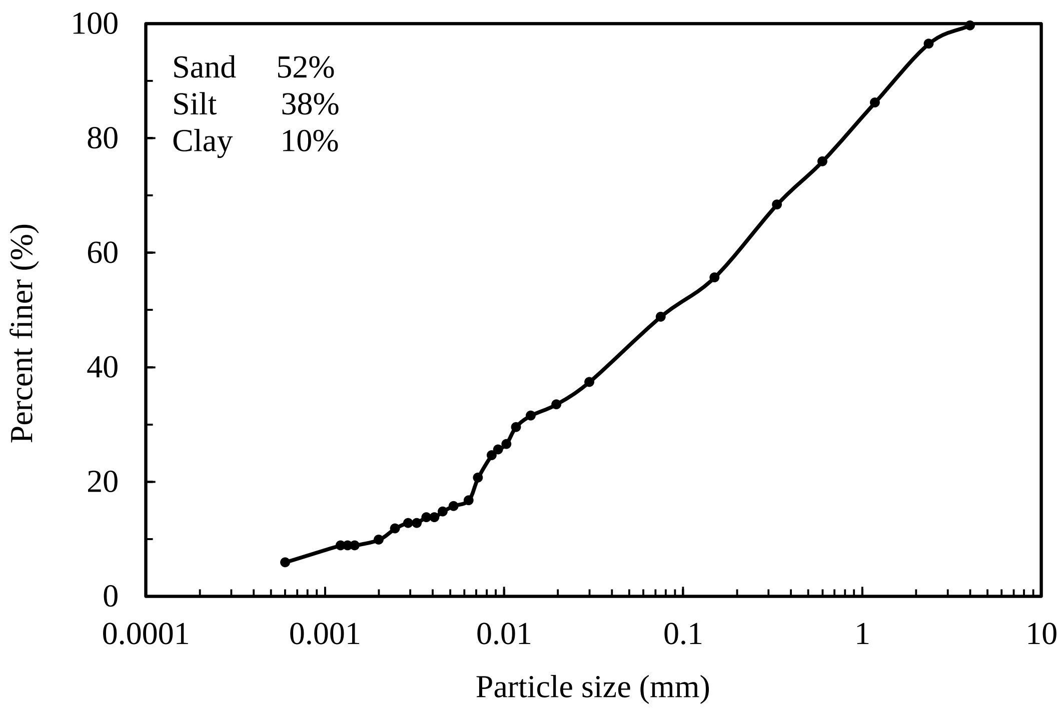

Figure 3.1. Grain size distribution of Kasama soil

Table 3.2. Characteristics of Kasama soil

Property	Values
G_s	2.67
Moisture content (%)	30
LL	59
PL	33.2
$\gamma_{d\,(max)}$ (kN/m^3)	13.8
OMC (%)	27.5
γ_{sat} (kN/m^3)	16.8
γ_{unsat} (kN/m^3)	14.1
ϕ' (^{o})	32^o
c' (kPa)	5.9
k (m/s)	3.8 x10^{-5}

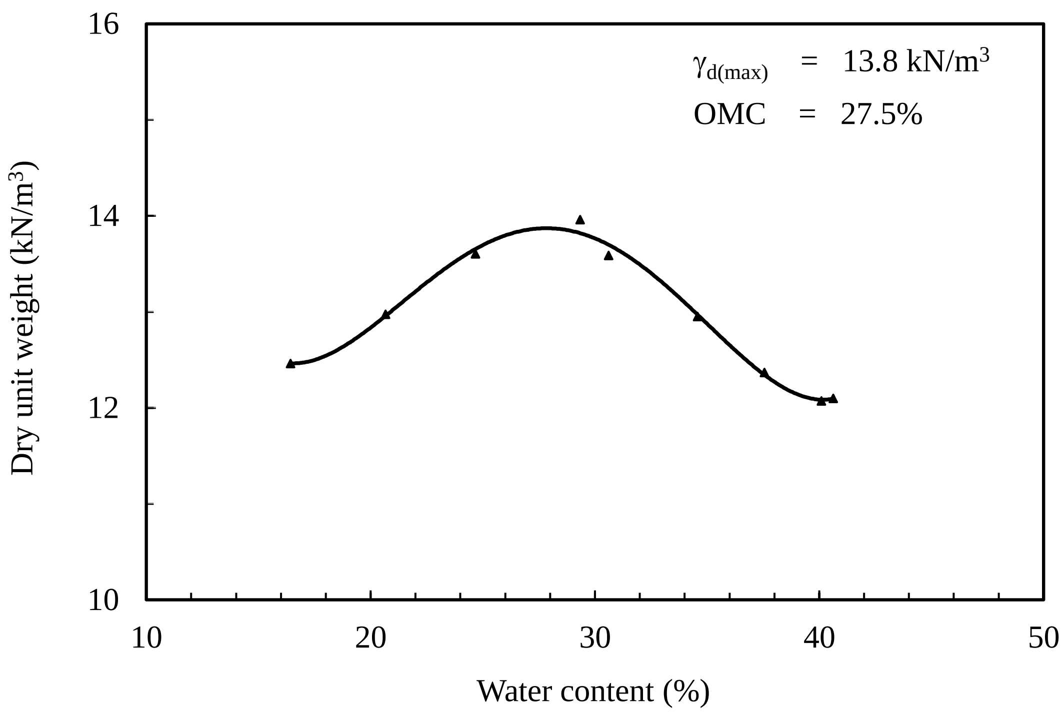

Figure 3.2. Standard proctor test on Kasama soil

The geometrical configurations were selected based on the common height of the reported levee failures due to animal burrows [60]. The 1:35 scaled-down section was built to model a 5-m high levee cross section with a 4-m wide crest width and the selected 1H:1V side slopes. As shown in Figure 3.3a, the levee model has a landside toe drain to keep the slope dry and reduce the number of parameters affecting the slope stability of the intact levee. Both intact and deteriorated models were constructed following the same procedure and tested under similar conditions.

3.4.1 Model construction and monitoring scheme

The levee model was constructed inside the centrifuge box using the compaction and excavation technique. This method involves two steps: (1) placement and compaction of the soil in equal thickness lifts (layers) up to the desired height, and (2) removal of the soil (excavation) in order to shape the levee cross section (Figure 3.3b). The desired levee profile was overlain on the glass walls of the centrifuge box before soil placement (points b through g). The levee is constructed in nine 2.5-cm thick lifts. Each soil layer is compacted at a moisture content of approximately 30% using a vibratory compactor. The toe drain material is placed within the bottom three layers using vertical and horizontal spacers. Upon placing the first two layers (Figure 3.3b), the vertical part of the granular toe drain is placed and compacted. The 100 psi (689.5 kPa) miniature pore pressure transducers (PPT) with thin cables (Model GE Druck PDCR 81-347) are placed within the model at preselected locations to monitor the pore pressure changes during the test (Figure 3.3b). The use of sufficiently long PPT wires minimizes the impact of wiring interference on the measured deformations. Core samples were collected from both the waterside and landside - away from the levee

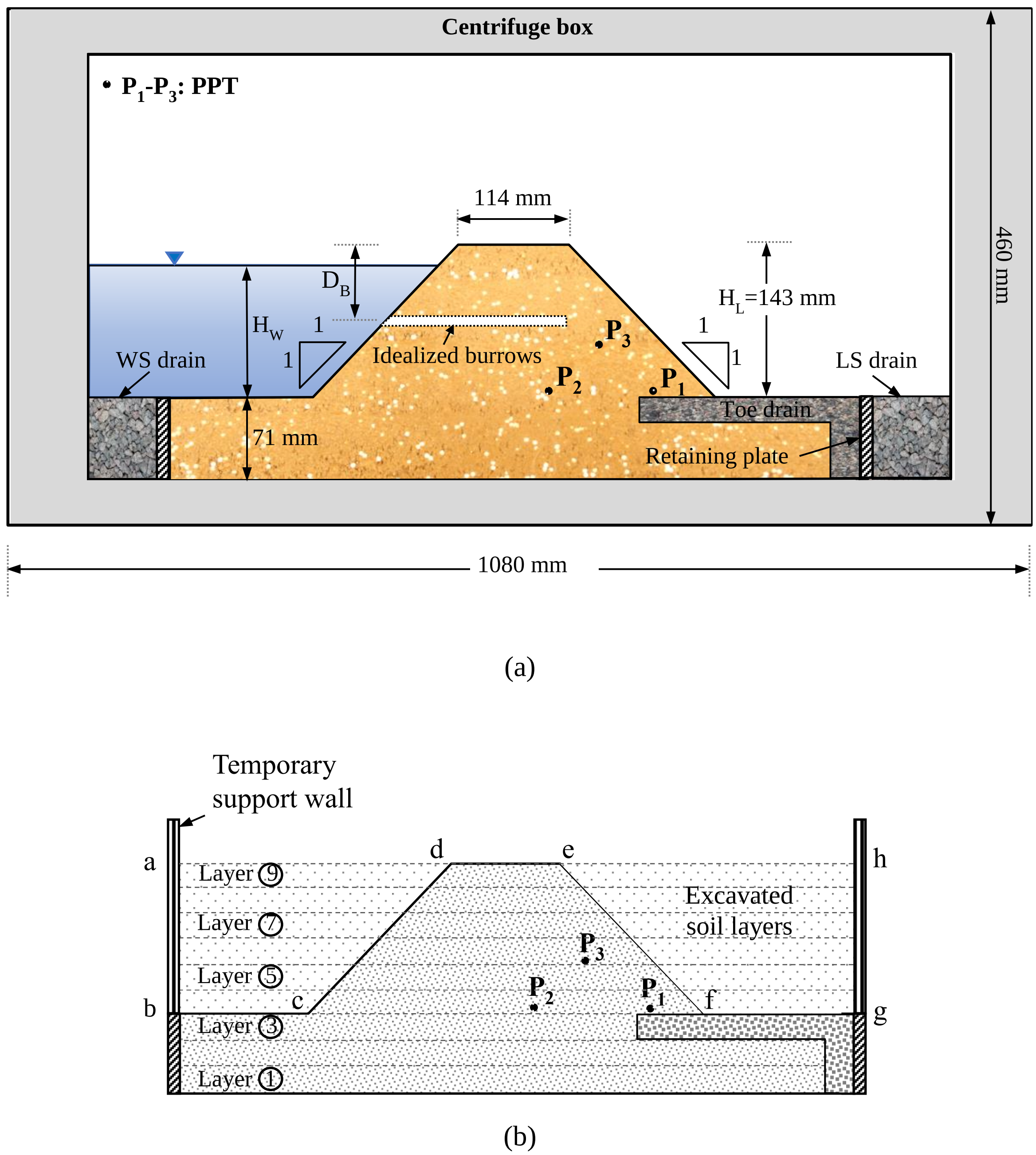

Figure 3.3. Model configurations: a) geometry; b) construction procedure and location of pore pressure transducers (P_1 through P_3)

section - to verify the degree of compaction and the water content before excavation. Following the placement of the top layer (layer 9 in Figure 3.3b), the excavation process was carried out from the waterside and landside (lines ab and gh) toward the predefined faces (lines cd and ef) of the levee cross section. This necessitated the removal of the soil volume within two trapezoidal areas: abcd and efgh. Excavation is performed slowly in order to minimize disturbance of the levee model. The model profile (points b through g) is continuously monitored during the construction and instrumentation stages. The foregoing scheme was adopted to build both of the intact and deteriorated levee models.

3.4.2 Introduction of idealized burrows into the deteriorated levee model

Burrows were introduced into the built model by initially placing a set of rods, comprised of six 8.5-mm prismatic cylindrical stainless steel rods, at the mid-height of the levee section. The rods are of the same length and spaced 50 mm apart in plan as shown in Figure 3.4.a. At 35g, the chosen 8.5-mm cavity diameters approximately resembles 300 mm diameter burrows which is consistent with the size of common wildlife intrusions [3]. The pre-installed rods placed within the model were removed during centrifuge flight using a specially designed pullout system as shown in Figure 3.4b. This system consists of a linear actuator, a pulling cable running over a fixed pulley, and vertical and horizontal support plates (Figure 3.4b). The friction along the rod-soil interface was minimized by precise machining and smoothing of the rod surfaces. The rods were marked at preselected equal intervals for tracking of the buried length using a monitoring system installed around the model. Upon reaching the target g-level (35g), the pullout of the rods array triggered. This technique ensures smooth sliding of the connection beam on the support plate until the rods were completely removed from the model.

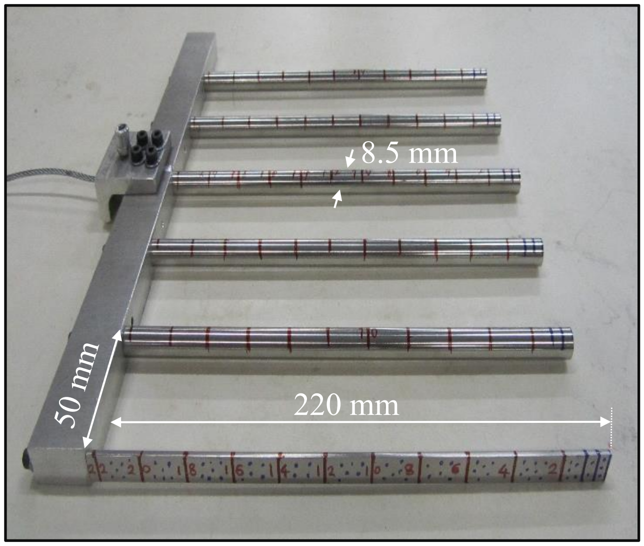

(a)

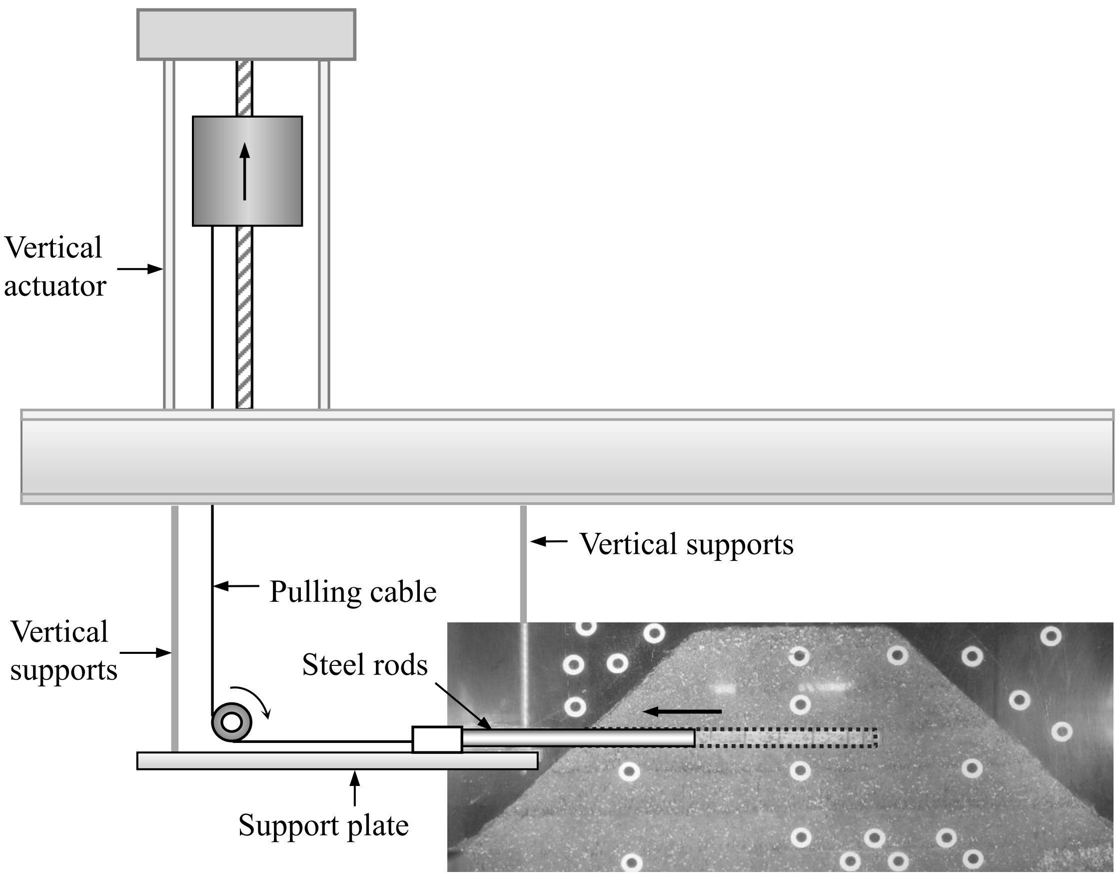

(b)

Figure 3.4. Burrow modeling technique: a) rod-set; b) pullout system

Three high resolution digital cameras (10.0 MP, 6x optical zoom) were placed outside the box to monitor the deformation field of the soil particles during the experiment. Still shots are taken every 5 seconds throughout the experiment. In addition, the top surface of the model, marked with white paint, is continuously monitored using HD camcorder. Crest settlement has been measured during the tests using two laser LVDTs attached to the box pointing down towards the levee surface. The test setup and monitoring system are illustrated in Figure 3.5.

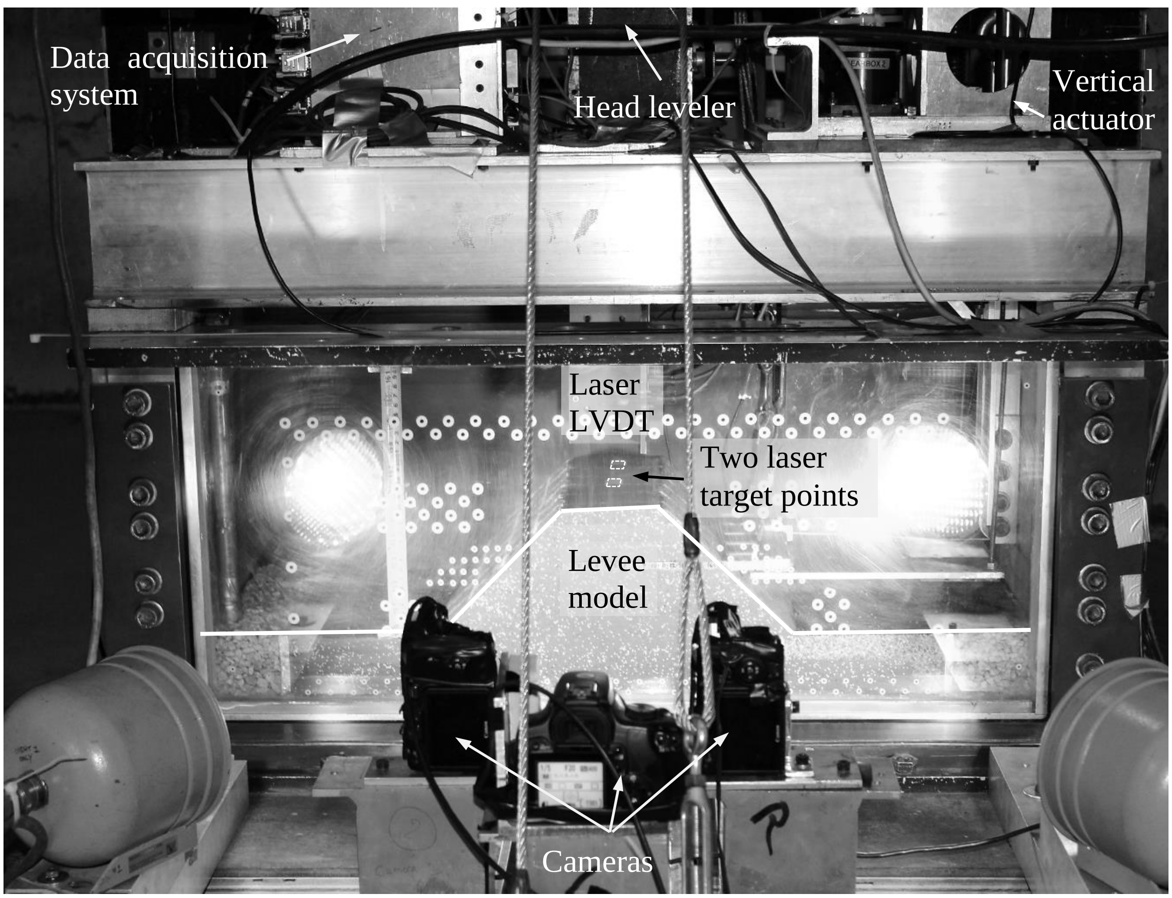

Figure 3.5. Test setup and monitoring system installed on the centrifuge box

3.4.3 Test procedure

The constructed levee model (14.3 cm height and 11.4 cm width) was tested at a centrifugal acceleration of 35g. The plane-strain box containing the model was equipped with a transparent face to allow for monitoring the deformation of the model. The centrifuge testing started by spinning the model up to an acceleration of 10g. The performance of the model and the installed instruments are checked at this acceleration level to ensure proper monitoring. The centrifuge acceleration continued to increase to the target g-level (35g), at which the rods were removed. The acceleration is held constant thereafter. Upon rod removal from the levee body, the water level on the waterside is raised gradually through the waterside main drain located to the left side of the model. A dedicated water pump was used to introduce water from the onboard water tank into the box. The water level is adjusted using the on-board head leveler and monitored using a PPT installed within the main drain.

Figure 3.6 shows a set of successive images that illustrate the rod removal process as captured by the cameras facing the model. It is crucial to ensure burrow stability before the water level was raised. Therefore, the vertical displacements (settlement) of the levee crest are closely monitored using two laser sensors directed towards the crest during the pullout process. The measured crest settlement versus elapsed time of the centrifuge spin is depicted in Figure 3.7. The rods pullout was performed between approximate elapsed times (t) of 2300 s to 3000 s marked by stages C and D, respectively (Figure 3.7). Insignificant settlements were noted during the removal of the rod system. Thus, the cavities introduction and pullout technique seem to provide repeatable initial conditions with a minimal effect on the levee integrity. By inspecting the measured crest settlement of the levee model to up to an elapsed time of 5000s, it is evident that the levee started to experience rapid increase in settlement shortly after the water level was raised (at approximate elapsed time of 4000 s as depicted in Figure 3.7).

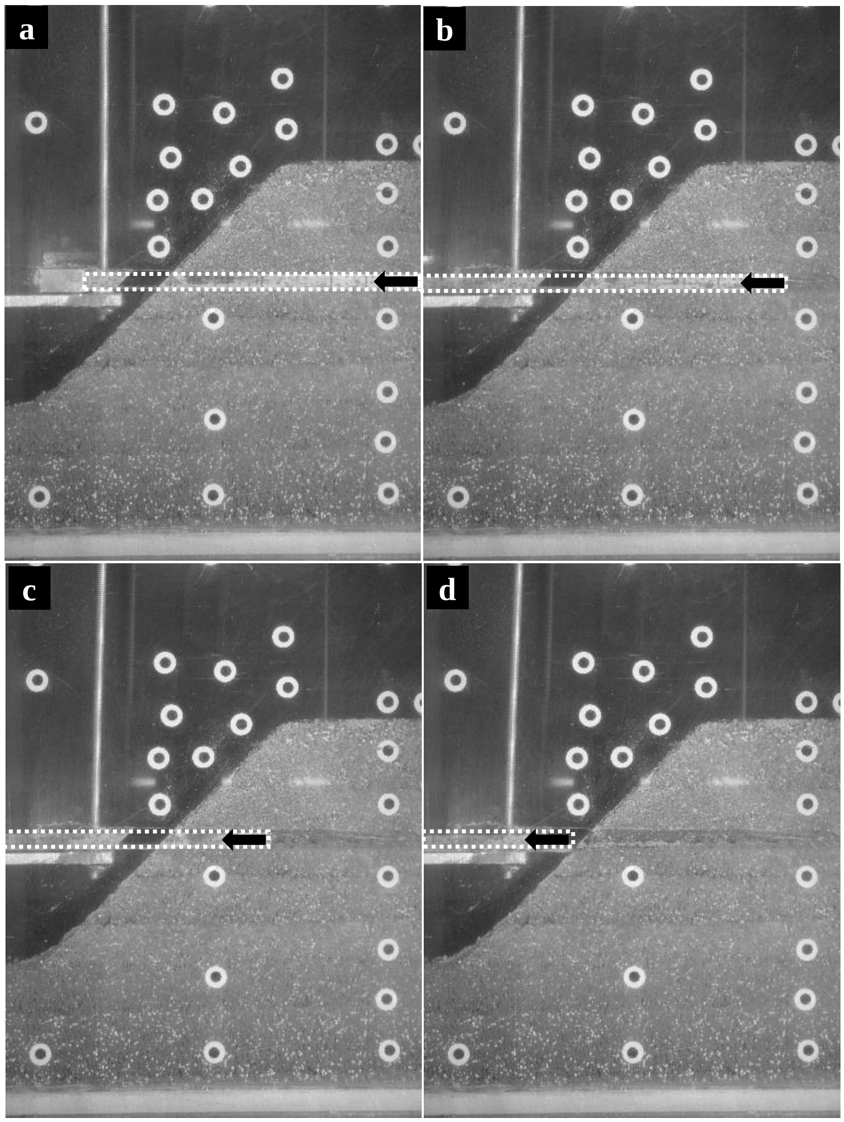

Figure 3.6. Rod set pullout process: a) initial; b) halfway; c) three-quarters; d) complete removal

All centrifuge tests reported in this study have been conducted at the C-Core centrifuge facility in Saint john's, Newfoundland, Canada. The facility has a 5.5m beam centrifuge with a maximum G-Level of 200g and 2200 kg payload capacity at 100g.

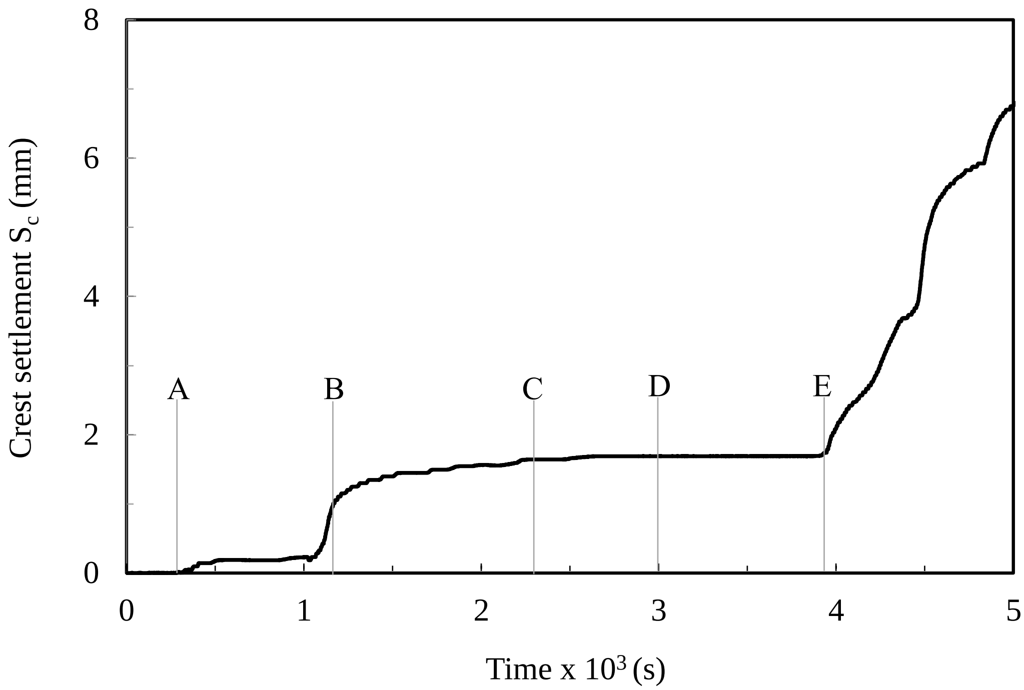

Figure 3.7. Progress of crest settlement during a typical centrifuge flight: a) spin-up; b) 35g; c) beginning of pullout; d) end of pullout; e) increase water level

3.5 Results and discussion

3.5.1 Levee deformation

The crest settlements of the intact and deteriorated levee models are shown in Figure 3.8. Crest settlement and levee distortion were closely monitored during testing. For both configurations, the crest experienced a small increase in settlement of about 2 mm prior to the commencement of water (t ≅ 4000 s). The rate of settlement rapidly increased in both cases to about 8 mm shortly afterwards (t ≅ 6000 s). This is attributed to the water flow through the levee and the associated increase in pore pressure within the body of the levee and its foundation. Beyond that point, the two configurations exhibit quite distinguishing responses. The crest settlement of the intact levee (indicated by the solid line) stabilizes at about 9 mm whereas the deteriorated levee (the broken line) experienced excessive settlement (the near vertical line) followed by a rapid failure.

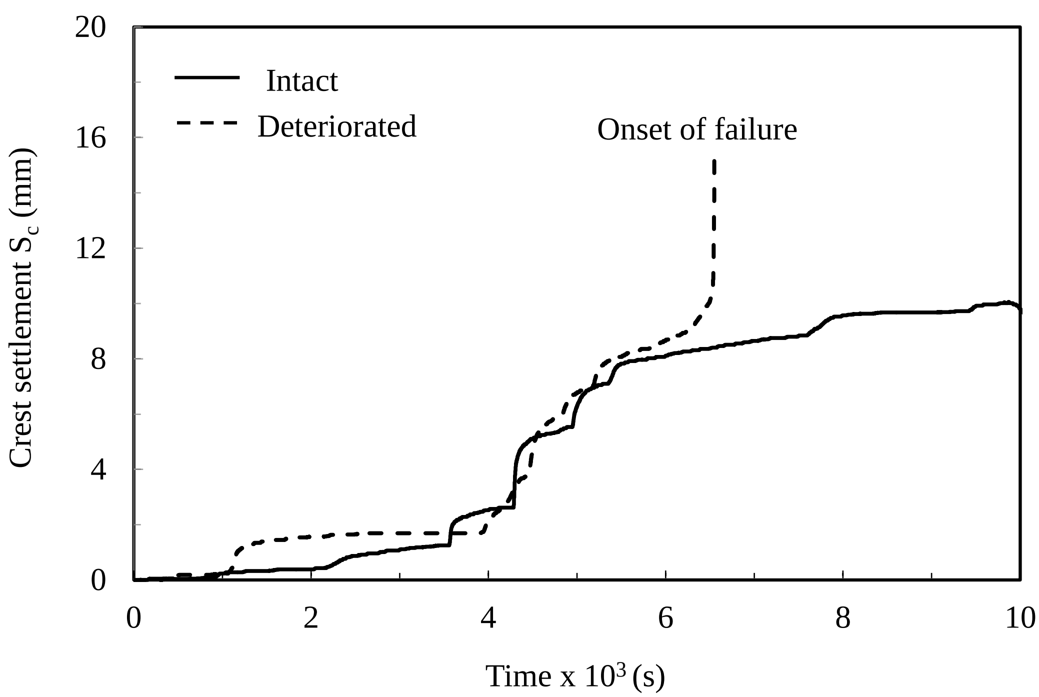

Figure 3.8. Crest settlement of intact and deteriorated levees

Selected snapshots of the levee cross-section were taken at different elapsed times, to examine the progression of geometrical changes to the original profile and the burrows following the increase in water level (Figure 3.9). The time elapsed is normalized with respect to the levee failure time (t_f). The rod location is indicated in dark color to allow for tracking the movement of the burrows during levee settlement. Figure 3.9a depicts the changes in the levee cross-section following the rod set removal and right before elevating the water level. Evidently, the levee geometry is essentially unchanged and the traced burrow geometry remains in line with the rod set location. When the water level reached about 25% of the levee height (at $t/t_f \cong 0.79$), downward movement of both the crest and the burrows is observed (Figure 3.9b). At t/t_f of about 0.87, where the water level stand right below the burrow, levee settlement increased and became slightly non-uniform with more settlement near the waterside (Figure 3.9c). When the burrows became fully inundated ($t/t_f \cong 0.97$), additional deformation was observed and the cylindrical shape of the burrow experienced a substantial distortion, creating non-uniform diameter as illustrated in Figure 3.9d.

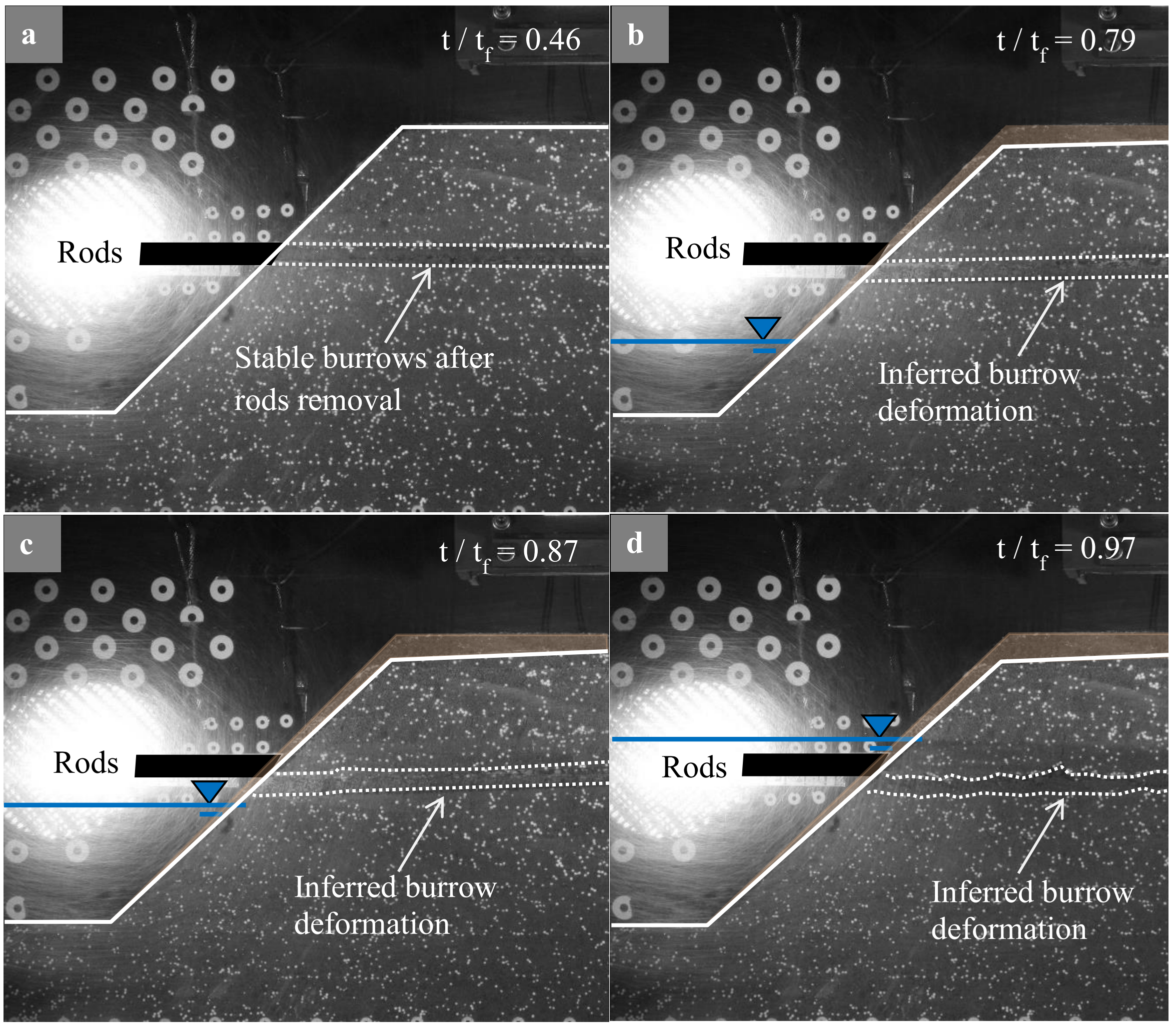

Figure 3.9. Observed crest settlement and traced deformation of burrows: a) immediately after rod removal; b) water flow reaches level of burrows; c) upstream water filled burrows; d) water level higher than burrows elevation

3.5.2 Hydraulic performance and progressive failure

The pore pressure readings taken at the three PPT locations (1, 2, and 3) during the experiments allowed for close investigation of the hydraulic performance of the levee. It is imperative to note that the previously described settlement and the associated changes in levee geometry may result in slight changes in the elevations of the installed PPT. This could subsequently lead to some variation in pore pressure readings. In order to consider this settlement effect, the total head (h_t) has been modified based on the elevation of the PPT after settlement (z_{mod}), rather than the raw pore pressure readings. The modified values are estimated as follow:

$$z_{mod} = z_o - \Delta_z \tag{3.1}$$

$$h_t = z_{mod} + h_p \tag{3.2}$$

Where:

z_o is initial height of the PPT above the datum (levee base);

Δ_z is settlement at the PPT location (linearly interpolated); and

h_p is the pressure head (obtained by dividing the pore pressure reading by the unit weight of water (γ_w).

The hydraulic gradient near the exit points was calculated based on the modified head by dividing the difference in total head (h_t) by the distance between the two PPTs. Figure 3.10 shows the changes in hydraulic gradient at the three preselected locations 1, 2 and 3 for both the intact and deteriorated levee. Based on this arbitrary definition, the hydraulic gradient is found to be notably higher for the deteriorated levee compared to the intact case. This was globally observed with an increasing trend towards the exit slope near the toe drain.

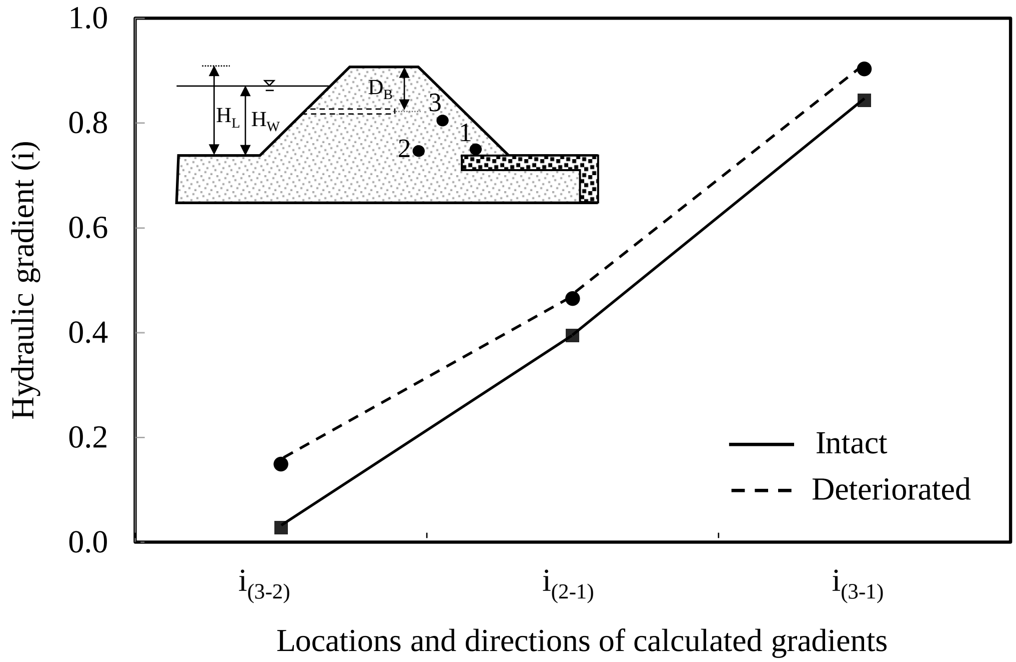

Figure 3.10. Estimated hydraulic gradients near the exit locations

The traced phreatic surfaces for the intact levee is depicted in Figure 3.11 at the maximum retained water level. The phreatic surface appears to follow the theoretical pattern with an uninterrupted path ending at the toe drain. The slightly darker shades in Figure 3.11 indicate the wet soil mass below the phreatic line. This is not; however, the case for the deteriorated levee as the presence of the water-filled cavities appreciably altered the seepage path.

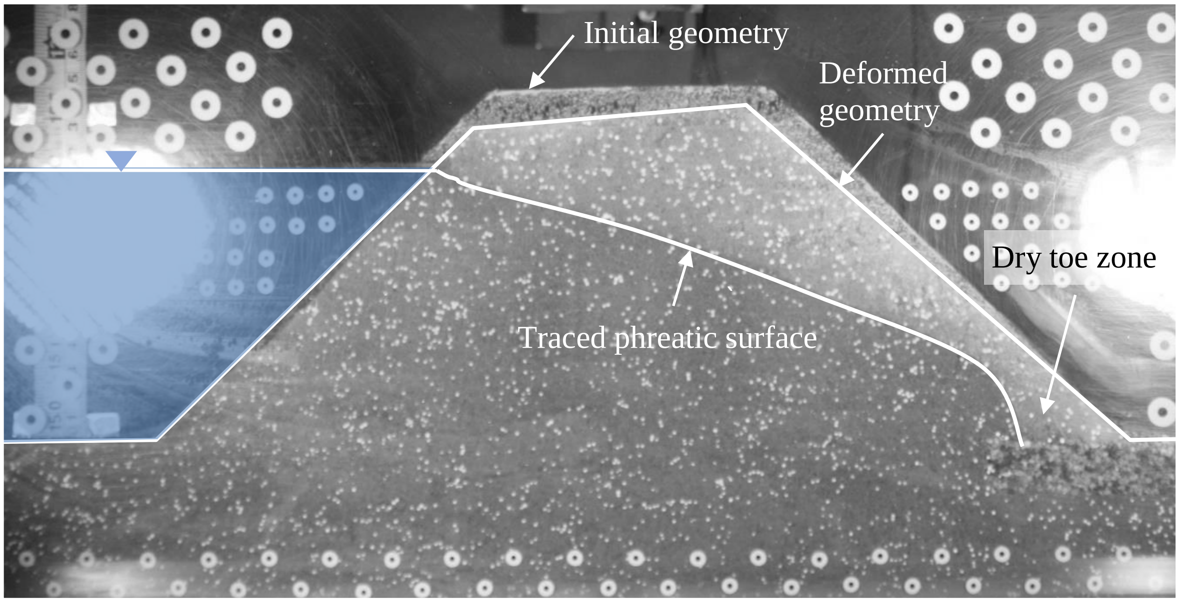

Figure 3.11. Observed seepage through the intact levee structure and the inferred phreatic surface

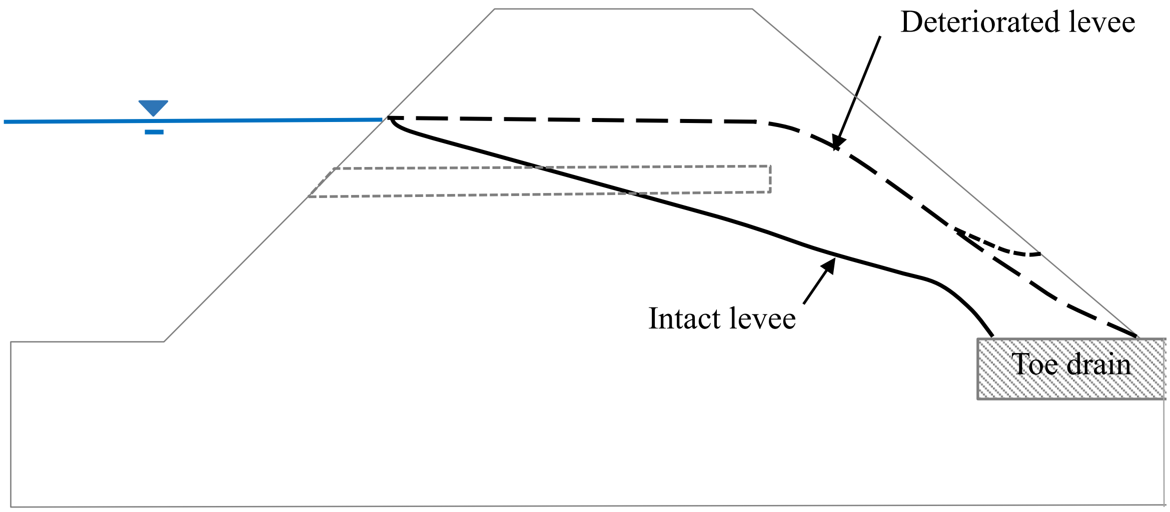

Figure 3.12. Conceptual comparison between traced phreatic surfaces for intact and deteriorated levees

The phreatic surfaces for both cases are conceptually illustrated in Figure 3.12. For the deteriorated levee, the phreatic surface became essentially horizontal along the burrow length and intersected with the landside slope. In this case, the phreatic surface further advances horizontally leaving a larger wet area above the toe drain with the water flow exiting through the slope. Piping was observed during the experiment immediately before slope failure.

Figure 3.13 shows the local and global failure mechanisms developing in a deteriorated levee for t/t_f ranging from 0.98 to 1.0. The inferred phreatic surface is overlaid on the profile of the deteriorated levee as schematically shown in Figure 3.13a. The noted changes to the default hydraulic response progressively lead to soil piping within the wet zone located above the toe drain, which results in local toe failure as shown in Figure 3.13b ($t/t_f \approx 0.99$). As illustrated in Figure 3.13c immediately following the toe failure and with further water seepage and soil erosion, a sudden global failure was developed ($t/t_f \approx 1$). The near circular slope failure started from the levee crest and ended at the toe with a large soil mass moving along with the seeping water towards the landside.

3.6 Summary and conclusions

The hydraulic performance and failure mechanism of a deteriorated levee impacted by animal burrows have been experimentally investigated in this study. Centrifuge tests were conducted on instrumented intact and deteriorated levee models. Crest settlement as well as the changes in pore pressures were measured during the experiment. Idealized cylindrical burrows were created on the waterside of the levee and extended to about 75% of the levee width (at the burrow location). Results confirmed that the presence of cylindrical cavities has a significant

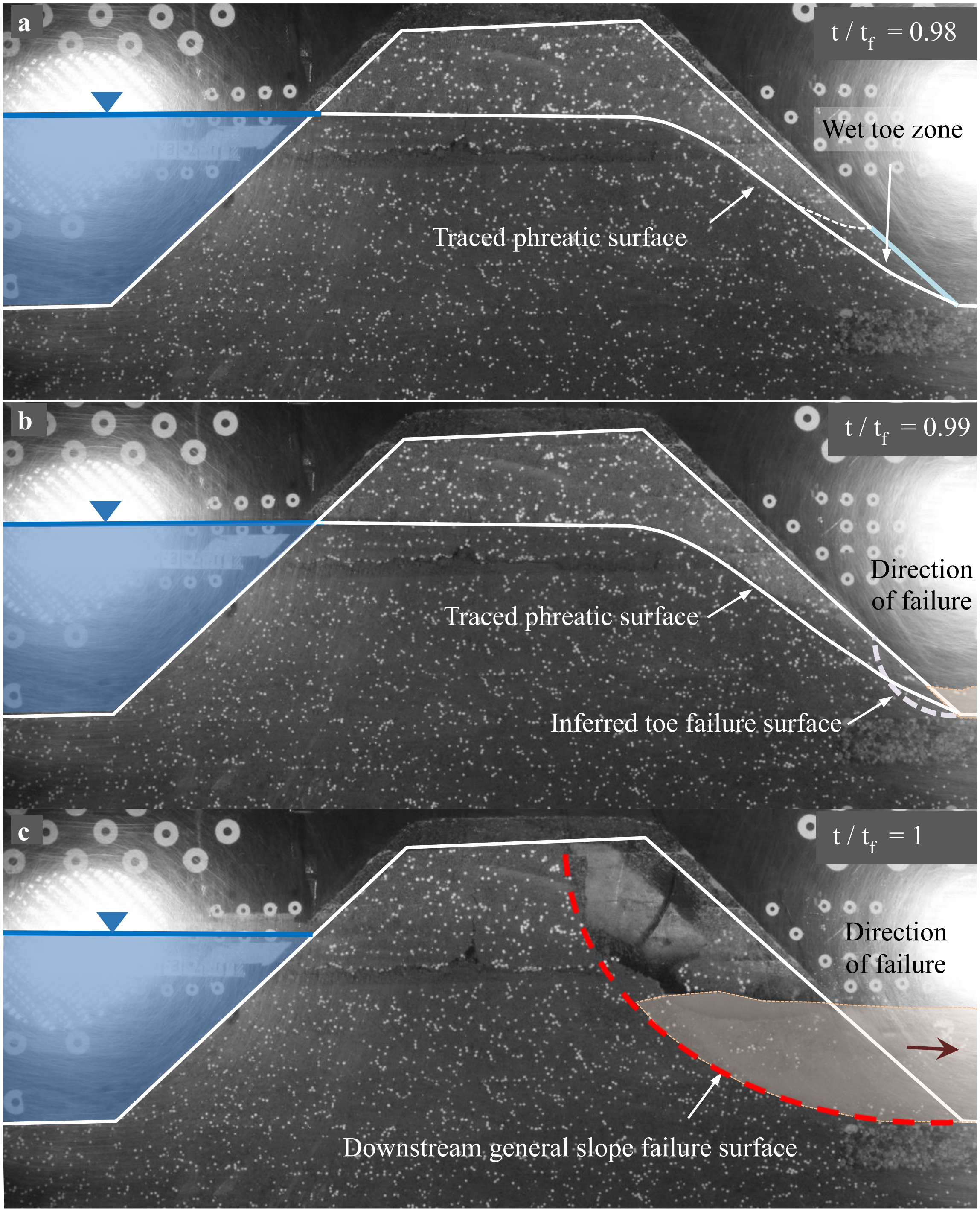

Figure 3.13. Progressive failure of levee with induced midnight burrows: a) initially stable slope; b) slope failure at the toe of the levee; c) extension of the local toe failure to a global slope failure

impact on the seepage pattern and as importantly on the overall stability of the levee. It has been demonstrated that cylindrical burrows can remain stable even when they are filled with water and this alters the phreatic surface leading to an appreciable increase in hydraulic gradient above the levee toe. These changes were found to cause local slope failure at the toe of the slope. The progressive development of global failure was found to occur abruptly after the local failure- resulting in water inundating landside. These findings could explain the unexpected and occasionally imminent failures of existing levees deteriorated by wildlife activities [3].

It should be noted that the complexity of real animal cavities does not warrant accurate duplication of burrow configuration that unarguably challenge any plausible optimization modeling scheme. Therefore, the results reported in this study reflect the behavior of the chosen levee geometry and soil type. Further investigation is, therefore, needed to study the response of earth structures with different side slopes and material types to other burrow configurations.

4 SYNTHESIS OF WILDLIFE-TRIGGERED FAILURES IN EARTH LEVEES

4.1 Preface

Chapter three details the experimental part of this research. It discusses the centrifuge models and the developed burrow simulation mechanism. The chapter also presents and analyzes the results of two centrifuge experiments: (1) intact levee model and (2) a levee with waterside burrows, including the failure mechanism. These results illustrate destructive impact that animal burrows have on earthen levees. In order to more comprehensively elucidate the nature of relationships between animal burrows and earthen levee collapses. Chapter four compares the distinct embankment failure mechanisms for each burrow attack side, i.e. waterside or landside. Building on Chapter three, the fourth chapter presents and analyzes the results of the final centrifuge experiment conducted on: (3) a levee with landside burrows. The fundamentally different failure mechanisms resulting from waterside vs. landside burrow attacks are subsequently outlined and discussed. Chapter four additionally presents levee deformation patterns calculated and depicted using the particle image velocimetry (PIV). Presentation of further numerical analysis of the results of the centrifuge experiments together with the finite element model used in the analysis conclude chapter four.

4.2 Introduction

The damage to earthen structures caused by invasive wildlife activities is observed worldwide. Such natural exploits are often associated with economic losses in infrastructures and adjacent properties. Animal burrows have been known to negatively influence the hydraulic performance of earth dams and in severe cases could potentially lead to a complete loss of their structural integrity. Failures and losses related to animal activities in earth structures are discussed in further detail by Bayoumi and Meguid [3]. These damages caused by nuisance activities could remain concealed for a long time until the safety of an earth structure is massively jeopardized [46].

Breaches of earth dams are typically driven by a variety of actions including excessive forces from the retained water (floods), low strength materials, or seismic activities. The consequences of wildlife activities in levees can be categorized into structural damage, surface erosion, and hydraulic alterations [6]. These adverse outcomes are often related. Changes to hydraulic performance is one of the most common causes of failure in earthen structures, which typically lead to internal erosion and piping [45]. While internal erosion naturally occurs in solid earth structures, the hostility of the consequences is exacerbated in the presence of cracks or cavities within the soil mass.

Controlling seepage through earth dams and levees is an important design requirement to prevent excessive uplift pressures, piping and erosion of material through losses into cracks, joints, and cavities ([61]; [62]; [63]; [64]). Extensive research has been done on intact earth structures to study the mechanisms of piping ([47]; [48]; [33]; [49]), erosion ([50]; [51]; [52]), and overtopping ([23]; [53]). A significant amount of the literature in the area of wildlife investigates the ecological impact of animal activities and habitat [3]. However, studies related to the synthesis of failure mechanisms of earth structures due to invasive wildlife activities are very scarce in the literature. Visual inspection of wildlife damage in earth structures might leave an average observer with the false impression that they are meant to be erratic and random. The convoluted nature of these burrow systems in earth dikes and dams hides ingenious engineering that could go beyond comprehension. This probably stands behind the limited effort in studying the underlying mechanics of deterioration and their impact on performance. Wildlife develops numerous strategies and techniques in attacking earth structures. Species dwelling in these structures typically have a strong preference either by intruding from the waterside or landside, occasionally both sides [3]. Equally important, predation and other ecological characteristics of wildlife have a significant impact on the location and geometry of burrow systems.

4.3 Scope

This research investigates the impact of location and elevation of animal burrows on the behavior of earth levees. Understanding of the failure mechanism of damaged earth structures - even at an abstract level - is thus pivotal for sound post-failure analysis and potentially adequate design. In doing so, equidistant horizontal cylindrical array of burrows is introduced at different elevations within a centrifuge levee model. This arbitrary damage configuration is supported by the dominance of near horizontal animal burrows in earth structures [20]. Both waterside and landside attacks are closely examined by monitoring the surface movement, global deformation, and changes in pore pressure distribution due to the introduction of these cylindrical-shaped burrows.

Description of the physical model, summary of the methodology used to introduce animal burrows within the model, and details of the performed centrifuge testing are presented herewith. The test results of an instrumented intact levee model, including surface displacements and pore pressures, are summarized, and compared with those measured for deteriorated levee cases. The effects of the configuration of animal burrows on the hydraulic performance and stability of levees are accordingly discussed. Three-dimensional finite element analyses are utilized to support the hypothesized reasons for the alternations to phreatic surface and the failure mechanisms of the deteriorated levees.

4.4 Experimental program

Hori et al. [56] successfully used the Kasama soil (silty sand) for centrifuge modeling of earth dams (Table 4.1). Its weak cohesive nature has bestowed favorable conditions for wildlife invasive activities. The low-to-medium plasticity offers wildlife a reasonable balance between stability of cavities and relative ease in digging. A side slope of 1H: 1V seems to warrant initial stability of the levee model and simultaneously - from experimental feasibility standpoint - provides an ample chance of failure in the case of deteriorated levee [65]. While relatively steep slope is uncommon for engineered earth dams, this configuration allows for viably investigating both serviceability (prior to failure) and ultimate limit states. A line of horizontal equispaced cylindrical burrows was introduced at different elevations within the levee section. Each test case has one set of burrows at the same elevation on either the waterside (WB) or landside (LB) of the model (Figure 4.1a). Centrifuge modeling enables close examination of the animal burrows' effect on the stability and hydraulic performance of the levee section in a controlled environment. For benchmarking, an intact levee section was tested in a similar fashion. The details of the experimental program reported by Saghaee et al. [65] are summarized below.

4.4.1 Setup and burrow configuration

A 1:35 scaled-down section was built to model a 5-m high levee with a 4-m crest width and 1H: 1V side slopes. The Kasama soil was compacted in the centrifuge box to a moisture content of approximately 30% in nine 25-mm thick lifts to the desired height. In order to eliminate the risk of disturbance, the levee section was shaped carefully and incrementally by removing the soil (excavation) to shape the predefined levee model (Figure 4.1a). Thin-wired 100-psi pore pressure transducers (PPT - Model GE Druck PDCR 81-347) were placed during the construction stage at preselected locations along the centerline of the model to monitor pore pressure changes during the test (Figure 4.1a). The use of sufficiently long PPT wires minimized the impact of interference on the measured deformations. The wires were monitored for unusual tension or movement during the experiments.

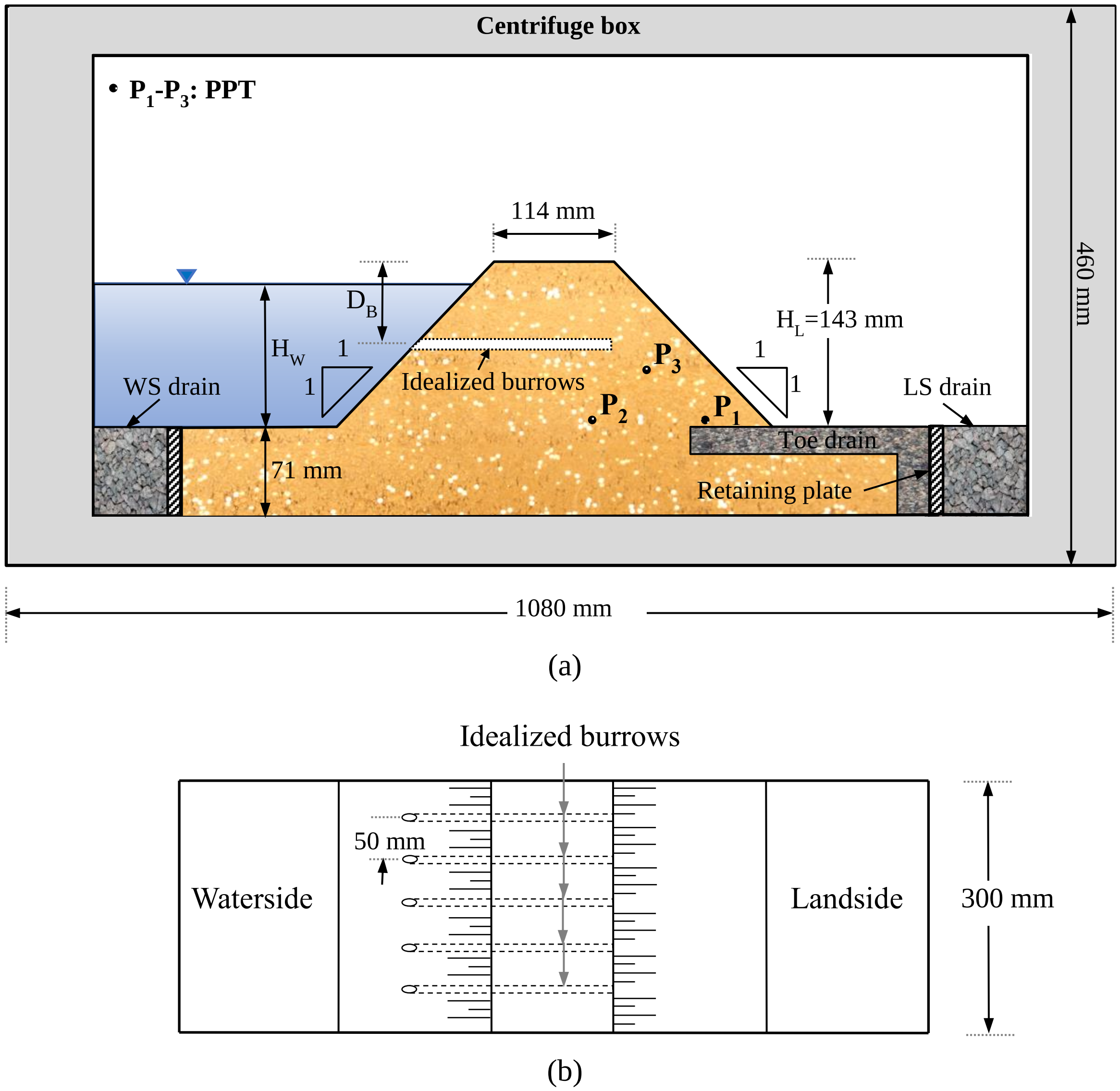

Figure 4.1. Model configurations: a) geometry and location of pore pressure transducers (P_1 through P_3); b) plan view of the model with waterside burrows [65]

Table 4.1.Characteristics of the Kasama Soil

Property	Values
G_s	2.67
Moisture content (%)	30
LL	59
PL	33.2
$\gamma_{d\,(max)}$ (kN/m^3)	13.8
OMC (%)	27.5
γ_{sat} (kN/m^3)	16.8
γ_{unsat} (kN/m^3)	14.1
ϕ' (^{o})	32^o
c′ (kPa)	5.9
k (m/s)	3.8 x10^{-5}

Animal burrows were modeled as cylindrical cavities using six stainless steel rods of 8.5 mm diameter, spaced at 50 mm apart (Figure 4.1b). At 35g-acceleration level, a customized pullout system gradually extracted the pre-installed rods during the centrifuge flight. This method has successfully introduced burrows at mid-height and three quarter of the levee height, D_B/H_L of 0.5 and 0.75, respectively. The model embankment (143 mm height and 400 mm width) experienced gradual spinning towards the targeted centrifugal acceleration (35g). The centrifuge box containing the model was equipped with a transparent face to allow for visual monitoring of the deformations during testing (Figure 4.2). The levee construction procedure and further modeling details are provided by Saghaee et al. [66, 67].

The foregoing configuration arbitrarily mimics site conditions whereby clustered animals (high population) exercise invasive activities. The burrow length and diameter are inspired by the typical activities of large digging carnivores. For example, the American badger is known to dig slightly elliptical openings averaging 20 to 30 cm in diameter and extend horizontally up to 9 meters into the ground [3]. Accurate modeling of real burrow network can be tedious and time-consuming; therefore, a row of cavities is deemed to warrant qualitative representativeness of sufficient damage that would eventually lead to failure. It is, therefore, important to realize that the study seeks understanding of seepage patterns and failure mechanism of deteriorated earth structures rather at the conceptual level.

4.4.2 **Material characterization**

The Kasama Soil was characterized for model construction and numerical simulation. This includes index tests, particle size distribution, standard proctor, shear strength and hydraulic conductivity tests. Figure 4.3a depicts the gradation curve for the Kasama Soil. The material is classified as silty sand (SM) in accordance with the USCS. Constant head permeability tests suggested a coefficient of hydraulic conductivity of approximately 3.8 x 10^{-5} m/s. The levee model was constructed inside the centrifuge box using the compaction and excavation technique. This method involves two steps: (1) placement and compaction of the soil in equal thickness lifts (layers) up to the desired height and (2) removal of the soil (excavation) in order to shape the levee cross section. This levee construction procedure was strictly followed for both the intact and deteriorated levee models. Saghaee et al. [65] discussed in further detail the compaction test in relation to the construction of the model. Drained strength and stiffness of the soil used to build the levee model were evaluated for consolidated-drained triaxial tests at three confining pressures: 50, 150, and 200 kPa (Figure 4.3b). Soil specimens were prepared in a mold and tamped in four layers following a procedure similar to that used to build the levee. The average moisture content of the prepared specimens was found to be approximately 30%, which is comparable to that of the levee model before raising the water level. The soil properties and parameters are summarized in Table 4.1.

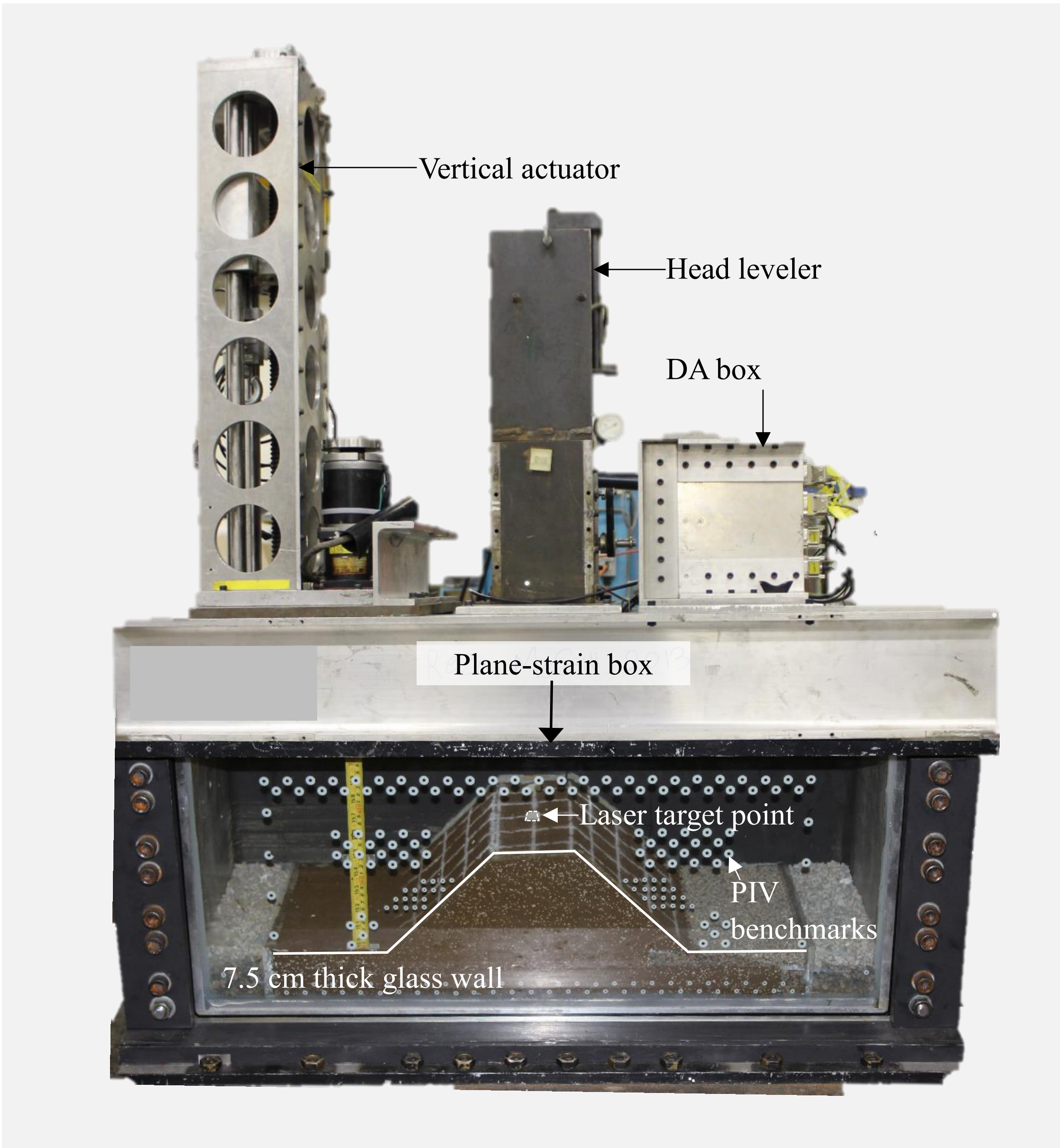

Figure 4.2. Test setup installed on the plain strain centrifuge box

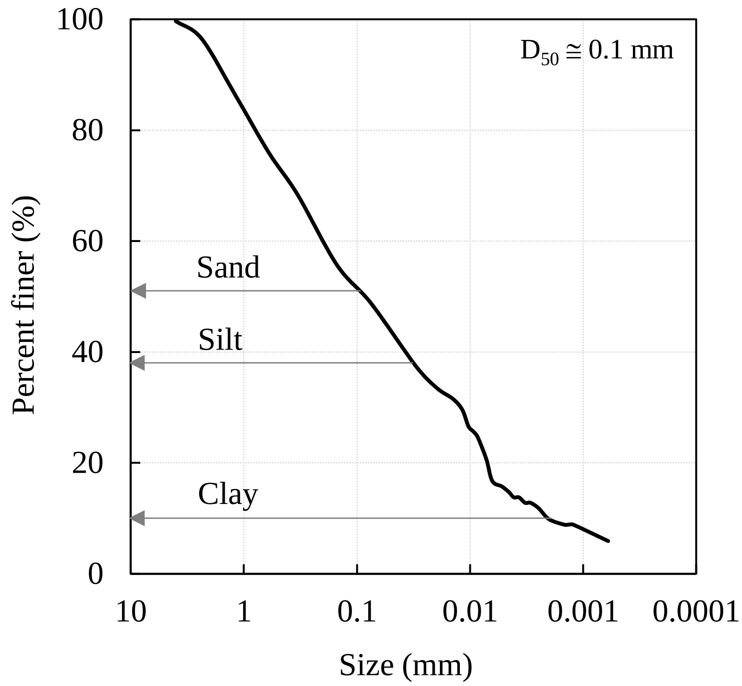

(a)

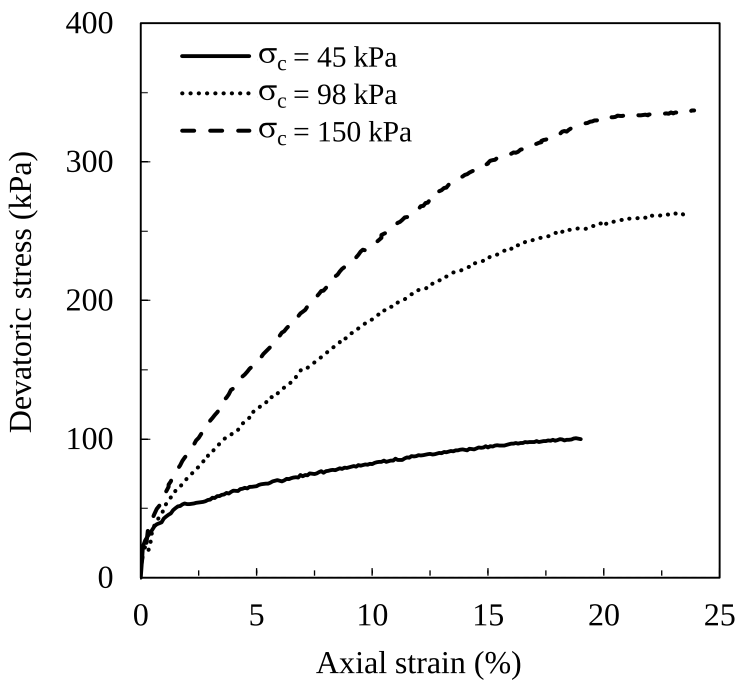

(b)

Figure 4.3. Kasama soil characterization: a) particle size distribution; b) triaxial consolidated-drained stress-strain curves for confining pressure (σ_c) of 45, 98, and 150 kPa

4.4.3 **Testing procedure**

The centrifuge testing started by spinning up the model to an initial acceleration of 10g. A payload (including the setup and the model) of about 800 kg reached the targeted centrifuge acceleration (35g) at an angular speed of 78 rpm. The overall performance of the model appeared to be adequate with the monitoring instruments functional at this acceleration level. The maximum error associated with stress non-linearity (approximately 0.7%) falls within acceptable limits [34]. Gradual pullout of rods commenced at a rate of 0.33 mm/sec immediately upon reaching the maximum acceleration. The negligible settlement observed at the crest during the pullout is indicative of repeatability of cavity introduction and initial conditions. Following rod removal from the levee body, the water level on the waterside was gradually raised at elapsed time of 4,000 second using a dedicated water pump. The process of increasing the water level lasted for about 200 seconds allowing for steady-state conditions (constant PPT readings) to be reached for each 20 mm increment. The water was then maintained at a target level (H_w) using onboard head leveler and subsequently monitored using a PPT installed within the main drain.

4.4.4 **Monitoring scheme**

Digital photography captured numerous images of soil deformations. Three high-resolution digital cameras (10.0 MP, 6x optical zoom) were affixed outside the centrifuge box to monitor the planar soil deformation through the transparent wall. Two cameras closely monitored waterside and landside slopes and the central camera covered the whole levee model including the foundation. The progression of geometrical changes of the cross section was snapshotted at 5-second intervals. A HD camcorder continuously monitors the profile of the model. Additionally, two laser LVDTs were used for measuring the crest settlement along the centerline of the model. High resolution still imaging during the centrifuge flights allowed for post processing of deformations using Particle Image Velocimetry (PIV) analysis [68]. A thin soil layer near the transparent wall was mixed with 5% styrofoam beads 1 mm in diameter to texturize the soil and allow for the deformation to be accurately measured.

4.5 Observations

The study investigated the impact of the burrow configuration (attack side and elevation) on the performance of the modeled levee. The following observations are used to envisage the nature of failure in deteriorated levees. The deformation, hydraulic performance and failure progress of the deteriorated models are separately discussed.

4.5.1 Deformation field

The measured crest settlement for both deteriorated models (WB and LB) are depicted against that of the intact model in Figure 4.4. All cases generally experience a gradual increase in crest settlement up to approximately 2 mm prior to elevating the water level (at t = 4,000 s). An abrupt increase in the crest settlement is noted shortly after the water level was raised. The deteriorated models exhibit a distinctive failure response commencing at elapsed time of about 6,000 s (Figure 4.4). The WB and LB models experienced excessive and abrupt settlement followed by rapid failure at elapsed times of approximately 6,500 s and 7,700 s, respectively. Comparatively, the crest settlement measured for the intact levee, however, plateaued at about 9 mm and showed no signs of distress up to the end of the experiment.

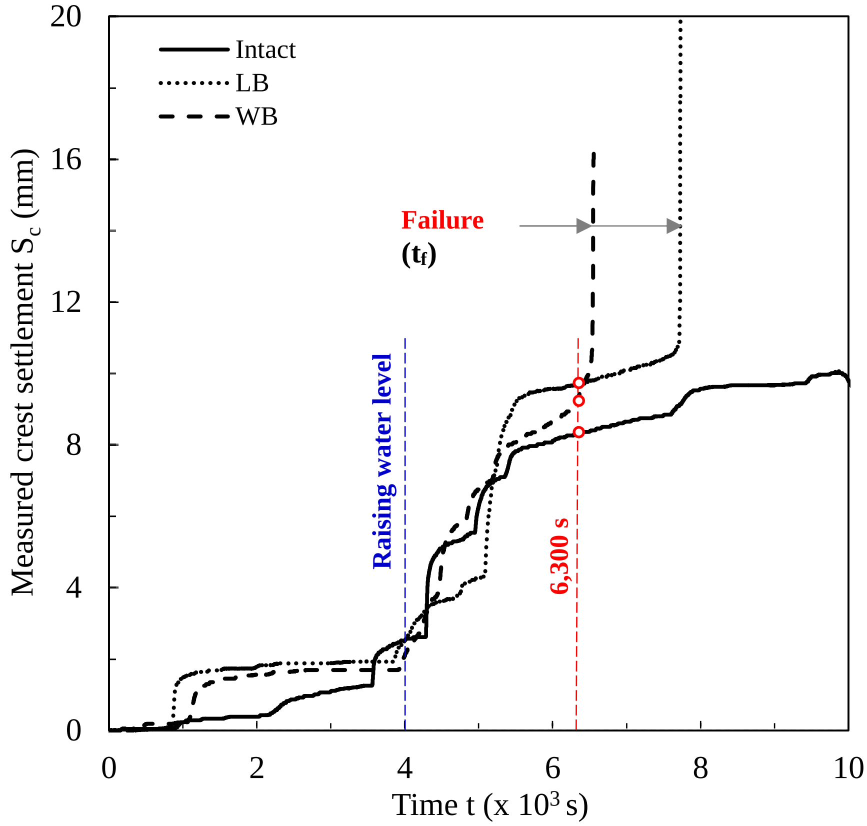

Figure 4.4. Measured changes in crest settlement with the increase in water level for Intact levee, levee with landside burrow (LB) and levee with waterside burrow (WB)

Contours of the vertical and horizontal deformations for all cases are post-processed using PIV analysis during raising the water level (from t = 4,000 s to t ≅ 6,300 s). The cumulative vertical and horizontal displacements from PIV analysis are illustrated in Figure 4.5, respectively. Positive vertical and horizontal displacements indicate downward and lateral movements toward landside, respectively. As expected, the maximum vertical and horizontal deformations of intact levee cross section are smaller than those of the deteriorated models (Figure 4.5b and 5c). Whilst similarity is apparent, the contours of the vertical displacements

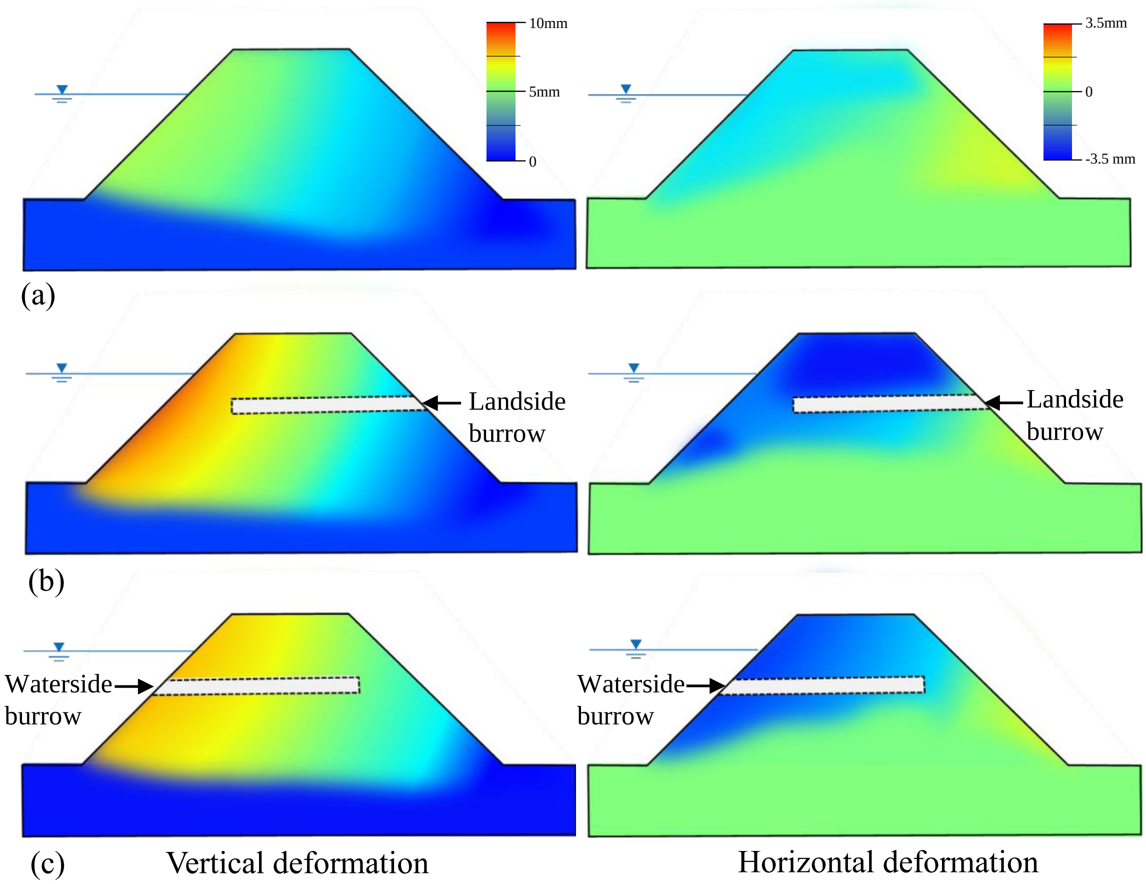

Figure 4.5. Contour plot of cumulative deformation due to rising water level from timestamp t ≅ 4,000 s to t ≅ 6,300 s for: a) intact; b) landside attack (LB); c) waterside attack (WB); (Positive direction is downward and toward landside)

(subsidence) for the WB model suggest higher settlement than the LB model. This is in line with the trends of crest settlement observed within the same time interval (Figure 4.4). The LB model exhibited larger vertical deformations at the closed end (Figure 4.5b). Horizontal deformations of the intact model are rather insignificant with an average hovering around zero displacement. The top of the foundation of the deteriorated models demonstrated moderate to high vertical settlements on the order of 4 to 8 mm increasing toward the waterside toe. This deformation pattern stands behind the noted tilt of the model toward the waterside.

The horizontal deformation contours for WB and LB models are similar – with larger horizontal deformations around the waterside slope. Based on the observed contours, the average horizontal displacements for the deteriorated models are around 40% of their vertical displacements. Considering the modeling scale at 35g, vertical and horizontal displacements of a full-size levee section could be approximately 25 cm and 10 cm, respectively.

4.5.2 **Hydraulic response**

Pore pressure readings obtained during the experiment allowed for gauging the hydraulic response of the model. As depicted in Figure 4.1a, the PPTs measured pore pressures at three locations within the landside toe: P_1, P_2 and P_3. It is worth noting that the previously described levee deformations might result in slight changes in the elevations of the installed PPTs. The total head (h_t) was accordingly calculated based on the corrected elevation of the PPT after settlement (z_{cor}) as follows:

where:

$$z_{mod} = z_o - \Delta_z \qquad 4.1$$

$$h_t = z_{mod} + h_p \qquad 4.2$$

z_o: the initial height of the PPT above the datum (levee base);

Δ_z: the corresponding settlement (linearly interpolated); and

h_p: the pressure head

Figure 4.6 illustrates the impact of attack side on the hydraulic gradient (i) for the intact, LB and WB models. The figure shows the gradients for the deteriorated models with burrows at their mid-height. The hydraulic gradient near the exit toe was calculated as the quotient of the total head difference and the distance between the respective PPTs. Compared with the intact case, the hydraulic gradient is found to be higher for the deteriorated models with an increasing trend towards the landside toe drain. The hydraulic gradient of WB case was greater than that of the LB case. It should be noted that although these gradients could be different from local gradients, they are yet indicative of the burrow configuration effect on hydraulic response.

Figure 4.7 depicts the traced (approximate) phreatic surfaces for the three cases overlain on high-resolution still images. The slightly darker shades indicate the wet soil (below the phreatic surface), whilst the light shade represent the partially-saturated and drier regions (above the phreatic surface). The intact model exhibits the classical steady-state flow of water with the phreatic surface between the maximum retained water level (waterside) and ending at the toe drain (Figure 4.7a). This is not the case for the deteriorated levees as the presence of the cavities alters the classical seepage path (Figure 4.7b and 7c). For the LB model, the water seeped through the waterside slope and favorably collected in the burrows. The phreatic surface was parallel to the burrows within the levee prior to running parallel to the landside slope towards the landside toe (Figure 4.7b). In the case of WB, the burrows allowed direct access for water with minimal head loss along their length. The preferential near horizontal flow path created early in the seepage process resulted in raising the phreatic surface, which eventually exited near the toe of the model (Figure 4.7c). Compared with the LB case, the higher profile of the phreatic surface for the WB model explains the higher measured exit gradients (Figure 4.6).

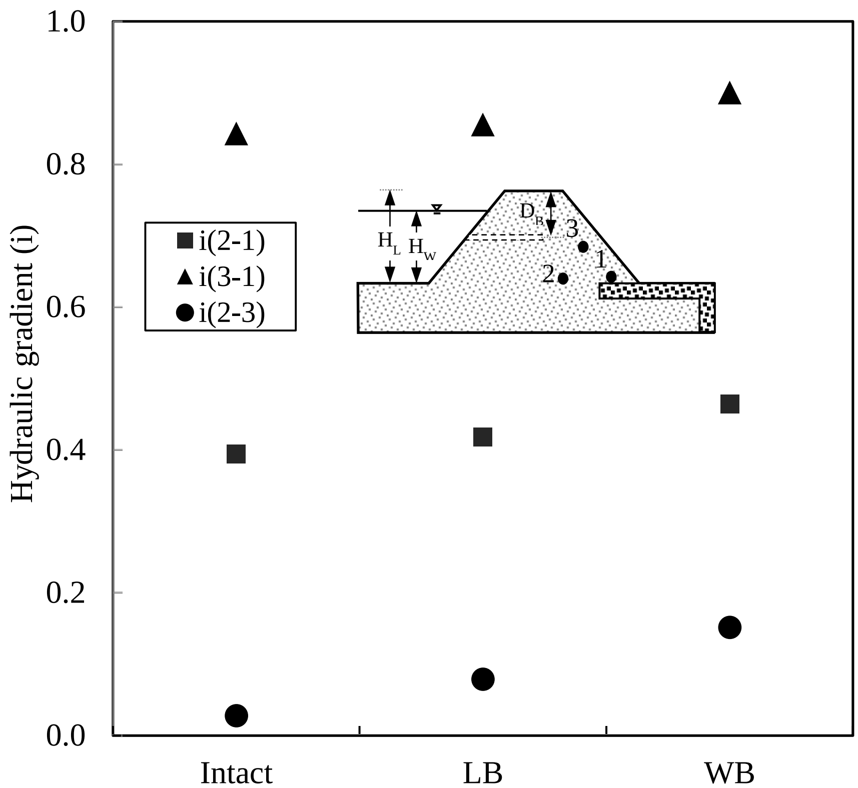

Figure 4.6. Hydraulic gradients near the exit for the deteriorated models with burrows at the mid height versus intact model

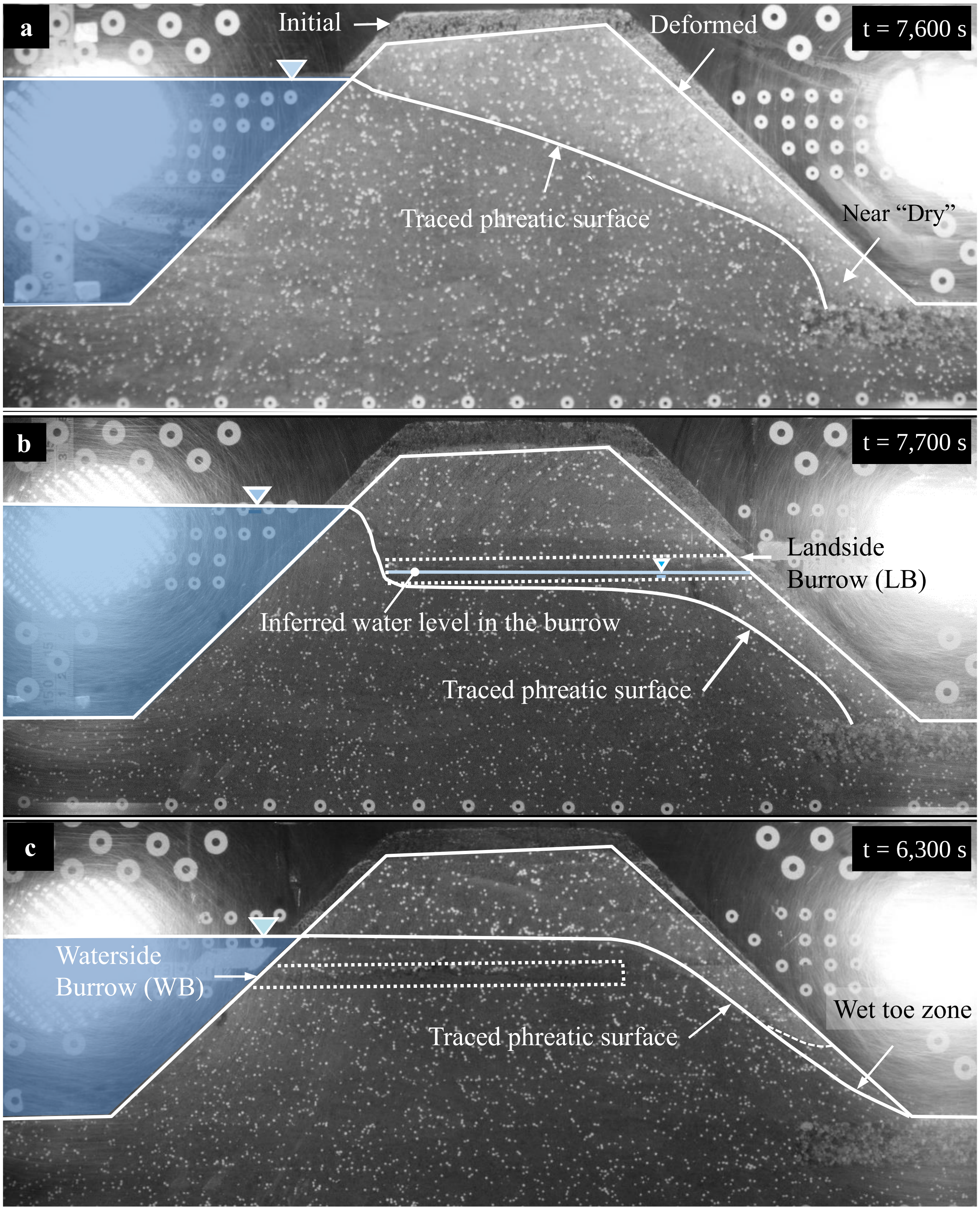

Figure 4.7. Inferred phreatic surface for the levee models: a) intact; b) LB (prior to failure); c) WB (prior to failure)

Subject to the dominating wildlife species at the levee location, attacks from the waterside could target lower elevations. Thus, a line of burrows at the bottom quarter (D_B/H_L = 0.75) of the model's height was introduced. Figure 4.8 depicts the effect of the burrow elevation on the hydraulic performance of the deteriorated levee. The normalized hydraulic gradient was used for this purpose. The measured gradient (i) is divided by H_W/H_L in order to relate head loss to water levels on the waterside. The low-elevation burrows (D_B/H_L = 0.75) yielded a hydraulic gradient of about twice that of the mid height burrows (D_B/H_L = 0.5) (Figure 4.8). Similar to the raw hydraulic gradient, the normalized gradient provides a somewhat qualitative measure of the hydraulic performance for deteriorated levees.

4.5.3 **Failure progress**

Still imaging of the models taken during the centrifuge flights was used to conceptualize the progress of failure. The investigated LB and WB cases show distinctive failure mechanisms despite their abrupt nature. The following summarizes the key observations for both models. The key characteristics and signs of failure of the levee model with landside burrows (LB) are captured in selected images from time stamp (TS = t/t_f) of 0.431 to 1.0 (Figure 4.9). The first visible landside crack appeared at a TS of 0.833 and laterally propagates as isolated distresses near the apex of burrows as shown in Figure 4.9b. Interconnectivity of cracks on the landside was spotted at a TS of 0.847 (Figure 4.9c). Sliding and separation of the bottom half of the landside slope seem to commence at a TS of 0.880 (Figure 4.9d). Further deepening of the cracks eventually has led to complete loss of structural integrity at a TS of 1.0 (Figure 4.9f).

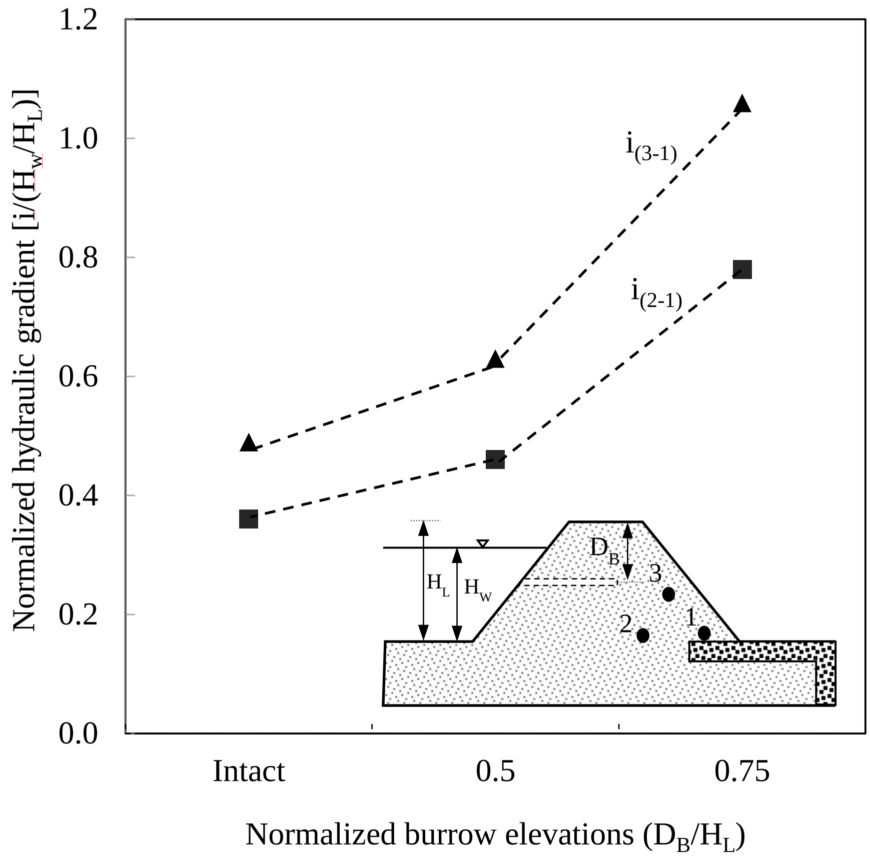

Figure 4.8. Effect of burrow depth on the hydraulic gradient near the exit for waterside burrows (WB) at H_w = 94 mm

Until a TS of 0.9963 the waterside burrows (WB) model showed no signs of through-seepage (Figure 4.10a). The rapid distress signs are subsequently captured in selected images from a TS of 0.9989 to 1.0 (Figure 4.10b thru f). The first appearance of seepage and washing of landside toe commence at TS of 0.9989 (Figure 4.10b). Subsequent deep horizontal cracks in landside slope (Figure 4.10c and d) propagate swiftly in a toppling mode (Figure 4.10e) until complete failure. At this stage, half of the landside section is almost washed instantly as illustrated in Figure 4.10f.

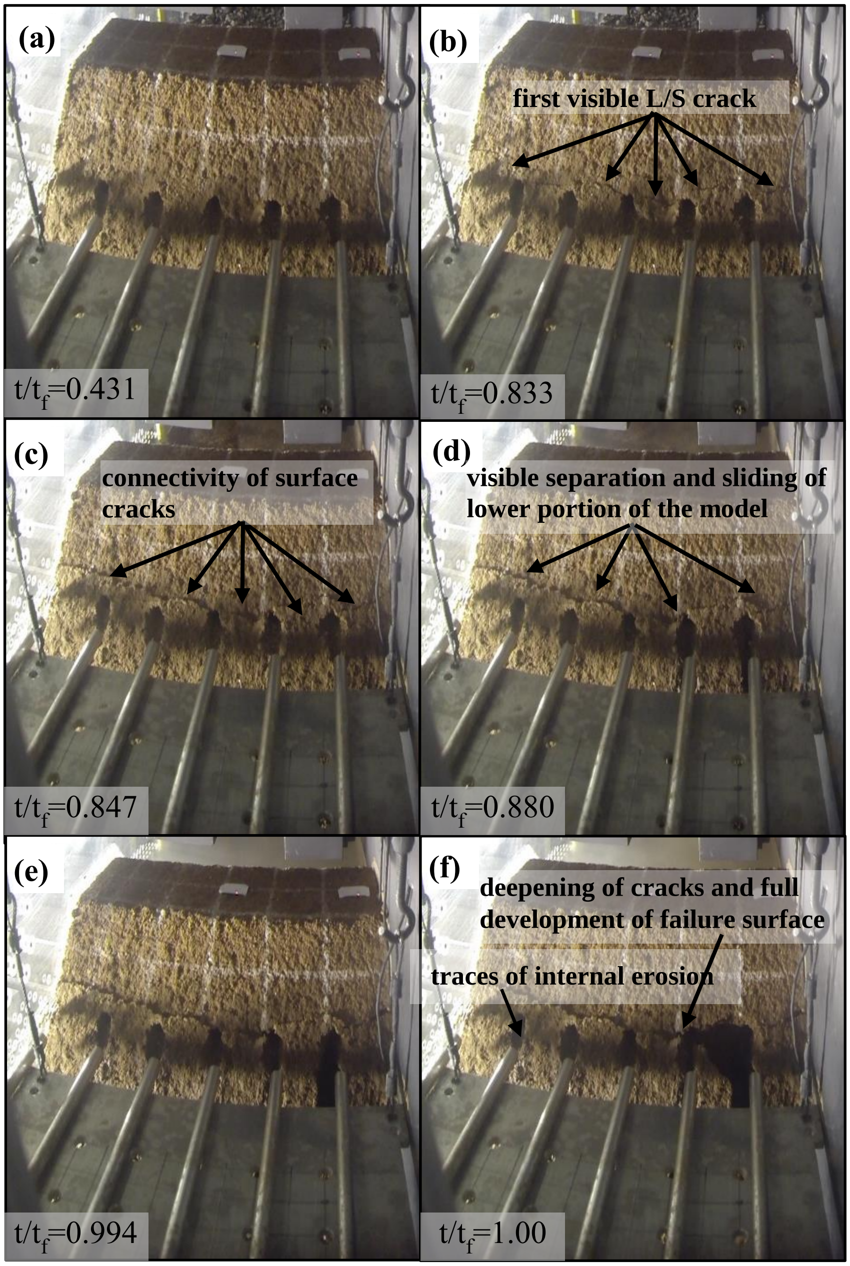

Figure 4.9. Failure of levee with landside burrows (LB) [t_f = time to failure]

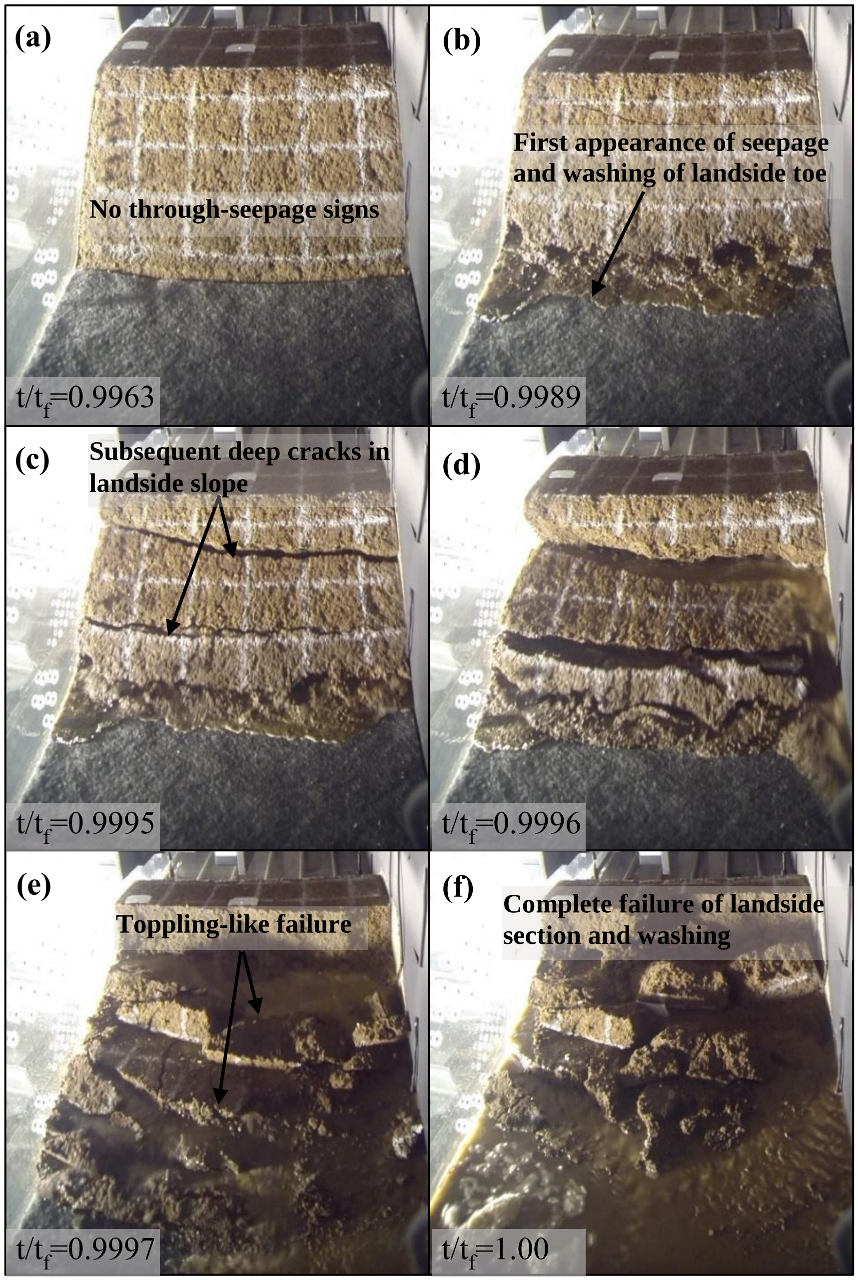

Figure 4.10. Failure of levee with waterside burrows (WB) [t_f = time to failure]

4.6 Numerical analyses

4.6.1 Model description

Three-dimensional finite element analysis was performed using Plaxis 3D software [69] to further support the visual observations of the physical model. This was of a particular importance given the distribution and shape of the burrows within the body of the model as well as the possible scale effects in the centrifuge model. A full-scale numerical model that captures the geometric features of the levee and the created burrows was developed. The conducted seepage analysis assumes a homogenous isotropic material under steady-state conditions. The stress and stability analyses were performed using the Mohr-Coulomb failure criterion. Utilizing geometrical symmetry, only one-half of the embankment was modeled to reduce the mesh size and the computation time needed for the analysis. The FE model dimensions, mesh and hydraulic boundary conditions are shown in Figure 4.11. To reduce the computational complexity of the 3D model, animal burrows were modeled as a highly permeable soil ($k = 100$ m/s) with negligible stiffness as compared to the surrounding soil. This was achieved by changing the properties of the levee material contained within the burrow geometries such that the new material would have insignificant resistance to deformation and water flow. This modeling approach eliminated numerical singularities that might have arisen if voids were to be explicitly modeled. It also enabled identical meshing for intact and deteriorated models. Quadratic tetrahedral 10-node elements allowed for the curvilinear modeling of the cylindrical cavities using a refined mesh around the burrows. The average element size of the mesh is 0.45 m with elements on the order of 0.15 m in the refined area in the vicinity of the burrows. Table 4.1 summarizes the properties and parameters used in the analyses.

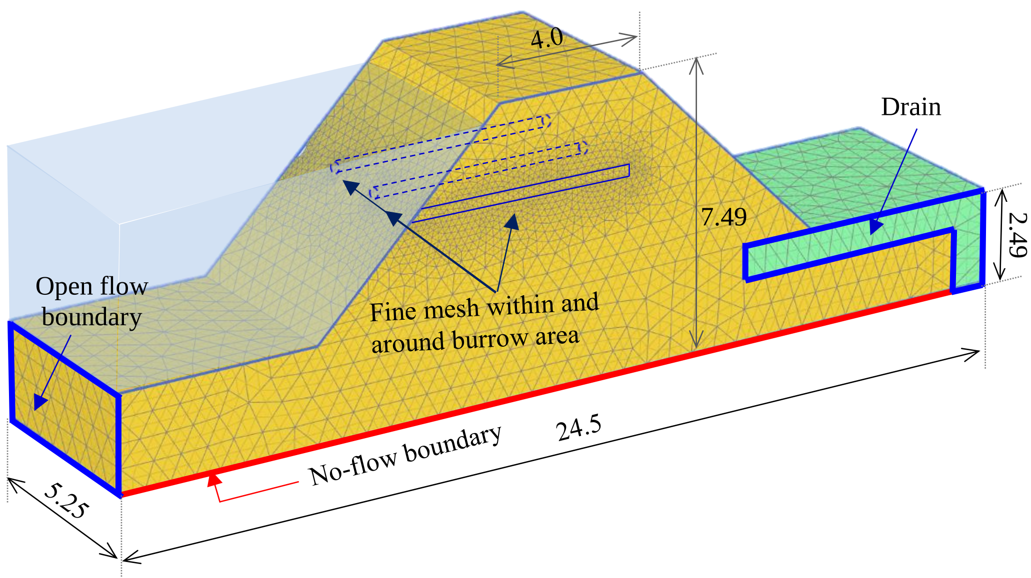

Figure 4.11. Vertical cross section through mid burrow of FEM model: geometry (in m) and boundary conditions

4.6.2 **Seepage analysis**

Figure 4.12 depicts the contours of pore pressure at 2D cross sections taken at the centerline of the intact and deteriorated models. The calculated pore pressure at four different locations within the body of the levee are given in Table 4.2. Comparatively, the phreatic line of LB model is somewhat similar to the intact model - with the dead end of the burrows dragging it further downward (Figure 4.12b). The traced phreatic line for LB model, as observed in the experiment (Figure 4.7b), is found to be in good agreement with that obtained using the numerical analysis. While pore pressures of LB are slightly lower than the intact model, the hydraulic gradients of the former are still higher. The pore pressure contours for the WB and

LB models are quite dissimilar. For the WB model, the prevalence of higher pore pressure is noted in the burrow region as well as the foundation level. The near horizontal extension of the contours is likely to be triggered by the burrow presence - very much similar to the traced phreatic line in Figure 4.7c.

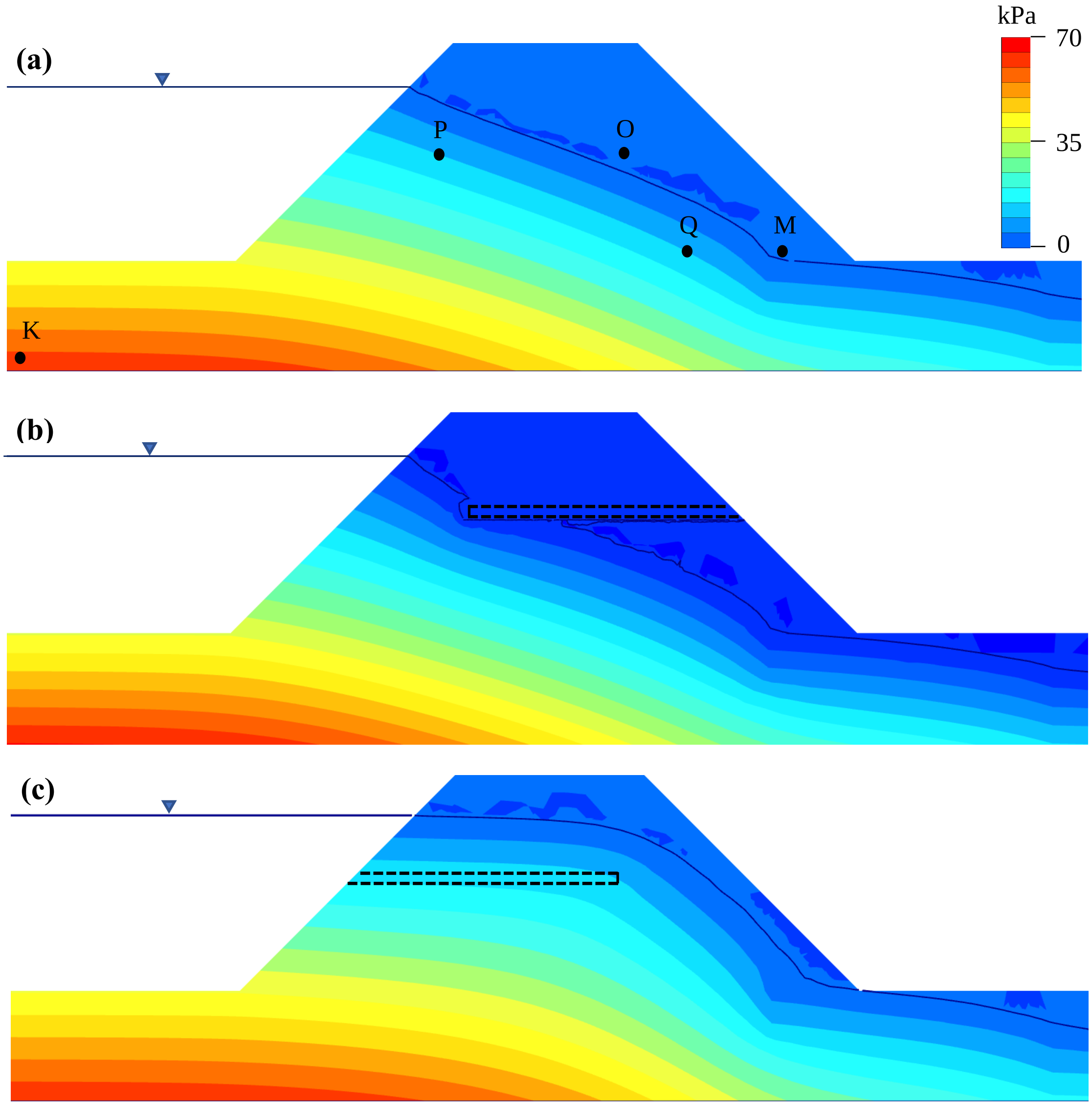

Figure 4.12. Steady state pore pressure distribution: a) intact; b) LB; c) WB

Figure 4.13 depicts the pore pressure distributions across the levee for three different elevations in the intact and deteriorated models. The results show that the increase in pore pressures is consistently and considerably higher for the WB compared with the LB and intact models. The increase was more pronounced near the landside slope. Compared with the intact model, the slightly lower phreatic line for the LB resulted in a small decrease in the pore pressures (Table 4.2). This general hydraulic performance for the deteriorated models is in fair agreement with the experimental observations expressed in terms of the arbitrary-defined hydraulic and normalized hydraulic gradients depicted in Figure 4.6 and 8, respectively.

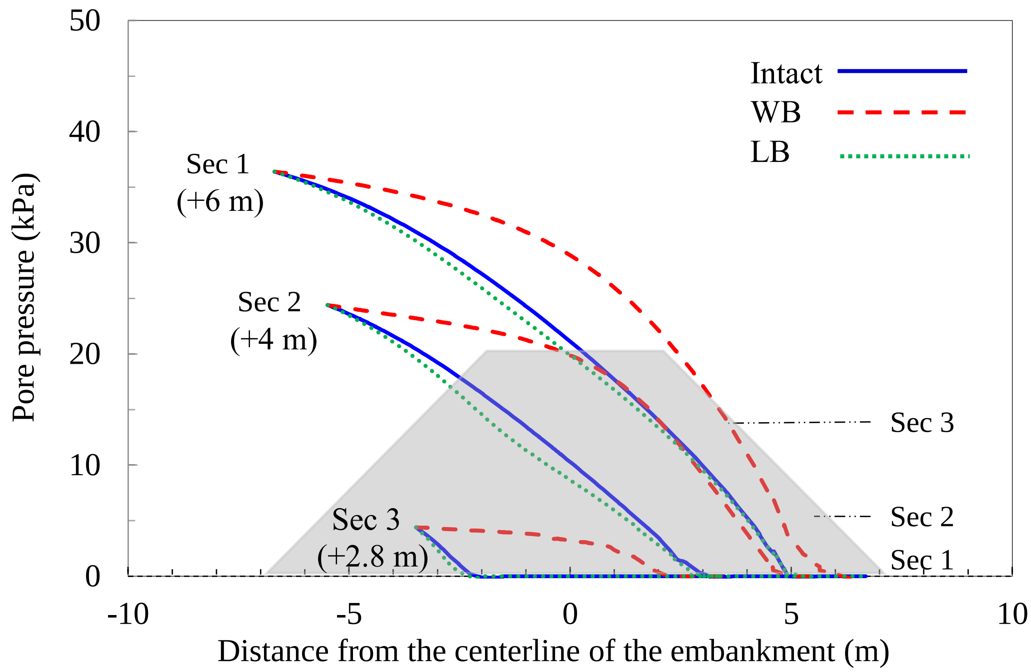

Figure 4.13. Pore water pressure distribution at horizontal sections across the levee

Table 4.2. Pore pressure comparison at selected points

Point	Pore water pressure (kPa)		
	Intact	LB	WB
K (WL)	63.75	63.75	63.75
M	0	0	1.68
O	0	0	11.92
P	5.54	1.24	12.49
Q	7.57	8.4	13.94

4.6.3 Stress analysis

The loss of structural strength within the body of the levee due to the presences of cavities is evident in the deteriorated models. To have an insight into the failure pattern and mechanism, the shear strain contours for WB model are shown in Figure 4.14a. The shear strain for the WB model bands along what seems to follow the failure surface. Additionally, strain concentrations extend along the burrow. The visually traced failure from the experiments (Figure 4.14b) as well as the model geometry at failure (Figure 4.14c) are qualitatively consistent with the numerical results. The progression of failure from the toe level towards the crest, as observed in the experiments, is intercepted by the weak plane at the burrow elevation. Such observation can be linked to the horizontal cracks that appear at the landside slope (Figure 4.10c) followed by excessive sliding (Figure 4.10d). The loss of strength is further exacerbated by the respective increase in pore pressures in the toe area –where failure surface is initiated– (Figure 4.12c). Further movement of the toe towards the landside deepen the horizontal cracks and eventually cause the observed toppling failure-like pattern (Figure 4.10e and f).

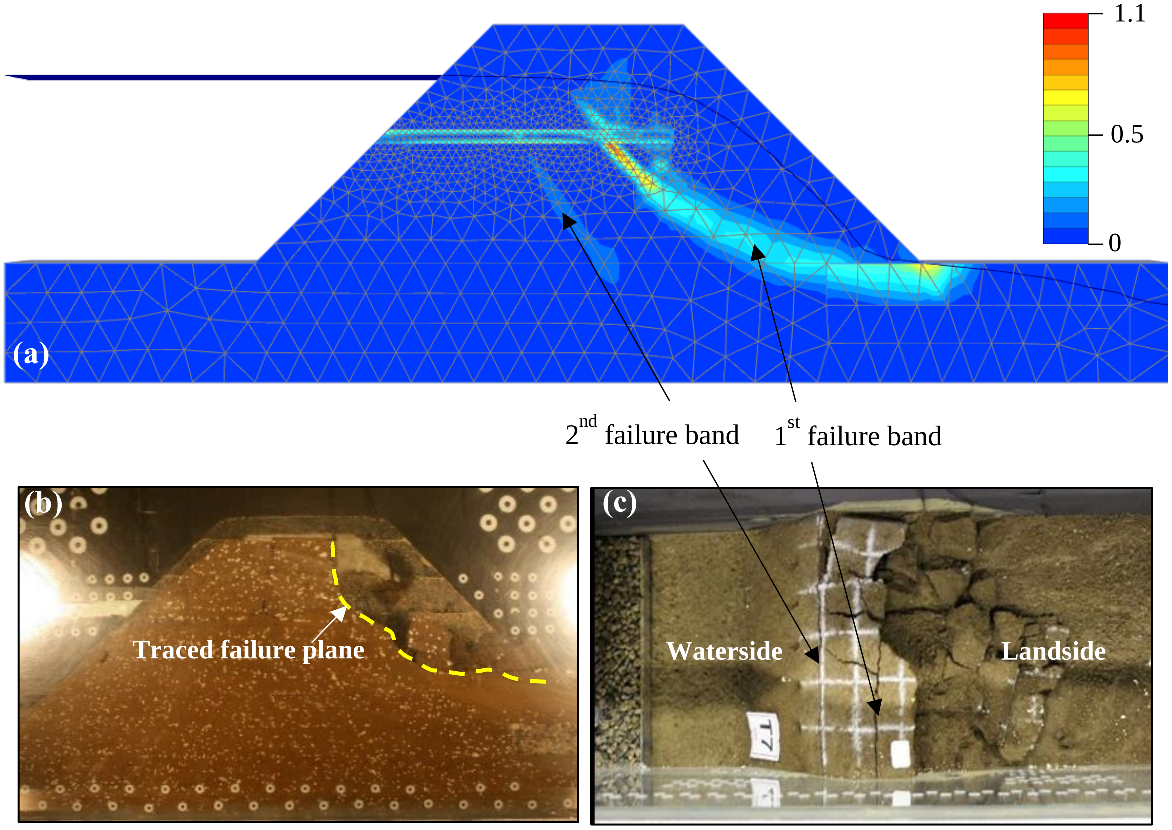

Figure 4.14. Stress analysis of WB model: a) shear strain (x10^{-3}); b) side view of the observed failure in WB model; c) top view of failed section

4.6.4 **Stability analysis**

To investigate the effect of strength reduction on the stability of levee slopes, the strength reduction method is used in this study, where the soil strength is artificially weakened until the soil fails [70]. This is established by decreasing the cohesion and tangent of the friction angle in the same proportion:

$$c' / c'_r = \tan \varphi' / \tan \varphi'_r = \textit{strength reduction ratio} \qquad 4.3$$

where c′ and φ′ are the input strength parameters for the Mohr–Coulomb failure criterion and c'_r and φ'_r are reduced strength parameters that are just large enough to maintain equilibrium. In FEM, no assumption needs to be made about the shape or location of the failure surface. Failure occurs through the zones within the soil mass in which the shear strength is unable to resist the applied shear stresses. Based on this approach and considering the toe of the landside slope (LS) as a reference point, the stability of both the intact and deteriorated levees is investigated. Figure 4.15 demonstrates that the safety factors for the intact and LB levees are about 1.3 whereas the deteriorated WB levee was on the verge of failure with a factor of safety approaching 1.0.

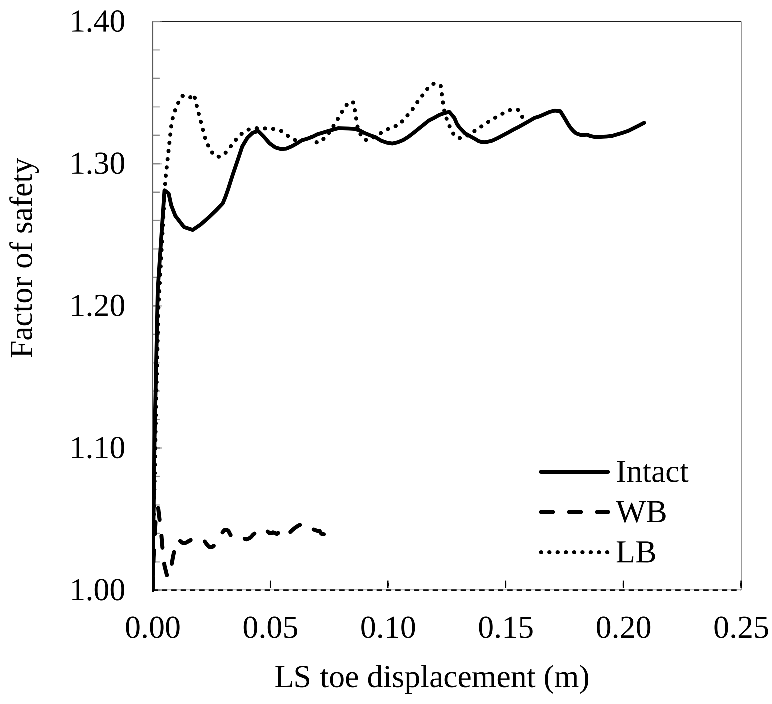

Figure 4.15. Factor of safety of the landside slope for LB and WB levees at time stamp T = 6,300 s

4.7 Synthesis of failure

Supported by the foregoing experimental observations and numerical results, the inferred scenarios, thus, represent the author's best judgement on the progression of failure in the deteriorated levee models.

4.7.1 Levee with landside burrows

Figure 4.16 summarizes a conceptual synthesis of the failure of LB model with the perceived chronological order indicated in boxes. The burrows evidently provide preferential path for the water flow toward the landside. Driven by the presence of cavities, the seeping water approaches the burrows from the closed end and the top possibly carrying some fines. The conducted analysis has shown that seepage into the burrows creates a concentrated flow around the burrows (see Figure 4.16b). This flow makes the walls of the partially filled burrows vulnerable to erosion. The seeping water with the carried/washed fines exit on the landside end of the burrows causing distress and disintegration of the surrounding area. This coupled with the free water seepage at the burrow level leads to structural deterioration locally propagating around individual burrows. Crest settlement started to develop progressively with the development of the visible landside cracks between the burrows (Figure 4.9b through e). Eventually, the structural integrity of the burrows is completely jeopardized (Figure 4.4 and Figure 4.9f).

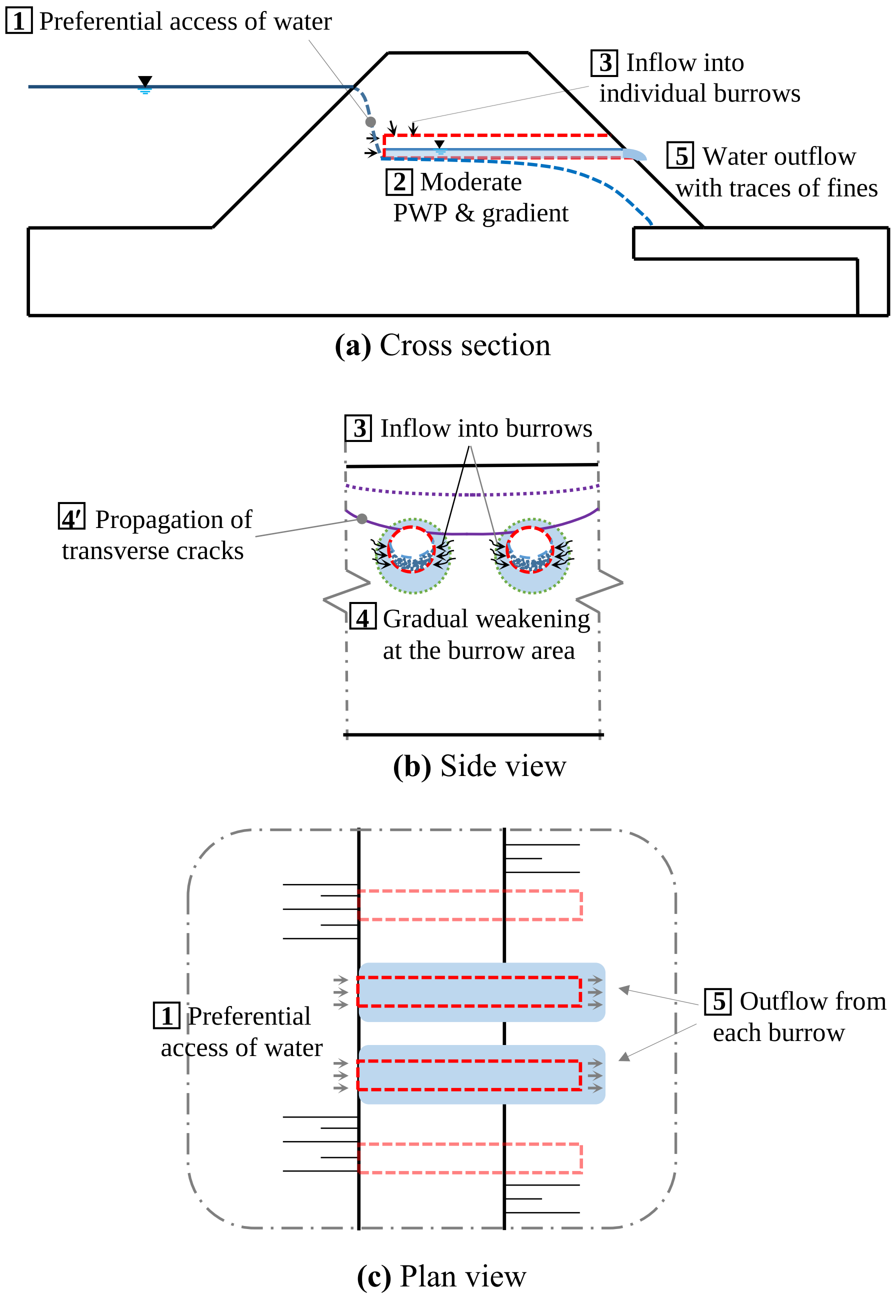

Figure 4.16. Schematic of the proposed failure scenario for the LB levee (sequence of distress events is indicated)

4.7.2 Levee with waterside burrows

A schematic of the proposed failure progression in WB levee section is shown in Figure 4.17. The burrows' proximity to water exacerbates flow and particle migration within the model and eventually weakens its structure. Unequivocally, this direct water access to the cavity system jeopardizes the hydraulic performance of the levee by raising the phreatic line. As compared with the LB case, the uninterrupted water entry obviously reduced head losses and yielded considerably higher pore pressures (Figure 4.13). The "buildup" of pore pressure –manifested in the higher phreatic line– is more intense because the water entering effortlessly at the waterside does not exit the burrow as easily. The "entrapment" of large pore pressures near the center of the model probably promotes transverse (lateral) seepage between the burrows. The lateral flow is associated with fines migration causing disintegration and weakening in the zone between the burrows, which is signified in the development of parallel cracks between the burrows. This flow pattern leads to erosion of the walls of the water-filled burrows. Subsidence develops across the levee section with interaction between adjacent burrows. As failure is approached, the high pore pressure leads to excessive seepage at the toe (Figure 4.10b) and the initiation of slip plane due to the loss of effective stress (shear strength). The intersection of the slip surface with the horizontal cracks around the burrow area forms a toe wedge (A) and a middle wedge (B). With further through seepage, the toe wedge slides and topples leading to crumbling of the middle wedge (Figure 4.10c and d). Under the high "blocked" pore pressure, the complete wash out of the levee section is inevitable. This mechanism justifies the rather steep trend of crest subsidence (Figure 4.4).

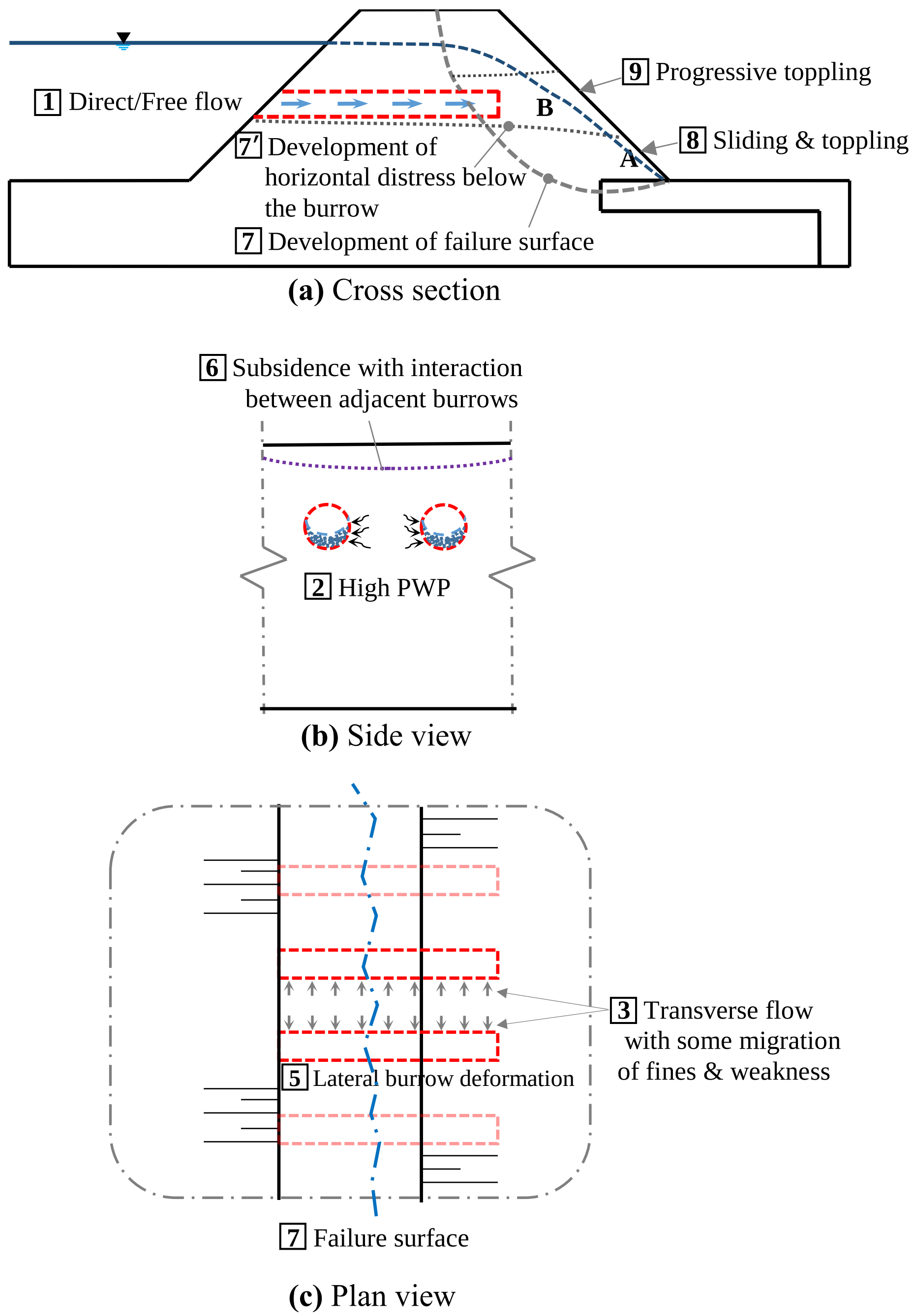

Figure 4.17. Schematic of proposed failure scenario for the WB levee (sequence of distress events is indicated)

4.8 Summary and closing thoughts

This study has investigated the effect of idealized configurations of wildlife attack on the hydraulic performance and structural integrity of earth levees. Animal invasive damage was modeled as idealized cylindrical cavities within the levee models. For this purpose, a series of centrifuge experiments on scaled-down levee sections having waterside and landside burrows at different levels were conducted. An identical intact section has undergone the same experiment for referencing. Compared with the intact levee, the deteriorated models exhibited peculiar seepage pattern. The experimental results indicated that the presence of the introduced cavities has dreadful impacts on the hydraulic performance and stability of levee. Utilizing the centrifuge observations, the study postulates distinguishing failure mechanisms associated with the attack side. Numerical simulations of the seepage and stress analysis have further supported the proposed hydraulic response and failure mechanism. The aforementioned findings collectively explain the unexpected and abrupt failures that could develop in levees deteriorated due to wildlife activities. The deduced failure scenarios advocate that subsidence in deteriorated levees is triggered by the combined effect of cavity destruction and loss of strength. Unmistakably, the use of crest settlement (subsidence) as a failure indicator in deteriorated levees is indicative but incomprehensive. Their apparent intactness prior to failure could be quite misleading. This has significant bearing on levee system management, as the damage (size of cavities) of concealed burrow systems within a levee section could be much larger than what the visible openings demonstrate [3]. Of note, the results reported in this study are rather limited by the investigated parameters including the levee and burrow geometries. Obviously, the size and density of the burrows could also be very critical. Thus, generalization of the outcomes requires further investigation on other materials, geometrical features of earth structures and deterioration levels and patterns.

5 EFFECT OF BURROW CHARACTERISTICS ON THE HYDRAULIC PERFORMANCE AND STABILITY OF LEVEES

5.1 Preface

Chapters three and four present the results of centrifuge experiments for three levee models: intact, with waterside burrows and with landside burrows. These results are presented and used to develop numerical models. Based on the finding in chapter four there is a need for a parametric study to better understand the impact of animal burrows on earthen levees under different geometric condition. Chapter five of this thesis focuses on this parametric study which is conducted using finite element modelling. The parametric study investigates the characteristics of burrows configurations, such as burrow length and burrow depth as well as the impact of change in the side slope ratio on the stability of each levee model. The details of the parametric study and the effects of each parameters on the seepage and the levee stability are presented in chapter five.

5.2 Introduction

Cases of levee failures due to animal burrows have been reported around the world [3]. Pin Oak levee in Missouri (US) is one of the recent cases that happened in 2008. The presence of small diameter rodent holes, has been found to be the cause of failure [71]. There are thousands of kilometers of exiting earthen levees around the world which need structural assessment. For instance, in the United States alone there are about 150,000 kilometers of levees which protect about 43% of the national population [6]. Understanding how these burrows affect the integrity of levees helps to accurately assess the serviceability and the safety of these structures. The author of this thesis has conducted physical modeling of earthen levees to explore the impact of internal deterioration caused by animal burrows on levee safety and performance. The results revealed that animal burrows have destructive effects on the safety of levees and may cause failure [65]. In addition to understanding the failure mechanisms of the deteriorated levee, evaluating the effect of burrow configuration on the levee performance is necessary for proper risk assessment. Previous studies performed by Saghaee et al. [65] confirmed that the attack side is determinative on the type of levee failure. Waterside burrows induce sudden failure without warning while landside burrows cause gradual failure with visible soil erosion signs on the slope. The configuration of animal burrows is complex and varies for different rodent species. However, there are parameters which define the configuration and have a considerable role in governing the behaviour of the deteriorated levees [20]. These parameters include burrow length (L_B), and burrow depth from the levee crest (D_B). This study aims to investigate the effect of these parameters on seepage and stability of deteriorated earthen levees.

5.3 Scope

The object of this study is to assess the effects of burrow configuration on homogenous earthen levees using a numerical analysis. Although, centrifuge modeling is an efficient technique to model deteriorated earthen levees, conducting a parametric study using centrifuge modeling is costly and time consuming. Therefore, finite element analysis is used in this study to perform the parametric study focusing on burrow length, burrow depth, and levee side slope ratio. These parameters are chosen due to their possible effect on the behaviour of the deteriorated levees. The above-mentioned parameters are studied for both waterside and landside burrows.

5.4 Finite element model

Homogenous intact levees are generally considered plane strain problems and are usually simulated using 2D models. However, in this research, due to the presence of animal burrows, 2D models are not able to accurately replicate the burrows; thus, 3D models are used. Finite element models are built based on the full-scale prototype of the centrifuge models presented in Chapter 3. Figure 5.1 demonstrates a sample finite element model used in these analyses. This model represents a homogenous earthen levee with side slope of 2H: 1V (2 horizontal to 1 vertical). To reduce the computational time, only half of the prototype is simulated. An "L" shaped toe drain is considered at the waterside of the embankment. The model has open flow boundaries at the two ends of the model and a no flow boundary at the base. Horizontal displacement in the X direction is restrained at both ends and side boundaries. The base of the model is restrained for displacement in all directions.

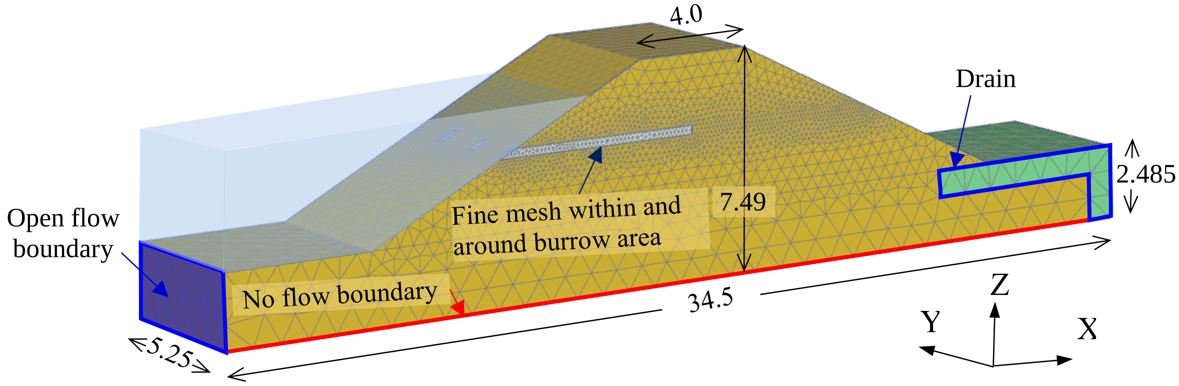

Figure 5.1. Typical finite element model for 2H:1V levee with mid-height waterside burrows (in m)

Burrows are modeled as horizontal cylindrical clusters inside the embankment with an open end on the slope. The diameter of the burrows is constant at 30 cm in all of the analysed models [72]. To simulate the introduction of the burrows, the original embankment material in the burrow cluster is replaced with a low stiffness material (E=10 kN/m^2) of high permeability (k=100 m/s). 10-node tetrahedral elements are used for the 3D mesh generation (Figure 5.2). The 3D finite element mesh is refined in the zone around and inside the burrows. The average element size in the burrows, embankment and the foundation are 0.16m, 0.45m and 0.75m respectively. Using fine mesh around the burrows is necessary to accurately create the cylindrical shaped burrows.

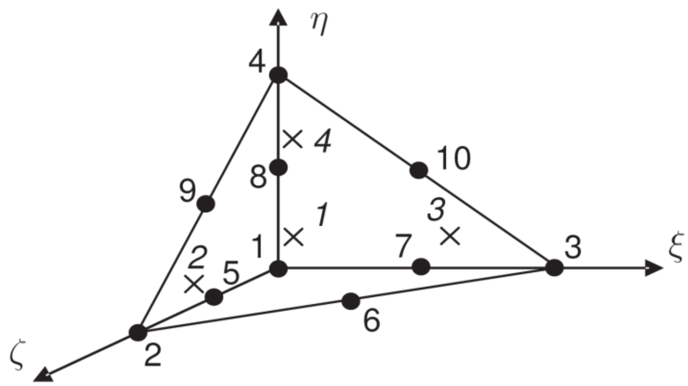

Figure 5.2. Second order 10-node tetrahedral element used in the 3D mesh

5.5 Parametric study

5.5.1 Effect of burrow length

In nature, the length of the burrows depends on many factors, such as the type and size of the rodent species and the levee construction material [3]. In order to study the effect of burrow length on the hydraulic performance and stability of the levee, three different lengths are considered in this study. Burrow lengths are normalized as a percentage of the length of the levee cross section at the burrow elevation. This normalized term is called here the length ratio (L_{Br}) and is defined in equation 5.1. Using L_{Br} helps to properly compare the results of the analyses.

$$L_{Br} = \frac{L_B}{L_C} \qquad 5.1$$

Where L_{Br} is the burrow length and L_C is the length of the levee cross section at the burrow elevation (Figure 5.3).

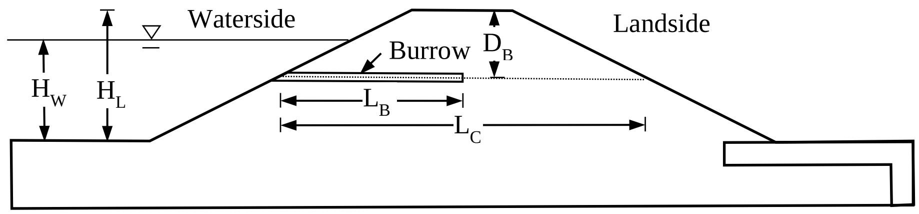

Figure 5.3. Definitions of the symbols used in this manuscript

Three different L_{Br} are chosen to study the effect of burrow length: 0.25, 0.5 and 0.75. In order to generate the same finite element mesh for all of the models, burrow clusters are extended to both side slope surfaces (L_{Br}=1). For the initial condition and the intact levee, the cylindrical burrows were filled with the material which has the same properties as the embankment (Kasama soil). Using stage construction provides the opportunity to have the same model geometry for different L_{Br} cases. Since pore pressure is one of the key parameters in the stability analysis of the levee, this parameter is extracted at three different cross sections in the embankment. These sections are located at elevations of +2.8m, +4m, and +6m from the bottom of the foundation, and referred to as Sec 1, Sec 2, and Sec 3, respectively (Figure 5.4). In all the graphs in this manuscript D represents the depth and L represents length. In this study, WB refers to the levee with waterside borrows and LB refers to the levee with landside burrows. Pore pressures are generally higher at deeper cross sections due to higher water head. For each section, the pore pressure curves start at the surface of the waterside slope with a value equal $P_{Steady} = \gamma_w \times h$, which h is the water height. Increasing of burrow length from L_{Br}= 0.25 to L_{Br}= 0.75 leads to an increase in the maximum pore water pressure at these three sections for WB. The pore pressure value at the centerline of the model (x=0 m) is chosen as a representative value for each section. These results are presented in Figure 5.5 for WB. Increasing the burrow length results in an increase in the pore pressure at all three sections. Pore pressure shows a 25% increase at the lowest section (Sec 1) in the case of L_{Br}=0.75 as compared to the intact levee. This increase is found to be higher at shallow sections (e.g. sec 1) and equal to 63%. The increase in pore pressure results in a decrease in effective stress and consequently soil shear strength [73].

For the levee with landside burrows (LB), changes in the pore pressure are presented in the Figure 5.6. For shallow burrows (D_{Br}=0.25) the variation is negligible as compared to the intact levee (Figure 5.6.a). For mid-height burrows (D_{Br}=0.5), change in pore water pressure is minimal for L_{Br}=0.25 and L_{Br}=0.5. However, in the case of L_{Br}=0.75 the pore pressure curve tends to bulk toward lower pore pressure (Figure 5.6.b). Increasing of burrows length causes decrease in pore pressure. This change is more significant in deeper burrows. The reason for the decrease in pore pressure is; burrows act as a temporary pressure releasing pipe in the embankment and help the pore water pressure to reach the atmospheric pressure in a short distance. Figure 5.7 indicates a decrease in pore pressure at the centerline of the embankment for the landside burrows (LB).

Reduction in shear strength of the embankment reduces the factor of safety and can cause slope instability. As presented in Figure 5.8.a, the factor of safety for the intact model is 1.30 which is reduced by 19% to 1.09 for L_{Br}=0.75. The reduction in the factor of safety also happens in other burrow depth ratios (Figure 5.8.a &b). The general factor of safety of the levee for LB is almost constant for the different burrow length ratios. The only exception in the case of deep burrows (D_{Br}=0.75) due to the decrease in pore pressure and increase in the factor of safety (Figure 5.9). It should be noted that the factor of safety mentioned here is for the landside slope and considers general slope failure. Local slope failure is not considered.

This factor of safety is calculated using the strength reduction method for a point located at the toe of the embankment.

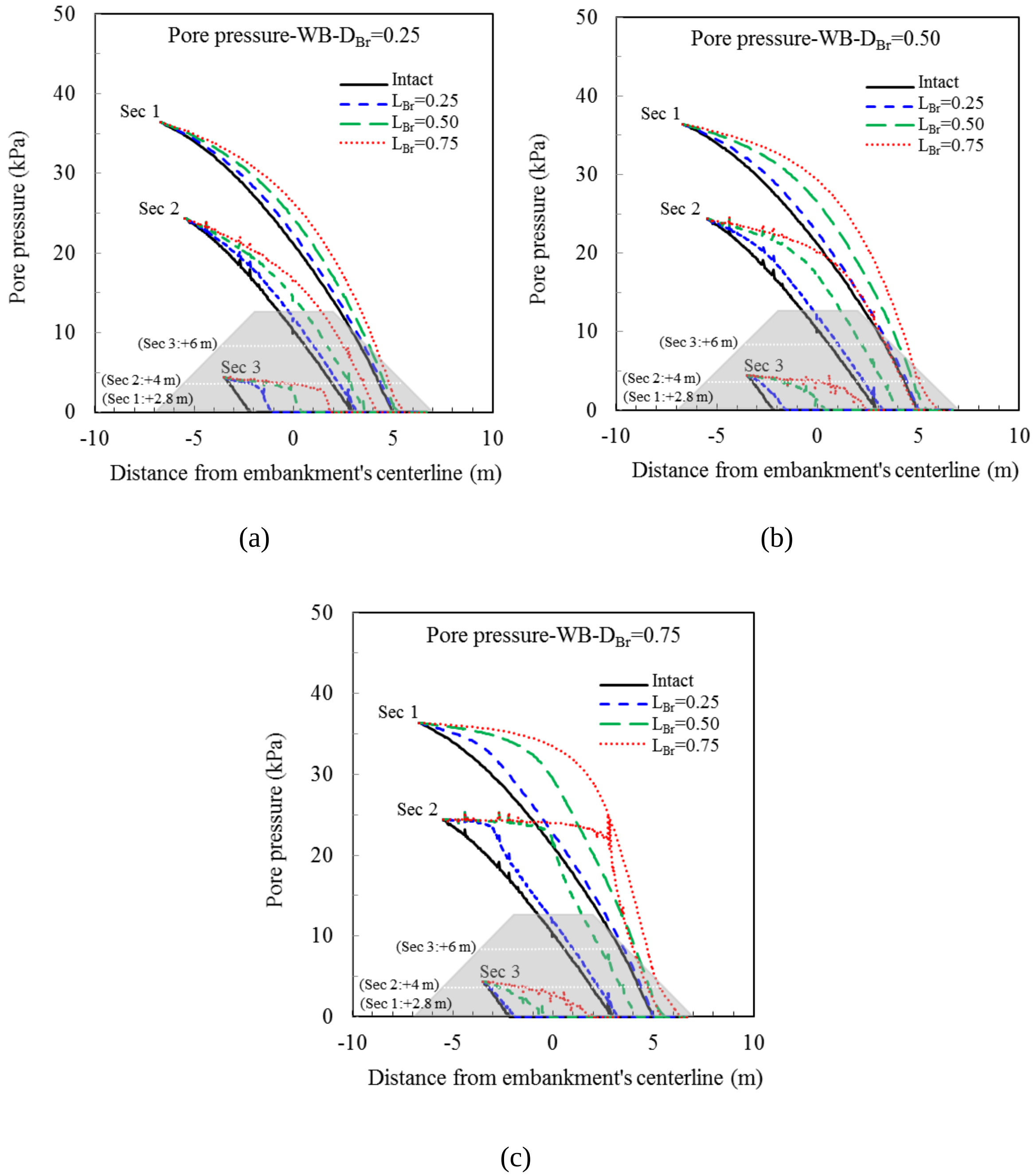

Figure 5.4. Pore pressure distributions at horizontal sections of levee with waterside burrows (WB) for different burrow depth ratios: a) D_{Br}=0.25; b) D_{Br}=0.5; c) D_{Br}=0.75

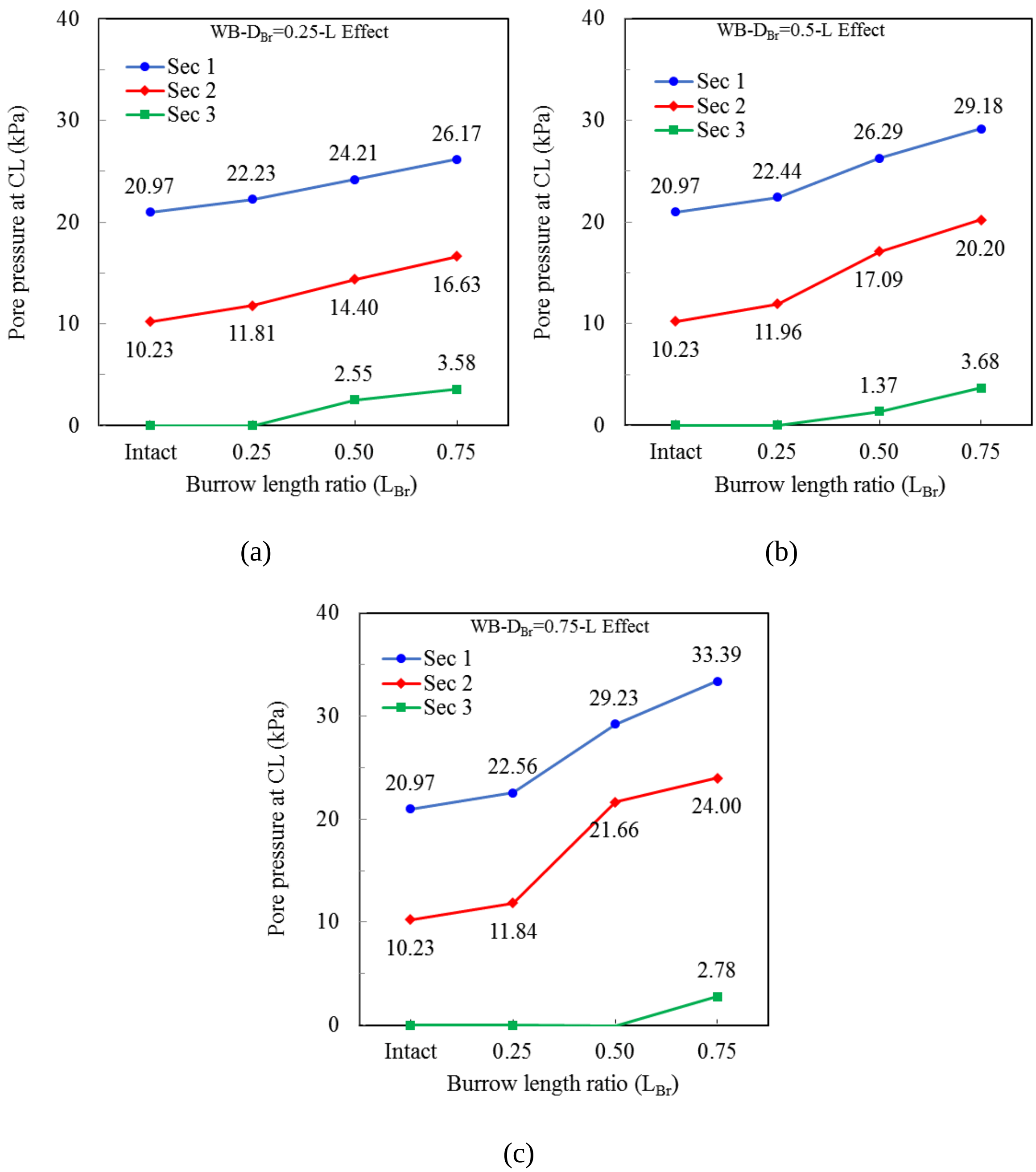

Figure 5.5. Pore pressure at the center line (CL) of the embankment for levee with waterside burrows (WB): a) D_{Br}=0.25; b) D_{Br}=0.5; c) D_{Br}=0.75

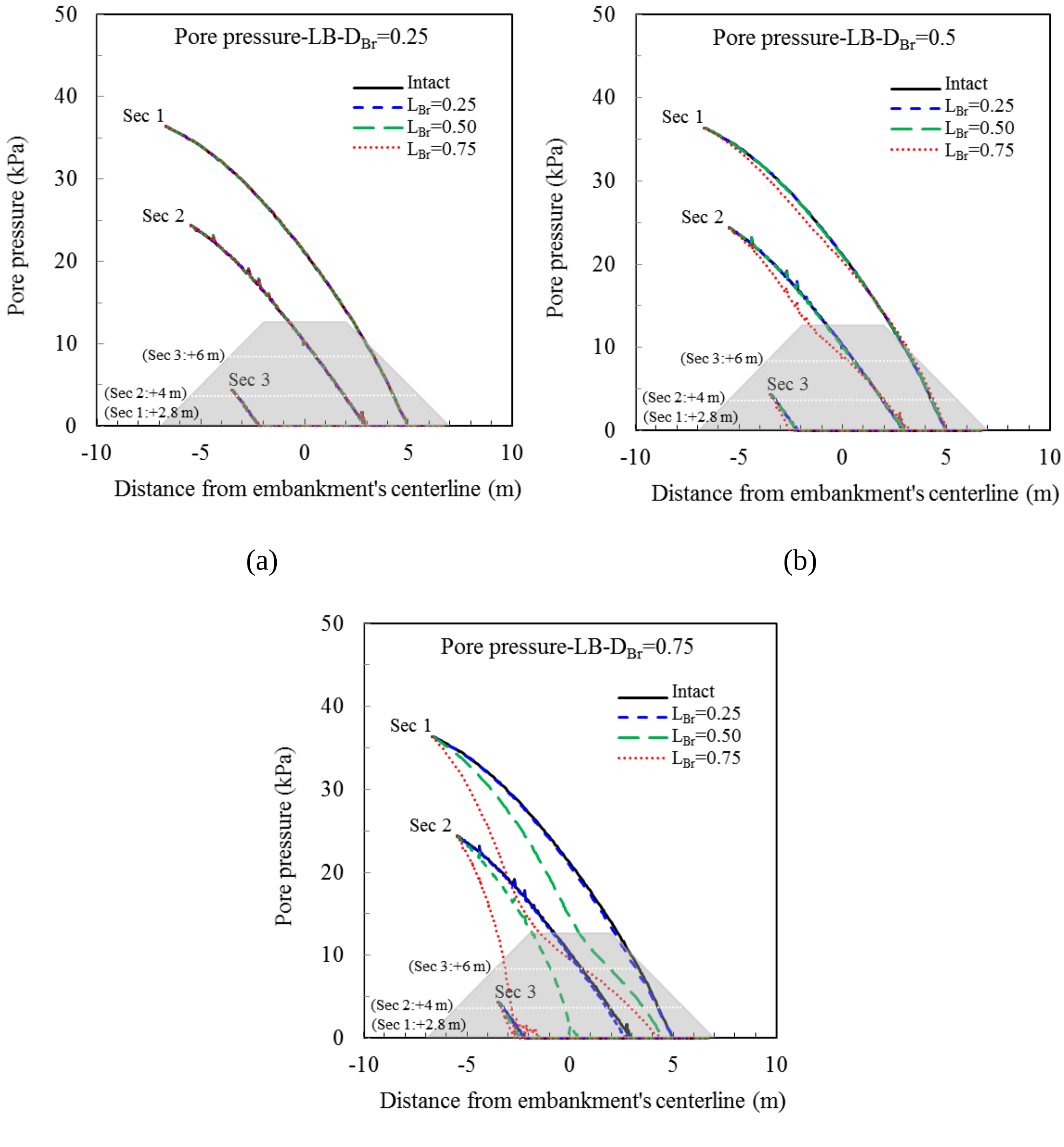

(c)

Figure 5.6. Pore pressure distributions on the horizontal section for landside burrows for different burrow depth ratios: a) D_{Br}=0.25; b) D_{Br}=0.5; c) D_{Br}=0.75

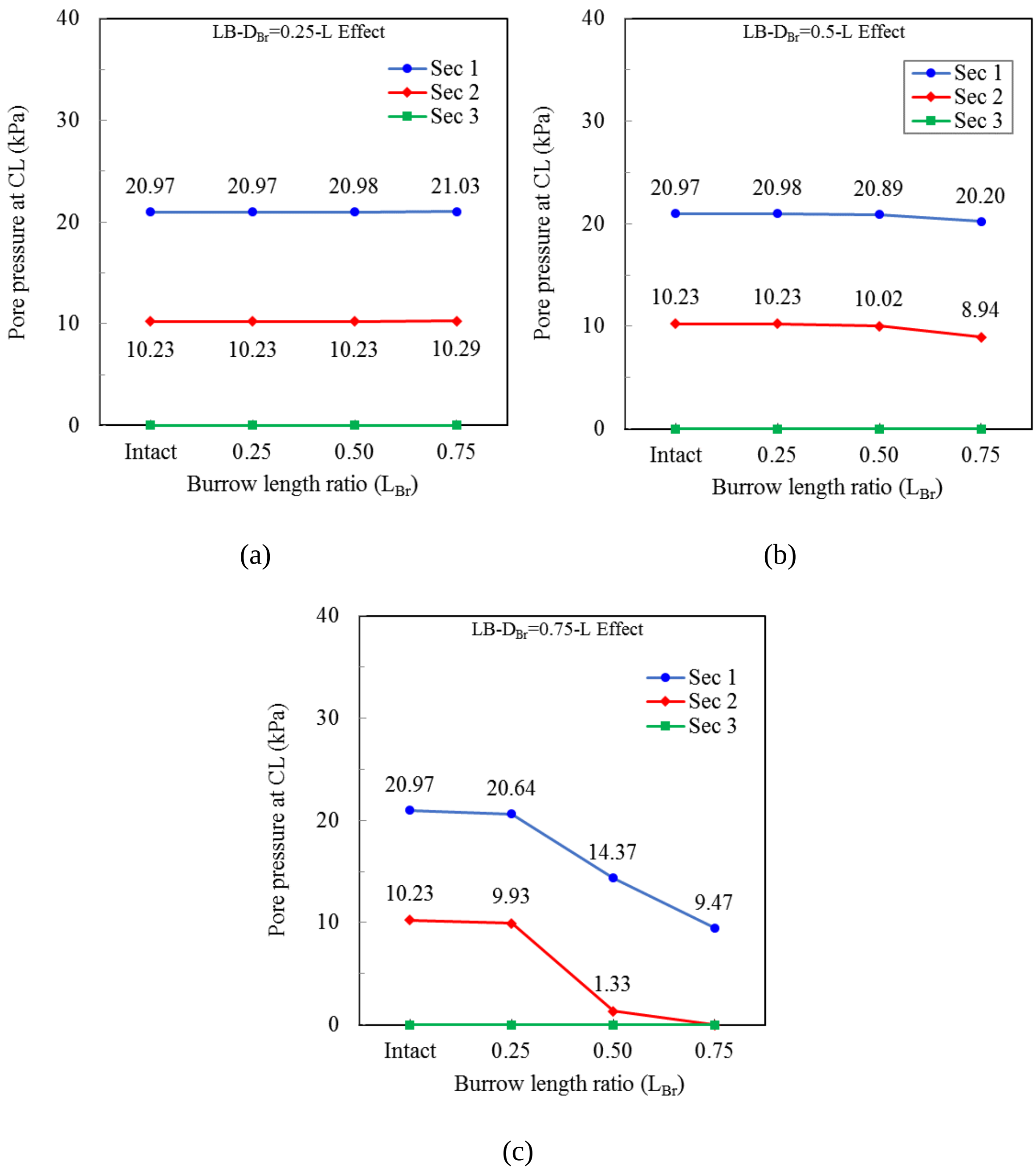

Figure 5.7. Pore pressure at the center line (CL) of the embankment for levee with landside burrows: a) D_{Br}=0.25; b) D_{Br}=0.5; c) D_{Br}=0.75

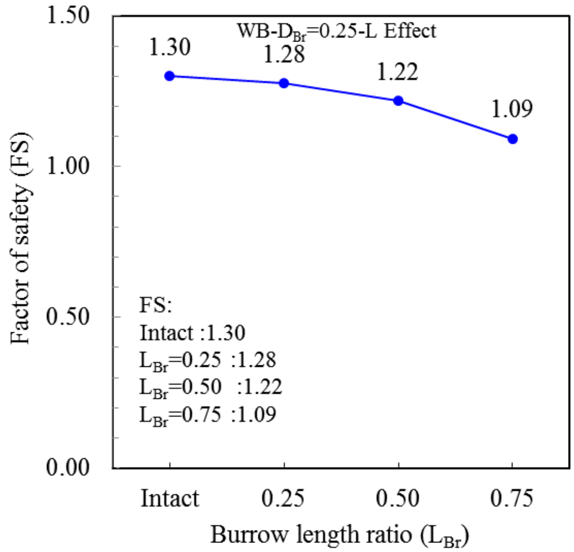

(a)

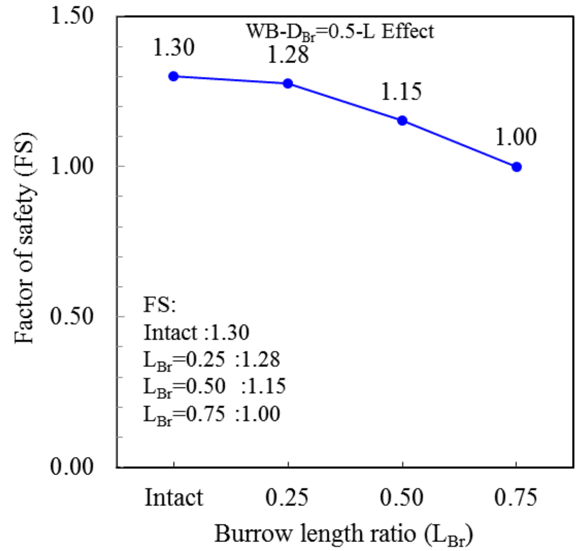

(b)

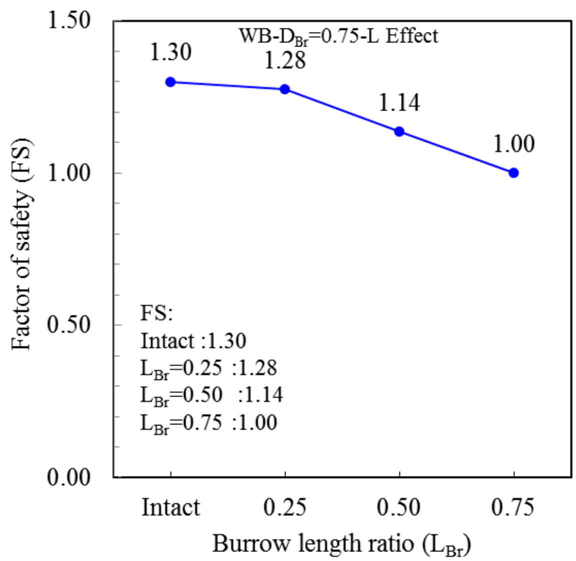

(c)

Figure 5.8. Factor of safety of the landside slope for the case of levee with waterside burrow (WB) for different L_{Br}: a) D_{Br}=0.25; b) D_{Br}=0.5; c) D_{Br}=0.75

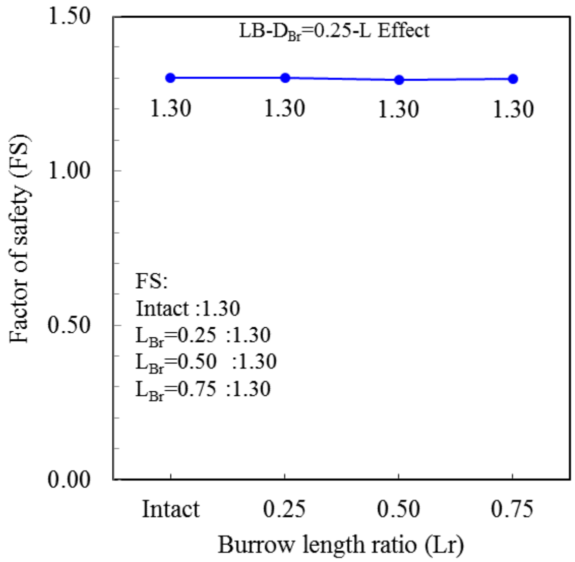

(a)

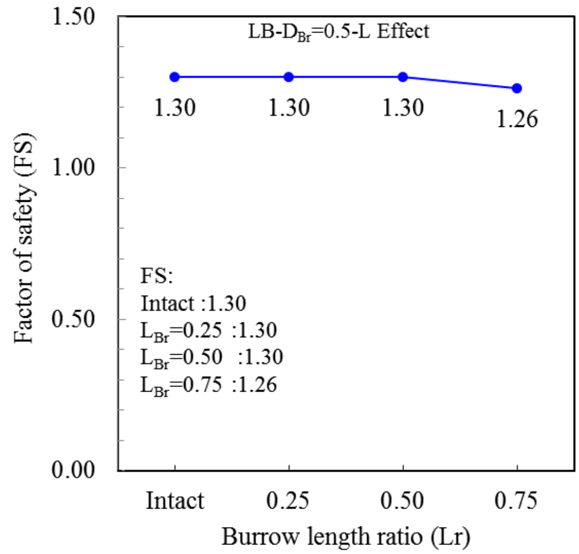

(b)

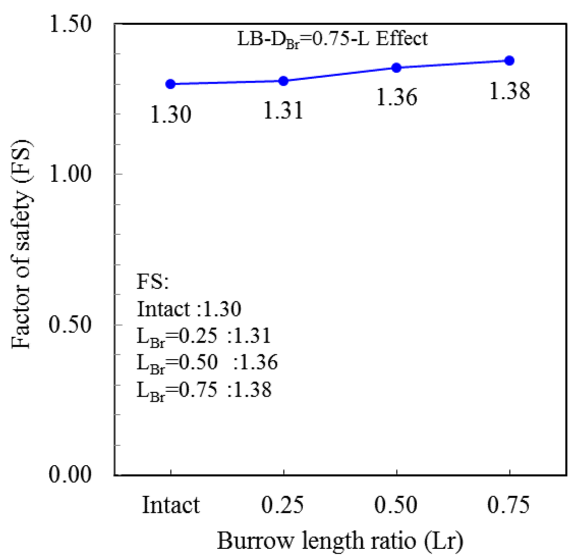

(c)

Figure 5.9. Factor of safety of the landside slope for the case of landside burrow (LB) for different L_{Br}: a) D_{Br}=0.25; b) D_{Br}=0.5; c) D_{Br}=0.75

5.5.2 **Effect of burrow depth**

In nature, burrow depth depends on the type of the animal and the attack side (waterside and landside) [3]. Since levees are flood protection structures, the waterside water level may be low most of the time [27]. A low water level gives the animal an opportunity to make deep burrows close to the foundation of the embankment. On the other hand, the landside slope is usually dry and favourable to be attacked by rodent species. In this study burrow depth is defined as the distance from the embankment crest to the centerline of the burrow (D_B in Figure 5.3) and consequently the depth ratio (D_{Br}) is defined used equation 5.2, where D_B is the depth of the burrow and H_L is the height of the embankment.

$$\mathrm{D_{Br}} = \frac{\mathrm{D}_B}{\mathrm{H}_L} \qquad 5.2$$

To study the effect of burrow depth on the seepage and stability of the levee, three different depth ratios are investigated. These depth ratios are D_{Br}=0.25, D_{Br}=0.5 and D_{Br}=0.75. The smaller depth ratio, 0.25, indicates shallower burrows which are closer to the crest. Comparison of the pore pressures on the horizontal sections (Sec 1 to Sec 3) of levee with waterside burrows for different depth ratios shows that an increase in pore pressure with the increase in burrow depth. For section 1 (Figure 5.10.a), increasing the burrow depth ratio from 0.25 to 0.75 results in an increase in pore water pressure by about 21% for L_{Br}=0.5 and 27% for L_{Br}=0.75. Pore pressure at section 1 for L_{Br}=0.25 is almost the same for all the depth ratios which is due to the minimal effect of the short waterside burrows on the phreatic surface. Regarding section 2, changing the depth ratio from 0.25 to 0.75 increases pore pressure by 50% and 44% for L_{Br}=0.5 and L_{Br}=0.75 (Figure 5.10.b). At the shallower section, section 3, pore pressure shows a modest decrease as the depth ratio is increased (Figure 5.10.c). For section 3, pore pressure in the case of intact levee and short burrows (L_{Br}=0.25) is equal to zero at the centerline which is consistent with the fact that the centerline of this section is located above the phreatic surface. Increasing the burrow depth does not have a significant effect on the pore pressure at the centerline of section 3. High water pressure inside deeper burrows can be considered the cause of increase in pore water pressure when the burrow depth for medium length (L_{Br}=0.5) and long (L_{Br}=0.75) burrows is increased.

For the case of levee with landside burrows (LB), analyses show that burrow depth has a significant effect on the pore water pressure compared to the intact levee particularly for deep burrows (D_{Br}=0.75). For shallower burrows, there is no change in pore pressure for both short (L_{Br}=0.25) and medium length (L_{Br}=0.5) burrows whereas a slight reduction of about 13% in pore pressure was calculated for long burrows (L_{Br}=0.75). The short length of shallower burrows cannot reach the phreatic surface to make changes in the pore water pressure at the centerline of the levee. The pore pressure decreases from 21 kPa at L_{Br}=0.5 for D_{Br}=0.5 to 14.4 kPa at D_{Br}=0.75, a 32% decrease (Figure 5.11. a & b). The depth ratio has more effect on long burrows (L_{Br}=0.75) and it reduces the pore water pressure from 20.2 kPa to 9.5 kPa (53%). The reason for this significant reduction in pore water pressure is that the presence of deep long burrows lowers the phreatic surface to the burrow elevation over a large section of the burrow length and at the centerline of the levee. Lowering the phreatic surface reduces the pore water pressure inside levee. As can be seen in Figure 5.11.c, burrow depth has minimal effect on the shallow part of the embankment (Sec 3) and the pore pressure remains zero for all cases. It is worth noting that, pore pressures are reported at the centerline of the levee and this does not mean that the pore pressure elsewhere is zero.

Factor of safety against instability of the landside slope is calculated to investigate the effect of animal burrows on the general stability of the levee. The results of the slope stability analysis for the waterside burrows (WB) are presented in Figure 5.12.a. Burrow depth does not have an effect on the factor of safety for short burrows (L_{Br}=0.25), however, it brings the factor of safety close to one for longer burrows. A factor of safety equal to and smaller than one is defined here as a failure. This figure shows that the burrow length has more effect on the factor of safety than the burrow depth for the WB levee.

Figure 5.12.b presents the factor of safety of the landside burrow levee (LB). As can be seen, burrow depth has almost no impact on the factor of safety of the embankment for shallow and medium depth burrows but it increases the factor of safety by about 10% for long burrows (L_{Br}=0.75). Deep burrows reduce pore pressure and consequently increase the global factor of safety of the slope. Since the failure mode of the embankment for landside burrows is a local slope failure at the burrow entrances and it is not a general slope failure, the increase in global factor of safety of the slope does not reflect a safer levee.

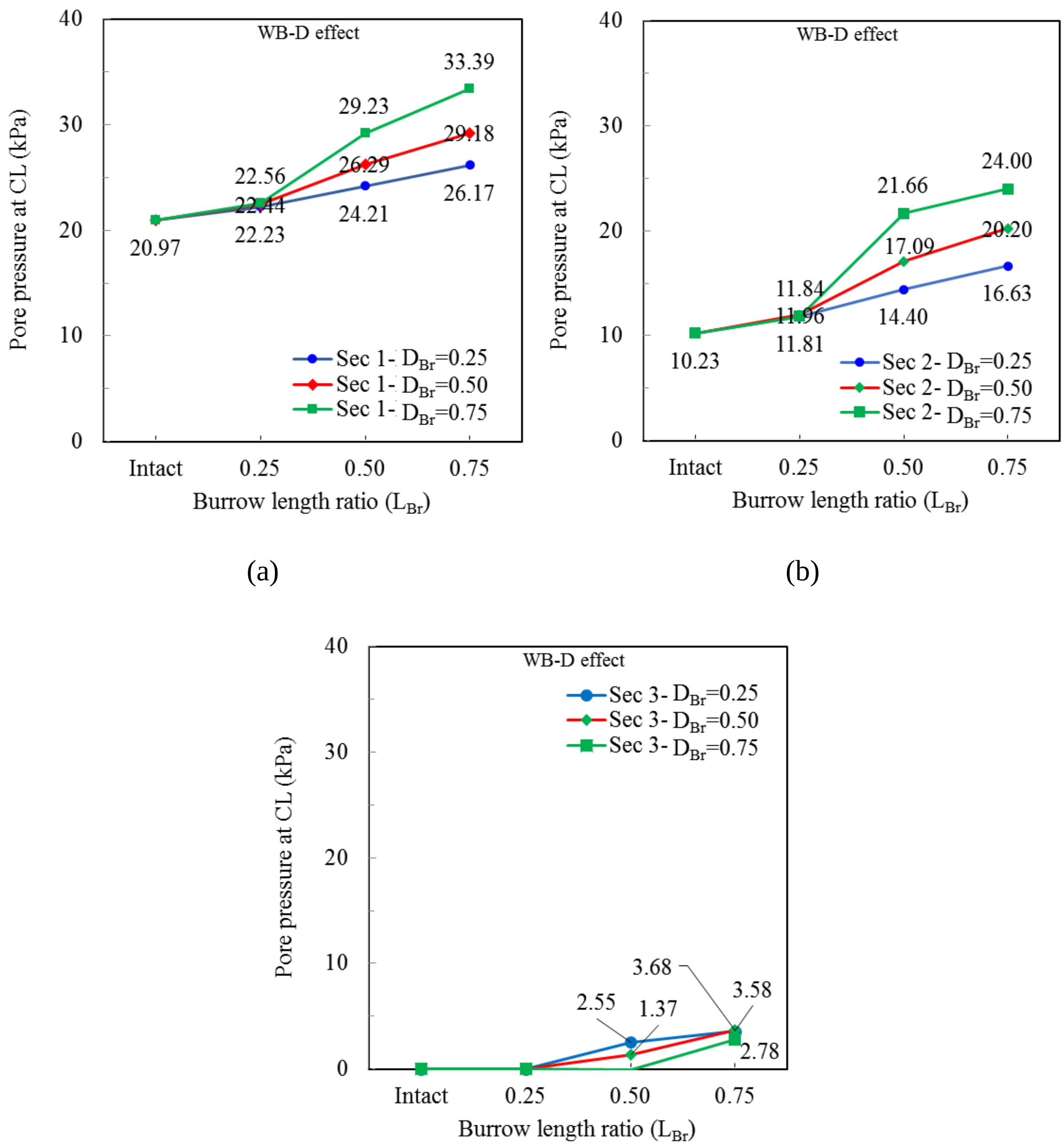

(a) (b)

(c)

Figure 5.10. Pore pressure at the centerline (CL) of the embankment for levee with waterside burrows (WB): a) section 1; b) section 2 and; c) section 3

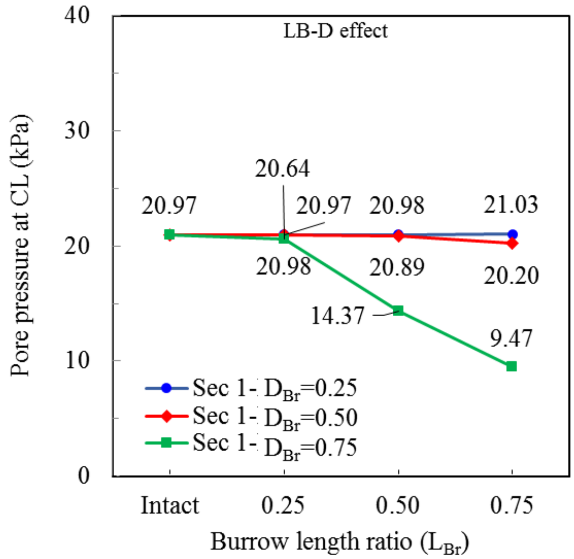

(a)

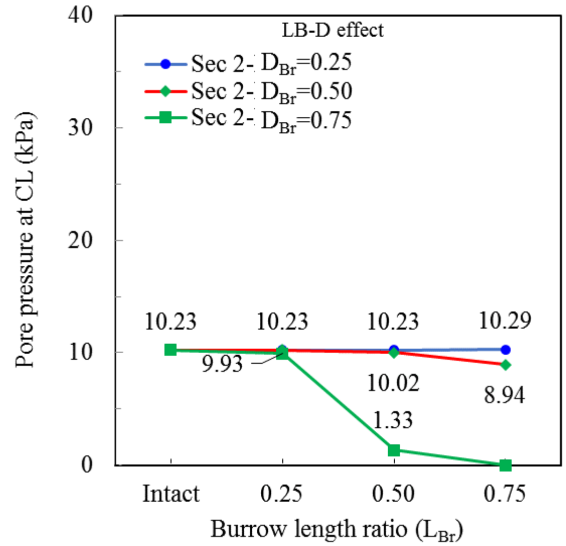

(b)

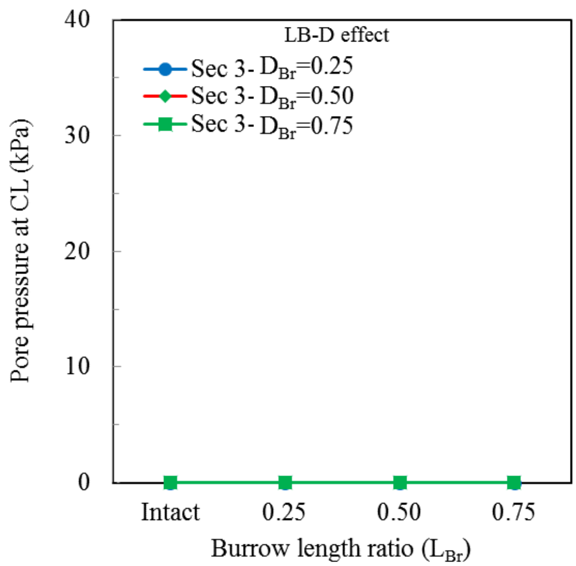

(c)

Figure 5.11. Pore pressure at the centerline (CL) of the embankment for levee with landside burrows (LB): a) section 1; b) section 2 and; c) section 3

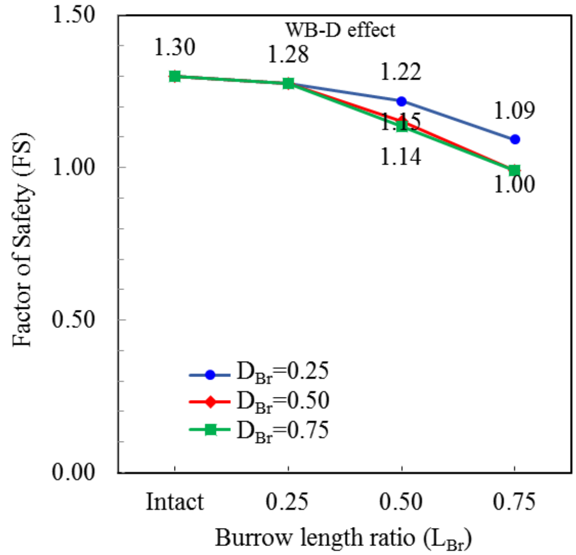

(a)

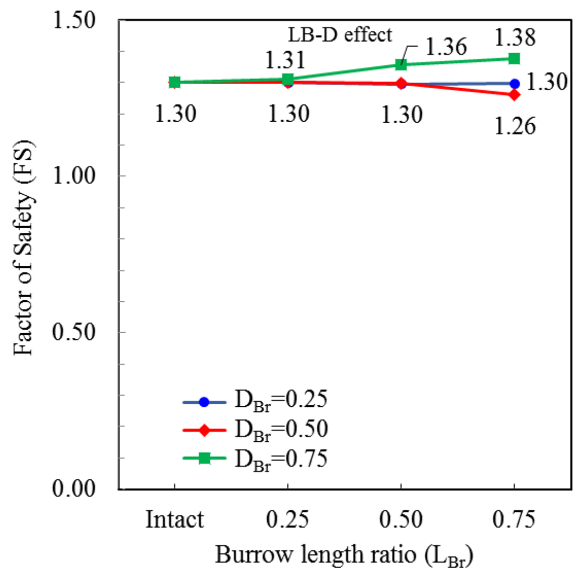

(b)

Figure 5.12. Calculated factor of safety against general slope failure: a) WB and b) LB

5.5.3 **Effect of embankment side slope ratio**

To study the effect of the side slope ratio on the stability of the deteriorated levee, three different side slope ratios of 1H: 1V, 2H: 1V, 3H: 1V are investigated. In all cases, waterside and landslide slopes are the same. The steep 1H: 1V slope was chosen to replicate the slope ratio of the physical models used in the experimental component of this study. The height of the embankment (H_L), the depth of foundation and the crest width are kept constant throughout the analysis. However, the length of the model increases due to flattening the side slopes. The dimensions of the landside drain are the same in all three cases. The length and the number of the elements in each model are presented in Table 5.1. In all cases, mid-height burrows are considered with three different burrow lengths. Figure 5.13 shows two of the finite element models used in this study.

Table 5.1. Information of the models used to study the effects of side slope ratio

Model	Side Slope	Model Height (m)	Model Length (m)	Number of Elements/Node	Average Element Size (m)
1H	1H: 1V	5	24.5	119494/172869	0.0897
2H	2H: 1V	5	34.5	120733/171510	0.1061
3H	3H: 1V	5	44.5	113090/161645	0.1245

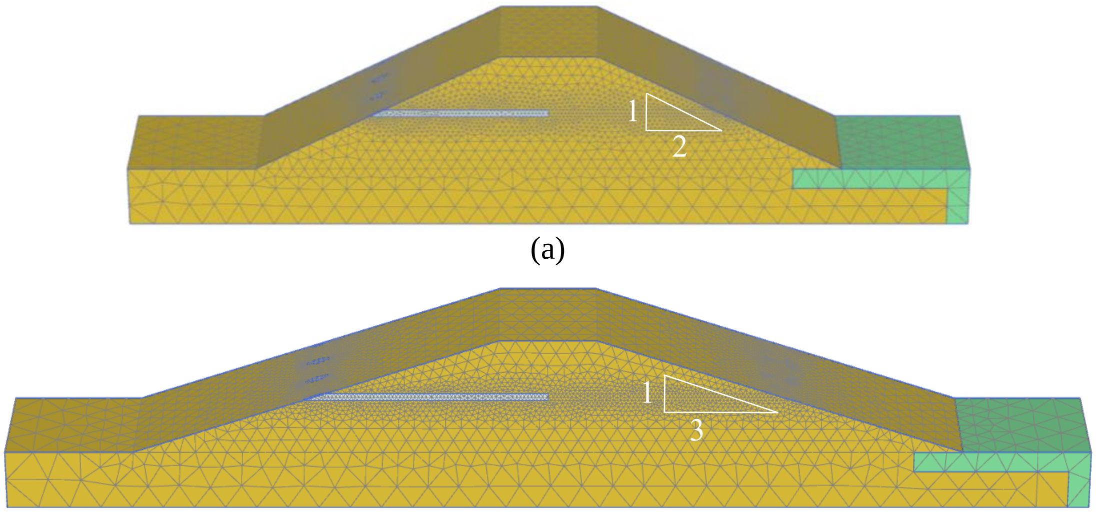

(a)

(b)

Figure 5.13. 3D finite element model of a levees with mid-height waterside burrows (WB): a) 2H:1V and b) 3H:1V

In order to investigate the effect of side slope ratio on seepage, pore pressure distributions are calculated on the three horizontal sections (Sec 1 at +2.8m, Sec 2 at 4m and Sec 3 at 6m). Pore pressure distributions are presented in Figure 5.14. For the case of waterside burrows (WB), the presence of the burrows increases the pore water pressure for all selected side slope ratios which agrees with the earlier findings. Increasing the slope ratio causes an increase in the representative pore pressure at the embankment centerline for all cases including the intact levee. This increase is due to the extension and raise of the phreatic surface at the centerline of the levee by flattening the slope while the crest width and toe drain size are kept constant. The various levee models with different slope ratios are superimposed in Figure 5.15 and the changes to the phreatic surface are illustrated. The trend and percentage change in pore pressure remains the same for all slope ratios (Figure 5.16).

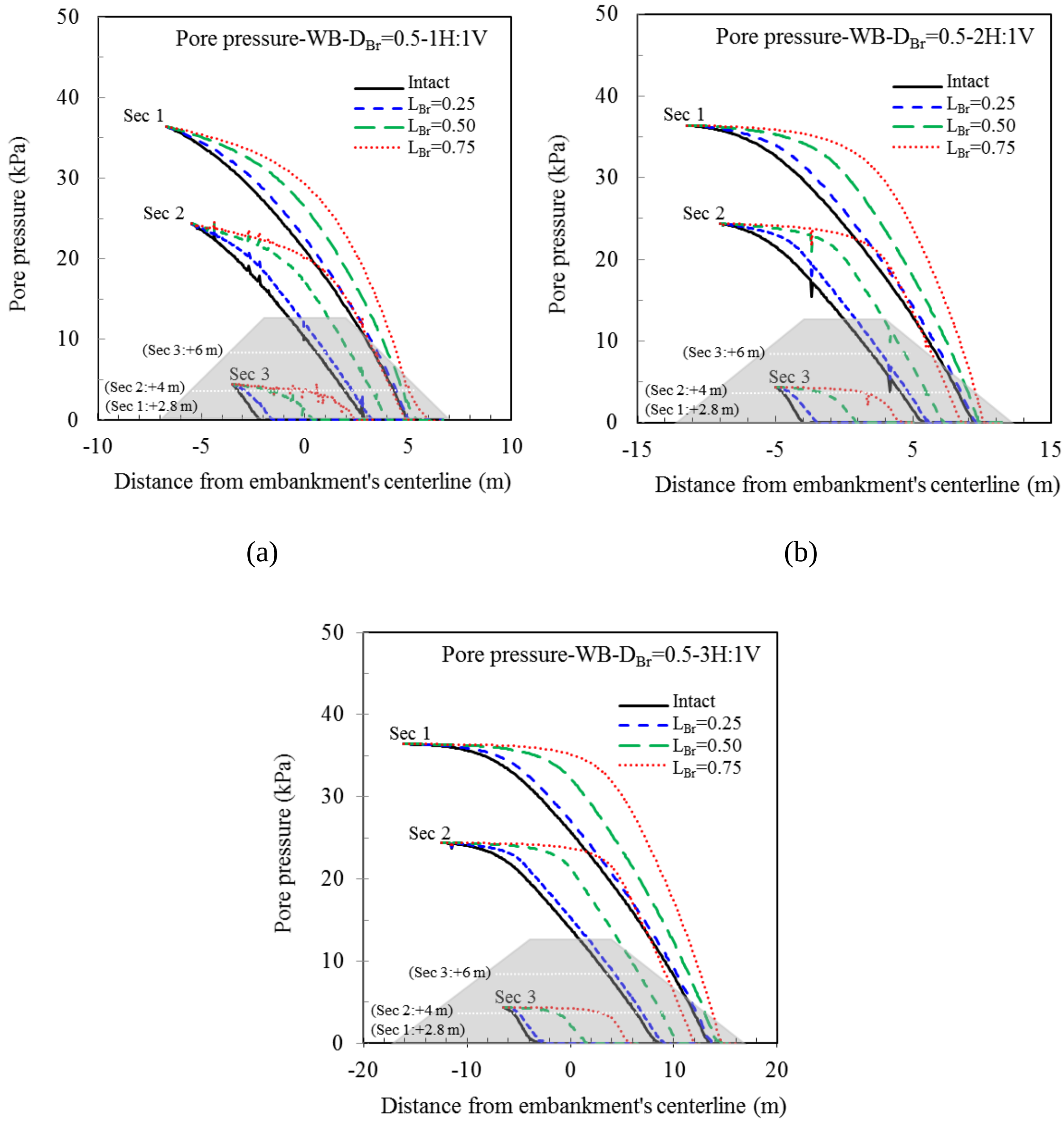

Figure 5.14. Pore pressure distributions of levee with waterside burrows (WB) on the horizontal sections for different levee side slope ratios: a) 1H:1V; b) 2H:1V; c) 3H:1V

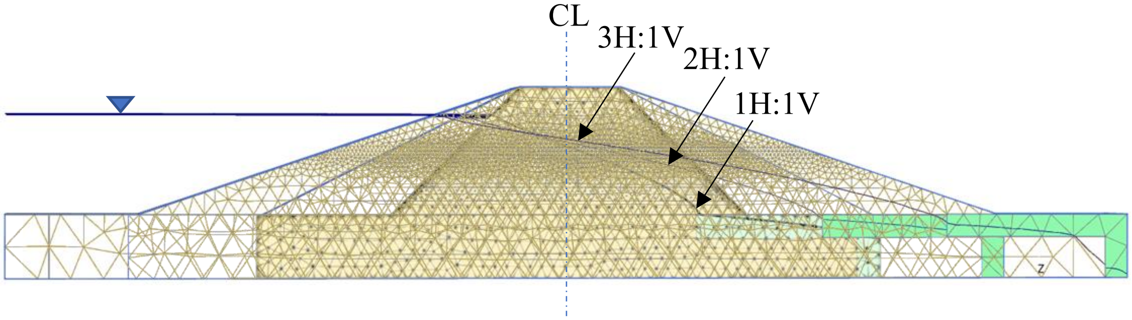

Figure 5.15. Change in phreatic surface due to change of slope ratio

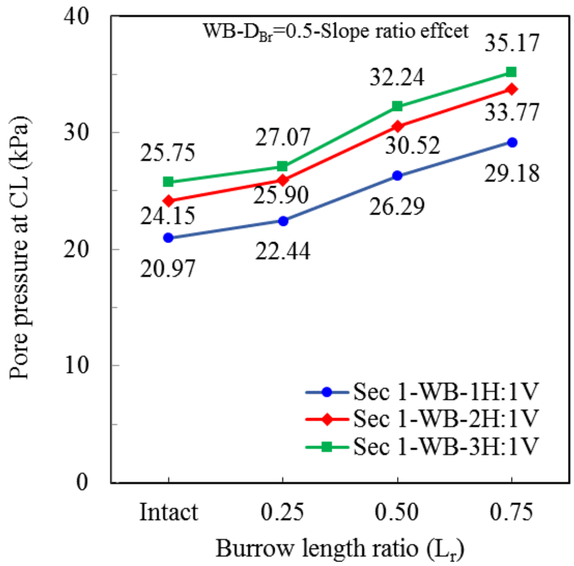

(a)

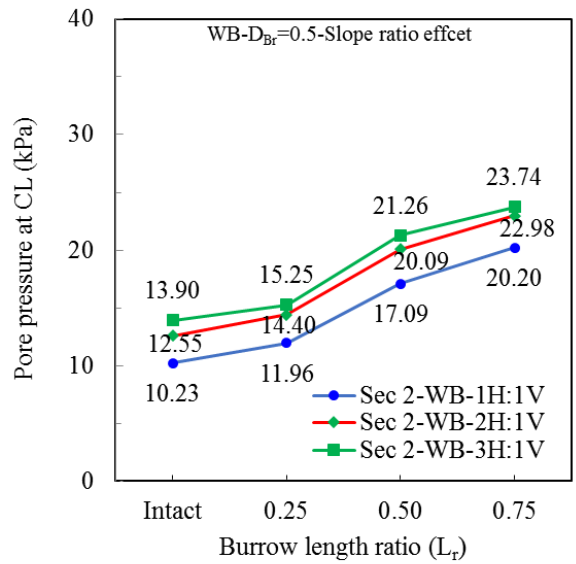

(b)

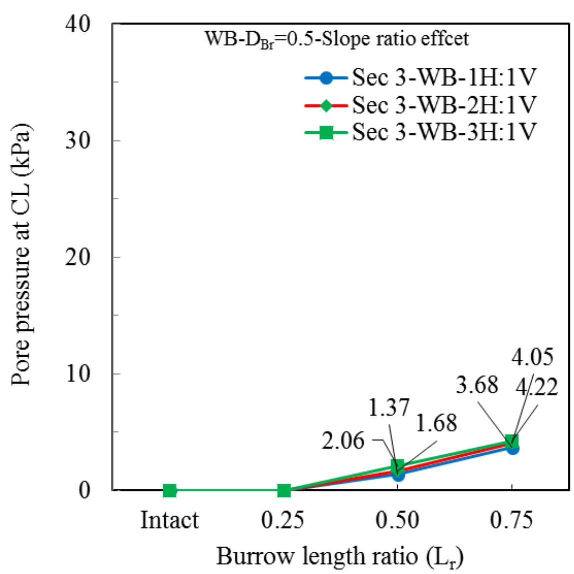

(c)

Figure 5.16. Pore pressure distributions of levee with waterside burrows (WB) on the horizontal section for different side slope ratios; a) Sec 1; b) Sec 2; c) Sec 3

Levees with landside burrows (LB) are also investigated for three different side slope ratios. Flattening the side slopes causes a convex curve showing a decrease in the pore pressure due to increase in burrow length ratio. These findings are consistent with the burrow length effect discussed earlier. The pore pressure curves for the long and medium length burrows for 2H: 1V and 3H: 1V show a slight increase around the levee toe. This increase is due to the displacement of the phreatic surface toward the landside slope (Figure 5.17).

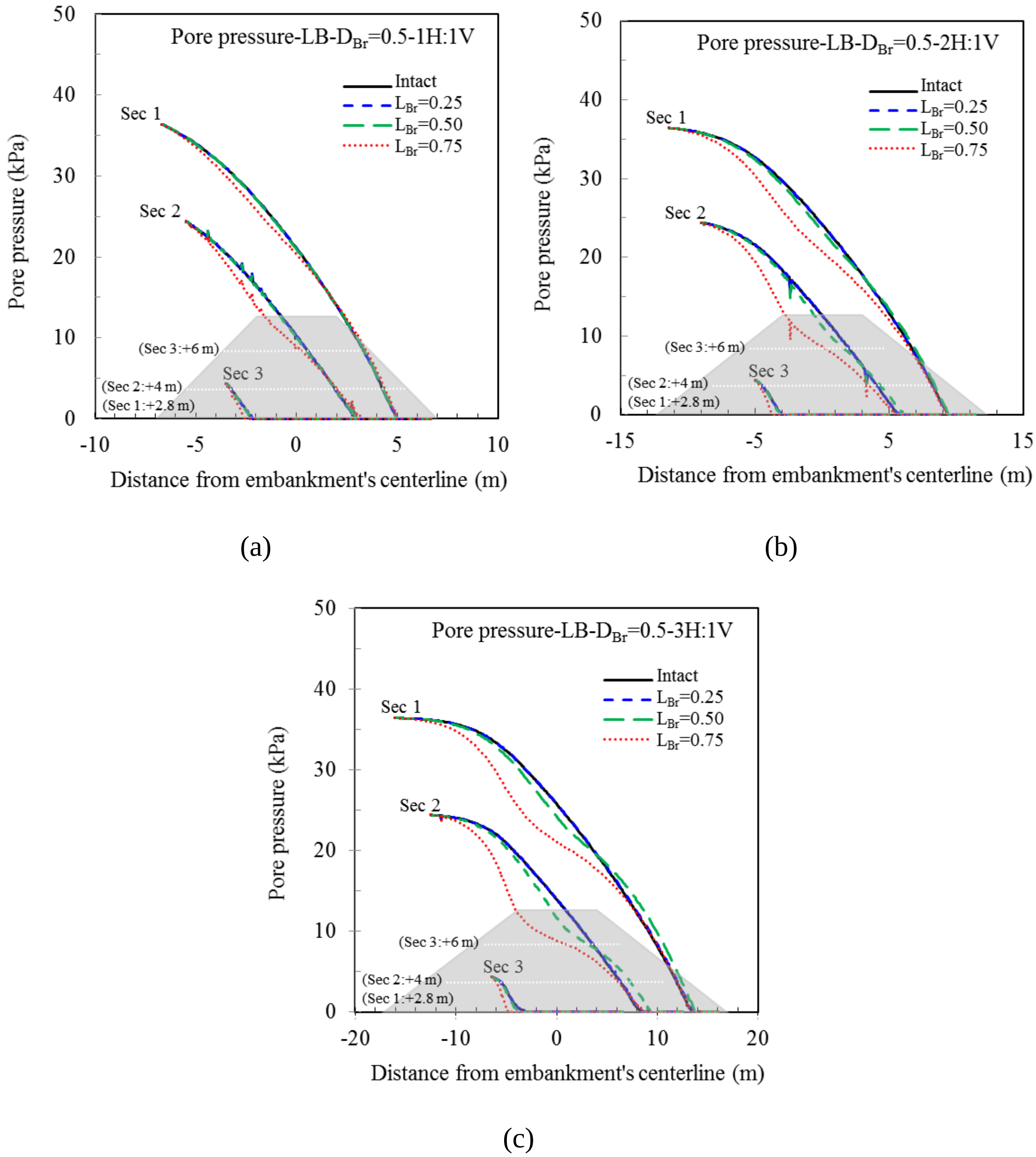

Figure 5.17. Pore pressure distributions of levee with landside burrows (LB) on the horizontal sections for different side slope ratios: a) 1H:1V; b) 2H:1V; c) 3H:1V

Figure 5.18 illustrates the pore pressure at the centerline of the model for different side slopes ratios and burrow lengths. For the medium and long length burrows pore pressure tends to converge to the same value after flattening the slope. The reason for this convergence is that by increasing L_{Br} the level of seeped water in the burrows becomes consistently the same at the centerline of the levee for all slope ratios. As can be seen in Figure 5.18.a and b, the difference between pore pressures at the same length are reduced by reducing the side slope ratios. The pore pressure at the same L_{Br} are higher in flatter slopes due to the increase in the horizontal path of the water through the embankment. For instance, in section 1 for intact and $L_{Br=}$ 0.25, calculation of the standard deviation (SD) for the three slope ratios, provides SD=1.9. However, SD for L_{Br}= 0.5 and L_{Br}= 0.75 are 0.8 and 0.2 respectively.

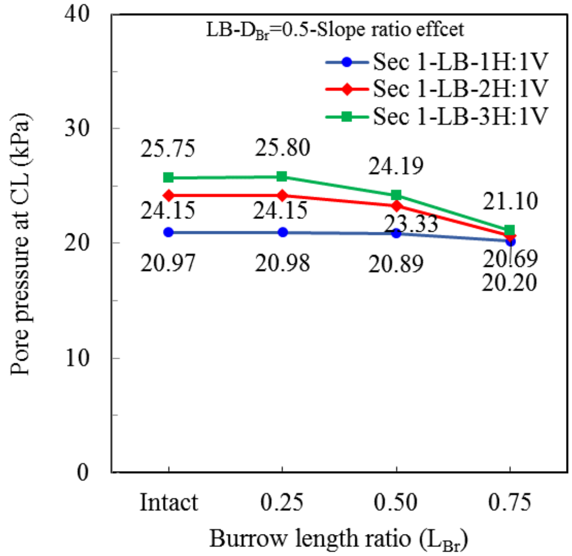

(a)

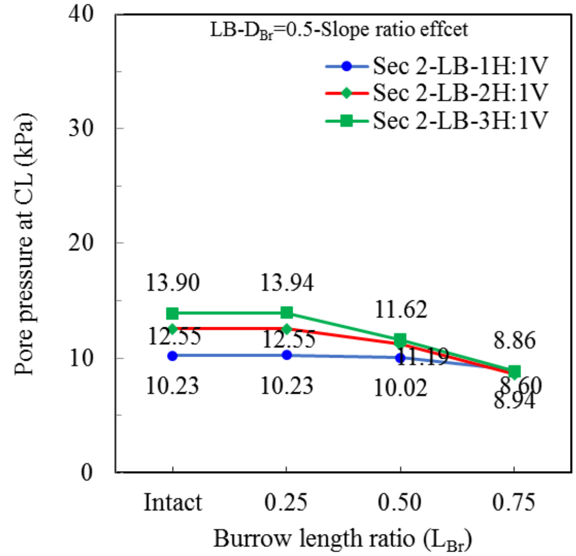

(b)

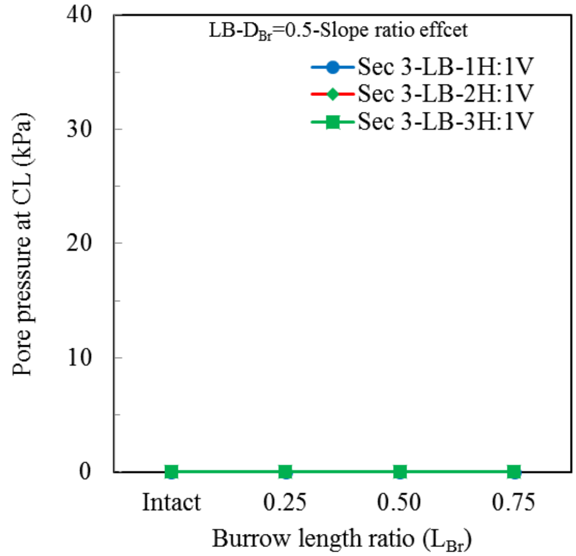

(c)

Figure 5.18. Pore pressure at the centerline of the embankment (CL) for levee landside burrows (LB) for different side slope ratios: a) Sec 1; b) Sec 2; c) Sec 3

Studying the factor of safety of the landside slope against global slope failure for both cases of WB and LB indicates that the factor of safety increases by flattening the slopes. Although, pore pressure at the centerline of the levee increases for larger slope ratios, the increase in the global factor of safety of the slope occurs due to the smaller disturbing force for flatter slopes. The rate of reduction in the factor of safety due to increasing the burrow length ratio is smaller for steep slopes (Figure 5.19.a) which is attributed to the smaller initial factor of safety of the corresponding intact levee. Alternatively, the factor of safety for the levee with landside burrows does not show a noticeable change (Figure 5.19.b). The maximum change in the factor of safety as compared to the intact levee which happens at L_{Br}=0.75 does not seem to be significant (about 3%). Although, the side slope ratio affects the initial factor of safety in the case of intact levee, the rate of reduction or increase is almost the same for all the slope ratios.

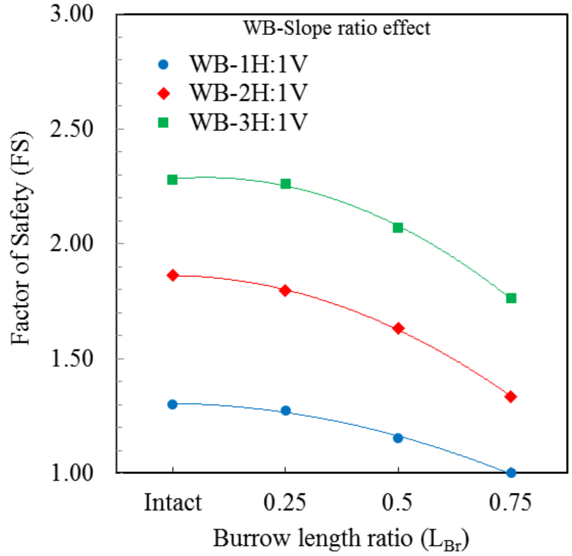

(a)

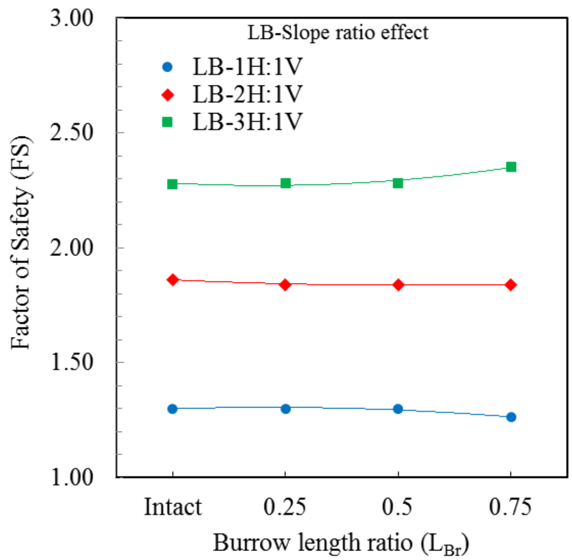

(b)

Figure 5.19. Factor of safety of the embankment for a) WB b) LB

5.6 Conclusions and limitations

This study investigates the effect of burrow configuration and levee geometry on the behavior of internally deteriorated earthen levees. The analyses are performed using 3D finite element models under steady state conditions. Effect of burrow length, burrow depth, and side slope ratio on pore pressure and factor of safety of the landside slope are investigated in the parametric study. The results of the study suggest that:

- For waterside burrows, increasing the length of burrows increases the pore pressure within the levee and moves the phreatic surface toward the landside slope. For levee with landside burrows, increasing the burrow length decrease the pore pressure inside the embankment. The presence of landside burrows is responsible for this decrease by shortening the free drain path in the embankment and consequently resulting a larger dry area. Although, it seems that longer burrows increase the global factor of safety of the slope in short term, they still endanger the safety of the embankment by causing local slope failure.
- The depth of burrows has an important role on seepage behavior and stability of the levees. Deep waterside burrows tend to significantly affect the pore pressure at the deeper level of the embankment which decreases the factor of safety of the landside slope faster and cause a rapid failure. For landside burrows, the burrow depth seems not to have a significant effect on the pore pressure distributions, except for the deepest burrow conditions which the presence of burrow decreases the pore pressure. Consequently, the factor of safety follows the same pattern and only increase in the

case of deep burrows. Generally, it can be concluded that the effect of burrow depth is more critical for the waterside burrows.

- The side slope ratio has different effects on the waterside and landside burrows. For waterside burrows, flattening the slope increases pore water pressure at the centerline of the model. The amount of increase is higher for longer burrows. Analyses show that even though the factor of safety of the levee with the steeper slope is lower, the rate of decrease in this factor is lower due to the increase in burrow length. In the case of landside burrows, side slope ratio seems to have a minimal effect on the factor of safety. For long landside burrows, pore pressure shows the same behavior for different slope ratios.

In this research, the analyses were done using limited number of geometric and material parameters. It is recommended that more variable related to burrow configurations are further investigated. These variables include a combination of landside and waterside burrows, soil properties, direction of burrow, and burrow size. The results of this study may provide an insight into the effects of selected variables on the hydraulic performance and safety of deteriorated earthen levees. The analyses reported in this research were performed under static loading conditions and, seismic analysis is needed for levees located in seismic zones.

6 CONCLUSIONS, LIMITATIONS AND RECOMMENDATIONS

The research presented in this thesis has investigated the effects of wildlife activities on earthen levees from a geotechnical engineering perspective. Invasive animal damages were modeled as idealized cylindrical cavities in earthen levee embankments. A series of centrifuge experiments were conducted on 1/35 scaled-down models with burrows at different elevations of the landside and waterside slopes. During the experiments, the models' responses were studied with respect to both stability and seepage. As reference points for the deteriorated models, intact models were also tested experimentally. Numerical models were then built based on the results of the centrifuge experiments and used to perform a parametric study on the deteriorated levee. The parametric study investigated the effects of burrow length, burrow elevation, burrow attack side, and side slope ratio on the stability and the hydraulic performance of earthen levees.

6.1 Conclusions

The following general conclusions can be drawn from the results presented in the chapters of this thesis:

- Animal burrows inside earthen levees have significant negative effects on the hydraulic performance and stability of an embankment. This finding confirms prior observation-based understandings.
- The rod-pullout mechanism developed to simulate burrows during a centrifuge flight is an effective and accurate solution for modeling idealized animal burrows in earthen levees.
- The attack side of animal burrows plays an important role in the type of damage and the failure mode of deteriorated earthen levees.
- Animal burrows can remain stable while being completely or partially filled with water. In such cases, changes occur in the seepage path through a levee embankment. For waterside burrows, change in the seepage path causes a high hydraulic gradient at the levee toe and leads to local toe failure. This initially local slope failure develops rapidly to global failure of the waterside slope. Failures due to the presence of waterside burrows occur suddenly and without warning.
- Animal burrows on the landside of earthen levees act as internal drains in the embankment. Water flows through the burrows and slides down the landside slope surface, causing local erosion and instability. Failures due to landside burrows are a result of gradual local failure around burrow openings, which extend and cause catastrophic embankment failures. Such failures happen slowly, and signs of deterioration can be observed on landside slope surface prior to levee collapses.
- Animal burrow length and depth have different effects on the waterside than on the landside of an embankment. When they occur on the waterside, both deeper burrows

and longer burrows decrease the factor of safety of a levee. However, when burrows occur on the landside of an embankment, neither burrow depth nor burrow length seem to have a significant effect on the factor of safety of a levee.

- The reduction of the factor of safety due to the presence of animal burrows seems to be minimally impacted by the side slope ratio of a levee embankment. Although it does not have an impact on the overall stability of the levee, the pore pressure at the centerline of the model is increased with flattening of the embankment slope for waterside burrows, and the increase is higher for longer burrows.

6.2 Limitations and recommendations for future studies

It should be noted that the results of this study are limited by the parameters investigated and the idealization applied. The complexity of animal burrow configurations in nature may limit the accuracy of any modeling scheme. It is recommended that additional experimental and numerical analysis be undertaken to model increasingly complex burrow configurations including multiple burrow directions and burrow connectivity. The analyses in this research were performed under static conditions. However, since many earthen levees are constructed in seismic zones, it is critical for future studies to consider the seismic behaviour of deteriorated earthen levees.

7 REFERENCES

1. Aanstoos, J., Hasan, k., O' Hara, C.G., Prasad, S., Dabbiru, L., et al. *Earthen levee monitoring with Synthetic Aperture Radar*. in IEEE Applied Imagery Pattern Recognition (AIPR). 2011. Washington,USA.

2. Steedman, S.R. and Sharp, M.K., *Physical modelling analysis of the New Orleans levee breaches.* Proceedings of the Institution of Civil Engineers-Geotechnical Engineering, 2011. 164(6): p. 353-372.

3. Bayoumi, A. and Meguid, M., *Wildlife and Safety of Earthen Structures: A Review.* Journal of Failure Analysis and Prevention, 2011. 11(4): p. 295-319.

4. Chen, Z., Stuetzle, C., Cutler, B., Gross, J., Franklin, R.W., et al. *Quantitative analysis of simulated erosion for different soils*. in Proceedings of the 18th SIGSPATIAL International Conference on Advances in Geographic Information Systems. 2010. San Jose, California: ACM.

5. Wang, P. and Kahawita, R., *Modeling the hydraulics and erosion process in breach formation due to overtopping*, in *Sedimentation and Sediment Transport: Proceedings of the Symposium held in Monte Verità, Switzerland, from September*

2nd – to September 6th, 2002, Gyr, A. and Kinzelbach, W., Editors. 2003, Springer, The Netherlands: Dordrecht. p. 211-220.

6. FEMA, *Technical Manual for Dam Owners:Impacts of Animals on Earthen Dams*, Federal emergency managment agency, Editor. 2005. p. 122.

7. Hanson, G.J., Tejral, R.D., Hunt, S.L., and Temple, D.M. *Internal Erosion And Impact Of Erosion Resistance*. in Collaborative Management of Integrated Watersheds. 2010. Sacramento, California: USSD.

8. Cobos Roa, D., Shriro, M., Sita, N., and Bray, J.D., *Field Evaluation of Burrowing Animal Impacts and Effectiveness of Remedial Measures*, in *Influence of Tree Roots and Mammal Burrowing Activity on Levee Integrity*. 2014. p. 75.

9. Van Vuren, D.H. and Ordeñana, M.A., *Factors influencing burrow length and depth of ground-dwelling squirrels.* Journal of Mammalogy, 2012. 93(5): p. 1240-1246.

10. Laundré, J.W. and Reynolds, T.D., *Effects of soil structure on burrow characteristics of five small mammal species.* Great Basin Naturalist, 1993. 53(4): p. 8.

11. Seabloom, E.W., Reichman, O.J., and Gabet, E.J., *The Effect of Hillslope Angle on Pocket Gopher (Thomomys bottae) Burrow Geometry*. Oecologia, 2000. 125(1): p. 26-34.

12. Hansen, D.T. *Risk Analysis, GIS and Arc Schematics: California Delta Levees*. in ESRI User Conference. 2008. San Diego California.

13. Mierzwa, M. and Suits, B., *Jones Tract 2004 Levee Break DSM2 Simulation*, in *Methodology for Flow and Salinity Estimates in the Sacramento-San Joaquin Delta and Suisun Marsh* 2005. p. 30.

14. Spragens, L., *Plant & Animal Impacts on Earthen Dams*, in *Future reaserch needed in dam safety*. 1999, FEMA: Lexington KY.

15. D'Alpaos, L., Brath, A., Fioravante, V., Gottardi, G., Mignosz, P., et al., *Relazione tecnico-scientifica sulle cause del collasso dell'argine del fiume Secchia avvenuto il giorno 19 gennaio 2014 presso la frazione San Matteo*. 2014. p. 92.

16. Bishop, I., Styles, P., Emsley, S.J., and Ferguson, N.S., *The detection of cavities using the microgravity technique: case histories from mining and karstic environments.* Engineering Geology Special Publication, 1997. 12: p. 13.

17. Weymouth, J.W., *Geophysical Methods of Archaeological Site Surveying.* Advances in Archaeological Method and Theory, 1986. 9: p. 311-395.

18. Kimchi, T., Reshef, M., and Terkel, J., *Evidence for the use of reflected self-generated seismic waves for spatial orientation in a blind subterranean mammal.* Journal of Experimental Biology, 2005. 208(4): p. 647-659.

19. Miller, R.D. and Steeples, D.W., *Detecting voids in a 0.6 m coal seam, 7 m deep, using seismic reflection.* Geoexploration, 1991. 28(2): p. 109-119.

20. Chlaib, H.K., Mahdi, H., Al-Shukri, H., Su, M.M., Catakli, A., et al., *Using ground penetrating radar in levee assessment to detect small scale animal burrows.* Journal of Applied Geophysics, 2014. 103: p. 121-131.

21. Di Prinzio, M., Bittelli, M., Castellarin, A., and Pisa, P.R., *Application of GPR to the monitoring of river embankments.* Journal of Applied Geophysics, 2010. 71(2–3): p. 53-61.

22. Schmocker, L. and Hager, W.H., *Modelling dike breaching due to overtopping.* Journal of Hydraulic Research, 2009. 47(5): p. 585-597.

23. Schmocker, L. and Hager, W.H., *Plane dike-breach due to overtopping: effects of sediment, dike height and discharge.* Journal of Hydraulic Research, 2012. 50(6): p. 576-586.

24. Bonelli, S., *Erosion in Geomechanics Applied to Dams and Levees*, ed. Nicot, F. 2013, Great Britain: WILEY.

25. Zachar, D., *Soil Erosion*. 1982: Elsevier Scinetific Publicatins Company 548.

26. Rao, X., Li, L., Amini, F., and Tang, H., *Smoothed Particle Hydrodynamics Modeling of Combined Wave and Surge Overtopping and Hydraulic Erosion of an Articulated Concrete Block-Strengthened Levee System.* Journal of Coastal Research, 2012. 28(6): p. 12.

27. Xu, Y., Li, L., and Amini, F., *Slope Stability Analysis of Earthen Levee Strengthened by High Performance Turf Reinforcement Mat under Hurricane Overtopping Flow Conditions.* Geotechnical and Geological Engineering, 2012. 30(4): p. 12.

28. Planès, T., Mooney, M.A., Rittgers, J.B.R., Parekh, M.L., Behm, M., et al., *Time-lapse monitoring of internal erosion in earthen dams and levees using ambient seismic noise.* Géotechnique, 2016. 66(4): p. 12.

29. Fisher, W.D., Camp, T.K., and Krzhizhanovskaya, V.V., *Anomaly detection in earth dam and levee passive seismic data using support vector machines and automatic feature selection.* Journal of Computational Science, 2016: p. 11.

30. Fell, R. and Fry, J.-J., *State of The Art on the Likelihood of Internal Erosion of Dams and Levees by Means of Testing*, in *Erosion in Geomechanics Applied to Dams and Levees*. 2013, John Wiley & Sons, Inc. p. 1-99.

31. Van Beek, V.M., Bruijn, H.T.J.d., Knoeff, J.G., Bezuijen, A., and Forster, U. *Levee Failure Due to Piping: A Full-Scale Experiment*. in International Conference on Scour and Erosion (ICSE-5) 2010. San Francisco, USA: ASCE.

32. Koelewijn, A.R., de Vries, G., Lottum, H.v., Förster, U., Beek, V.M.v., et al. *Full-scale testing of piping prevention measures: Three tests at the IJkdijk*. in ICPMG – Physical Modelling in Geotechnics: Proceedings of the 8th International Conference on Physical Modelling in Geotechnics. 2014. Perth, Australia: Taylor & Francis Group.

33. Van Beek, V.M., Knoeff, H., and Sellmeijer, H., *Observations on the process of backward erosion piping in small-, medium- and full-scale experiments.* European Journal of Environmental and Civil Engineering, 2011. 15(8): p. 22.

34. Taylor, R.N., *Geotechnical Centrifuge Technology*. 1995, london: Blackie academic & professional.

35. Das, B.M., *Advanced Soil Mechanics*. Vol. 1. 2008, London & New York: Taylor & Francis.

36. Ainsworth, A., Ellis, E.A., Baker, N., Cox, C., and Yu, H.S. *A new geotechnical centrifuge at the University of Nottingham, UK*. in Proceedings of the Sixth International Conference on Physical Modelling in Geotechnics, 6th ICPMG. 2006. Hong Kong: Taylor & Francis

37. Ubilla, J., Sasanakul, I., Abdoun, T., Sharp, M., Steedman, S., et al., *New Orleans Levee System Performance during Hurricane Katrina: London Avenue and Orleans Canal South.* Journal of Geotechnical and Geoenvironmental Engineering 2008. 134(5): p. 13.

38. Cappa, R., Yniesta, S., Lemnitzer, A., Brandenberg, S.J., and Stewart, J.P. *Centrifuge experiments to evaluate the seismic performance of levees on peaty soils in the Sacramento-San Joaquin delta*. in Association of State Dam Safety Officials Annual Conference. 2014.

39. Maharjan, M. and Takahashi, A., *Liquefaction-induced deformation of earthen embankments on non-homogeneous soil deposits under sequential ground motions.* Soil Dynamics and Earthquake Engineering, 2014. 66: p. 113-124.

40. Koito, N., Horikoshi, K., and Takahashi, A. *Physical modelling of backward erosion piping in foundation beneath levee*. in 8th International Conference on Scour and Erosion. 2016. Oxford, UK: Taylor & Francis Group.

41. Lee, C.W., Kim, Y.S., Park, S.Y., Kim, D.G., and Heo, G., *The behavior characteristics of a reservoir levee subjected to increasing water levels.* Journal of Civil Engineering and Management, 2017. 23(1): p. 12.

42. Jafari, N.H., Stark, T.D., Leopold, A.L., and Merry, S.M., *Three-dimensional levee and floodwall underseepage.* Canadian Geotechnical Journal, 2015. 53(1): p. 12.

43. Shi-igai, H. and Kono, T. *Analytical Approach on Wave Overtopping on Levees*. in 12th International Conference on Coastal Engineering 1970. Washington,USA.

44. Kaunda, R.B., *A neural network assessment tool for estimating the potential for backward erosion in internal erosion studies.* Computers and Geotechnics, 2015. 69: p. 6.

45. Fell, R., Wan, C.F., Cyganiewicz, J., and Foster, M., *Time for development of internal erosion and piping in embankment dams.* Journal of Geotechnical and Geoenvironmental Engineering, 2003. 129(4): p. 7.

46. Blach, M., Jurist, K., and Morton, S., *Anticipating California Levee Failure: Government response strategies for protecting natural resources from freshwater oil spills*. 2010, U.S. Department of the Interior Region IX. p. 18.

47. Van Beek, V.M., Knoeff, J.G., Rietdijk, J., Sellmeijer, J.B., and Cruz, J.L.D.L. *Influence of sand and scale on the piping process—experiments and multivariate analysis*. in Physical Modelling in Geotechnics. 2010. switzerland: Taylor & Francis Group, London.

48. Sellmeijer, H., López de la Cruz, J., Van Beek, V.M., and Knoeff, H., *Fine-tuning of the backward erosion piping model through small-scale, medium-scale and IJkdijk experiments.* European Journal of Environmental and Civil Engineering, 2011. 15(8): p. 15.

49. Zhou, X.J., Jie, Y.X., and Li, G.X., *Numerical simulation of the developing course of piping.* Computers and Geotechnics, 2012. 44(0): p. 5.

50. Bonelli, S. and Brivois, O., *The scaling law in the hole erosion test with a constant pressure drop.* International Journal for Numerical and Analytical Methods in Geomechanics, 2008. 32(13): p. 22.

51. Boukhemacha, M.A., Bica, I., and Mezouar, K., *Theoretical Mathematical Modeling For Piping Erosion Near Conduits.* Mathematical Modelling in Civil Engineering, 2011. 7: p. 7.

52. Xu, F., Zhou, H., Zhou, J., and Yang, X., *A Mathematical Model for Forecasting the Dam-Break Flood Routing Process of a Landslide Dam.* Mathematical Problems in Engineering, 2012: p. 16.

53. Sharp, J.A. and McAnally, W.H., *Numerical modeling of surge overtopping of a levee.* Applied Mathematical Modelling, 2012. 36(4): p. 11.

54. Sills, G., Vroman, N., Wahl, R., and Schwanz, N., *Overview of New Orleans Levee Failures: Lessons Learned and Their Impact on National Levee Design and Assessment.* Journal of Geotechnical and Geoenvironmental Engineering, 2008. 134(5): p. 9.

55. Witmer, G.W. and Engeman, R.M., *Subterranean Rodents as Pests: The Case of the Pocket Gopher*. 2007, University of Nebraska - Lincoln: Verlag Berlin Heidelberg p. 13.

56. Hori, T., Mohri, Y., and Niwano, K., *Model tests for chemical injection to an outlet pipe of small earth dams.* Japan Geotechnical Society, 2007.

57. ASTM, *Standard Test Methods for Particle-Size Distribution (Gradation) of Soils Using Sieve Analysis*, in *ASTM D6913*. 2009, American Society for Testing and Materials: USA. p. 34.

58. ASTM, *Standard Test Method for Particle-Size Analysis of Soils*, in *ASTM D422*. 2007, American Society for Testing and Materials: USA. p. 8.

59. ASTM, *Standard Test Methods for Laboratory Compaction Characteristics of Soil Using Standard Effort (12 400 ft-lbf/ft3 (600 kN-m/m3))*. 2012, American Society for Testing and Materials: USA. p. 13.

60. Laundn, J.W. and Reynolds, T.D., *Effects Of Soil Structure On Burrow Characteristics Of Five Small Mammal Species.* Great Basin Naturalist, 1993. 53(4): p. 9.

61. Sherard, J.L., Woodward, R.J., Gizienski, S.F., and Clevenges, W.A., *Earth and Earth-Rock Dams*. 1963, New York.: John Wiley & Sons.

62. Arulanandan, K. and Perry, E.B., *Erosion in Relation to Filter Design Criteria for Earth Dams.* Journal of the Geotechnical Engineering Division, ASCE, 1983. 109(5): p. 16.

63. FEMA, *Filters for Embankment Dams*, Federal emergency management agency, Editor. 2011. p. 332.

64. Sherard, J.L. and Dunnigan, L.P. *Filters and Leakage Control in Embankment Dams*. in Seepage and Leakage from Dams and Impoundments. 1985. New York: American Society of Civil Engineers.

65. Saghaee, G., Mousa, A.A., and Meguid, M.A., *Experimental evaluation of the performance of earth levees deteriorated by wildlife activities.* Acta Geotechnica, 2016. 11(1): p. 10.

66. Saghaee, G., Mousa, A.A., and Meguid, M.A. *An experimental procedure to simulate the effects of animal burrows on existing levee structures*. in Eurofuge 2012. Delft, The Netherlands: Delft University of Technology and Deltares.

67. Saghaee, G., Mousa, A.A., and Meguid, M.A. *On the effects of animal burrows on the performance of homogeneous earthen structures*. in Geo-Manitoba. 2012. Winnipeg, Canada: Candaian Geotechnical society

68. White, D.J., Take, W.A., and Bolton, M.D., *Soil deformation measurement using particle image velocimetry (PIV) and photogrammetry*. Geotechnique, 2003. 53(7): p. 13.

69. Plaxis, *Plaxis 3D AE Scientific Manual*, Plaxis, Editor. 2015: The Netherlands. p. 66.

70. Plaxis, *Plaxis 3D AE Reference Manual*, Plaxis, Editor. 2015: The Netherlands. p. 438.

71. Harder, L.F., Vroman, N., Sills, G.L., Groves, C., and Kelley, J.R. *Inspection of Levee Distress and Breaches During the Spring 2008 Midwest Flood*. in Association of Dam Safety Officials Conference. 2009. Florida, USA.

72. Van Vuren, D.H. and Ordeñana, M.A., *Habitat Associations of Burrowing Mammals along Levees in the Sacramento Valley, California*, in *California Levee Vegetation Research Program*. 2011, University of California: Davis, USA.

73. Fredlund, D.G., Morgenstern, N.R., and Widger, R.A., *The shear strength of unsaturated soils.* Canadian Geotechnical Journal, 1978. 15(3): p. 8.